

 National Library of Canada

Cataloguing Branch  
Canadian Theses Division

Ottawa, Canada  
K1A 0N4

Bibliothèque nationale du Canada

Direction du catalogage  
Division des thèses canadiennes

## NOTICE

The quality of this microfiche is heavily dependent upon the quality of the original thesis submitted for microfilming. Every effort has been made to ensure the highest quality of reproduction possible.

If pages are missing, contact the university which granted the degree.

Some pages may have indistinct print especially if the original pages were typed with a poor typewriter ribbon or if the university sent us a poor photocopy.

Previously copyrighted materials (journal articles, published tests, etc.) are not filmed.

Reproduction in full or in part of this film is governed by the Canadian Copyright Act, R.S.C. 1970, c. C-30. Please read the authorization forms which accompany this thesis.

**THIS DISSERTATION  
HAS BEEN MICROFILMED  
EXACTLY AS RECEIVED**

## AVIS

La qualité de cette microfiche dépend grandement de la qualité de la thèse soumise au microfilmage. Nous avons tout fait pour assurer une qualité supérieure de reproduction.

S'il manque des pages, veuillez communiquer avec l'université qui a conféré le grade.

La qualité d'impression de certaines pages peut laisser à désirer, surtout si les pages originales ont été dactylographiées à l'aide d'un ruban usé ou si l'université nous a fait parvenir une photocopie de mauvaise qualité.

Les documents qui font déjà l'objet d'un droit d'auteur (articles de revue, examens publiés, etc.) ne sont pas microfilmés.

La reproduction, même partielle, de ce microfilm est soumise à la Loi canadienne sur le droit d'auteur, SRC 1970, c. C-30. Veuillez prendre connaissance des formules d'autorisation qui accompagnent cette thèse.

**LA THÈSE A ÉTÉ  
MICROFILMÉE TELLE QUE  
NOUS L'AVONS RECUE**

HEAT TRANSFER IN TURBULENT RECIRCULATORY  
FLOWS AFFECTED BY BUOYANCY FORCES IN  
RECTANGULAR CAVITIES

by

Zakaria E. Abdelrehim

A thesis submitted to the School of Graduate Studies in partial  
fulfillment of the requirements of the degree of

MASTER OF APPLIED SCIENCE

in the

Department of Mechanical Engineering

University of Ottawa

Ottawa, Canada

1979

Z.E. Abdelrehim, Ottawa, Canada, 1979



i

ABSTRACT

The transport of momentum and heat in turbulent flow is often affected by buoyancy forces. In the present investigation, a turbulent recirculatory flow inside a rectangular cavity is studied. The flow is driven by the combined effects of shear, induced by a moving lower wall, and buoyancy, induced by a temperature difference between the upper and lower walls.

The analysis is based on the development of a two equation turbulence model proposed by Jones and Launder [24]. In this model, the equations for the kinetic-energy of turbulence, dissipation rate of the kinetic-energy of turbulence and mean-square temperature fluctuations are solved numerically, together with the momentum and energy equations, using the control volume approach. A numerical technique based on the Gosman procedure [2] is developed to solve the equations.

The flow of water and liquid sodium is investigated for Reynolds numbers up to  $10^6$ . The effect of buoyancy forces is analyzed. The flow patterns, temperature distributions, average Nusselt numbers and turbulence characteristics are presented.

The obtained results and observed trends are in good agreement with analytical and experimental work reported by other investigators [1, 3 and 15].

ACKNOWLEDGEMENT

I wish to express my sincere appreciation to my supervisor Dr. Martha Salcudean for her invaluable guidance and assistance in obtaining the results of this project. I am particularly grateful to Dr. Salcudean for the research assistantship I received during the course of this project.

I also wish to extend my thanks to the Department of Mechanical Engineering, the University of Ottawa, for the teaching assistantship I received throughout the investigation.

TABLE OF CONTENTS

	<u>Page</u>
ABSTRACT .....	i
ACKNOWLEDGEMENT .....	ii
TABLE OF CONTENTS .....	iii
LIST OF TABLES .....	v
LIST OF FIGURES .....	vi
NOMENCLATURE .....	ix
CHAPTER	
1 INTRODUCTION .....	1
2 SURVEY OF LITERATURE .....	4
2.1 STEADY FLOWS IN RECTANGULAR CAVITIES .....	4
2.2 MATHEMATICAL MODELS OF TURBULENCE .....	8
2.2.1 The Basis of Constructing a Turbulence Model .....	8
2.2.2 Algebraic Turbulence Models .....	9
2.2.3 Differential Turbulence Models .....	12
2.2.3.1 One equation models of turbulence .....	13
2.2.3.2 Two equation models of turbulence .....	14
3 MATHEMATICAL FORMULATION .....	19
3.1 INTRODUCTION .....	19
3.2 GOVERNING EQUATIONS .....	19
3.3 GENERAL TRANSPORT EQUATION .....	26
3.4 BOUNDARY CONDITIONS .....	29
3.5 NEAR WALL REGIONS .....	29
3.5.1 Modification of the Momentum Transport Equation .....	29
3.5.2 Modification of the Energy Transport Equation .....	30
3.5.3 Modification of the Transport of Dissipation Rate Equation .....	31
3.5.4 Modification of the Transport of the Mean Square Temperature Fluctuation Equation .....	32

	<u>Page</u>
4 THE FINITE DIFFERENCE CALCULATION PROCEDURE . . .	33
4.1 INTRODUCTION . . . . .	33
4.2 DERIVATION OF THE GENERAL TERMS . . . . .	33
4.2.1 The Grid Network . . . . .	33
4.2.2 The Derivation Procedure . . . . .	34
4.3 THE CALCULATION OF THE SOURCE TERM . . . . .	38
4.4 STABILITY OF THE SOLUTION PROCEDURE . . . . .	40
4.5 DERIVATION OF THE PRESSURE EQUATION . . . . .	43
5 COMPUTATIONAL PROCEDURE . . . . .	46
5.1 INTRODUCTION . . . . .	46
5.2 GRID DESIGN . . . . .	46
5.3 SOLUTION OF THE ALGEBRAIC EQUATION . . . . .	46
5.4 UNDER-RELAXATION FACTOR . . . . .	50
5.5 SUMMARY OF THE COMPUTER PROGRAM . . . . .	51
6 DISCUSSION OF RESULTS . . . . .	54
6.1 INTRODUCTION . . . . .	54
6.2 FLOW DISTRIBUTION . . . . .	54
6.2.1 The Effects of Reynolds Number . . . . .	54
6.2.2 The Effects of Buoyancy Forces . . . . .	56
6.3 TEMPERATURE DISTRIBUTION . . . . .	58
6.3.1 The Effects of Reynolds Number . . . . .	58
6.3.2 The Effects of Buoyancy Forces . . . . .	59
6.4 THE HEAT TRANSFER CHARACTERISTICS . . . . .	60
6.5 THE TURBULENCE CHARACTERISTICS . . . . .	62
7 CONCLUSIONS AND SUGGESTIONS . . . . .	64
7.1 CONCLUSIONS . . . . .	64
7.2 SUGGESTIONS FOR FURTHER RESEARCH . . . . .	65
REFERENCES . . . . .	98
APPENDICES	
A TRI-DIAGONAL MATRIX ALGORITHM . . . . .	101
B A SAMPLE COMPUTER PROGRAM . . . . .	107

v

LIST OF TABLES

<u>Table</u>		<u>Page</u>
3.1	The Values of the Model Constants .....	27
3.2	General Form of the Transport Equation ....	28

LIST OF FIGURES

<u>Figure</u>		<u>Page</u>
3.1	Physical Model .....	66
3.2	Near Wall Region .....	66
4.1	Grid Network .....	67
5.1	Line Iteration Procedure .....	68
5.2	Computational Flow Chart: Main Program ..	69
5.3	Computational Flow Chart: Subroutine CALCU .....	70
6.1a	Velocity Distribution Re = $1.3 \times 10^2$ , Pr = 3, Gr/Re <sup>2</sup> = 0 .....	71
6.1b	Velocity Distribution Re = $1.3 \times 10^3$ , Pr = 3, Gr/Re <sup>2</sup> = 0 .....	72
6.1c	Velocity Distribution Re = $10^5$ , Pr = 3, Gr/Re <sup>2</sup> = 0 .....	73
6.2	Movement of the Primary Eddy Centre   .....	74
6.3a	Velocity Distribution Re = $10^2$ , Pr = 0.01, Gr/Re <sup>2</sup> = 0 .....	75
6.3b	Velocity Distribution Re = $5 \times 10^3$ , Pr = 0.01, Gr/Re <sup>2</sup> = 0 .....	76
6.3c	Velocity Distribution Re = $10^6$ , Pr = 0.01, Gr/Re <sup>2</sup> = 0 .....	77
6.4a	Velocity Distribution Re = $8.4 \times 10^4$ , Pr = 3, Gr/Re <sup>2</sup> = 0 .....	78
6.4b	Velocity Distribution Re = $8.4 \times 10^4$ , Pr = 3, Gr/Re <sup>2</sup> = 1 .....	79
6.4c	Velocity Distribution Re = $8.4 \times 10^4$ , Pr = 3, Gr/Re <sup>2</sup> = 2 .....	80

<u>Figure</u>		<u>Page</u>
6.5a	Velocity Distribution Re = $10^3$ , Pr = 0.01, Gr/Re <sup>2</sup> = 0 .....	81
6.5b	Velocity Distribution Re = $10^3$ , Pr = 0.01, Gr/Re <sup>2</sup> = 1 .....	82
6.6	Isotherms, Pr = 3, Gr/Re <sup>2</sup> = 0 .....	83
6.7a	Vertical Centre-line Temperature Distribution, Pr = 3, Gr/Re <sup>2</sup> = 0 .....	84
6.7b	Horizontal Centre-line Temperature Distribution Pr = 3, Gr/Re <sup>2</sup> = 0 .....	85
6.7c	Right Side Wall Temperature Distribution Pr = 3, Gr/Re <sup>2</sup> = 0 .....	86
6.7d	Left Side Wall Temperature Distribution Pr = 3, Gr/Re <sup>2</sup> = 0 .....	87
6.8	Isotherms, Pr = 0.01, Gr/Re <sup>2</sup> = 0 .....	88
6.9a	Horizontal Temperature Distribution Re = $2.7 \times 10^5$ , Pr = 3 .....	89
6.9b	Vertical Temperature Distribution Re = $2.7 \times 10^5$ , Pr = 3 .....	90
6.10	Isotherms, Re = $10^3$ , Pr = 0.01 .....	91
6.11	Mean Nusselt Number .....	92
6.12	Variation of the Turbulence Kinetic Energy with Reynolds Number .....	93
6.13	Variation of the Effective Viscosity with Reynolds Number .....	94
6.14	Vertical Turbulence Kinetic Energy Distribution, Re = $8.4 \times 10^4$ .....	95

Figure

Page

6.15	Vertical Effective Viscosity Distribution Re = $8.4 \times 10^4$ .....	96
6.16	Vertical Distribution of the Mean Square Temperature Fluctuation Re = $8.4 \times 10^4$ .....	97

NOMENCLATURE

Symbol  
English Letters

Definition

A	Control volume cross-sectional area, $m^2$
$A_p$	$\sum a_i - S_p$
a	Coefficient of the finite difference equation
C	Convective term, $C = \rho UA$
$c_p$	Specific heat at constant pressure, $J/kg \cdot ^\circ K$
c	Empirical constant appearing in the K- $\epsilon$ model, see table (3.1)
D	Diffusion term, $D = \Gamma A / \Delta y$
d	Cavity width, m
E	Constant in the logarithmic law of the wall
F	Flux at control volume boundaries
G	Generation term
Gr	Grashof number, $Gr = g\beta\delta Td^3/\nu^2$
$Gr/Re^2$	Mixed convection parameter
g	Gravitational acceleration, $9.806 m/s^2$
h	Cavity height, m
K	Kinetic-energy of turbulence, $K = \frac{1}{2}(\overline{u_i^2})$
$l$	Characteristic turbulence-length scale
$l_m$	Prandtl's mixing-length
$l_{m,\phi}$	Prandtl's mixing-length of scalar quantity
NI, NJ	Number of grid mesh in x and y direction respectively

Symbol

Definition

$\bar{Nu}$	Average Nusselt number, $\left. \frac{dT}{dn} \right _{n=0}$
$Nu_b$	Average Nusselt number computed with buoyancy forces
$n$	Coordinate normal to the wall
$P$	Pressure, $N/m^2$
$Pr$	Prandtl number, $Pr = \frac{c_p \mu}{\lambda}$
$Q$	Heat flux, $W/m^2$
$q$	Mean-square temperature fluctuation, $^{\circ}K^2$
$Re$	Reynolds number, $Re = \frac{U_o d}{\nu}$
$S_{\phi}$	Source term, see table (3.2)
$S_{\phi V}$	Integral source term, $S_{\phi V} = S_{\phi 1} \phi_p + S_{\phi 1}$
$S_{false}$	False source term
$S_p$	$S_{p1} + \max \left( \sum_i c_i, 0.0 \right)$
$S_{p1}$	Component of linearized source term
$S_u$	$S_{u1} + \max \left( \sum_i c_i, 0.0 \right)$
$S_{u1}$	Component of linearized source term
$T$	Temperature, $^{\circ}K$
$T_1$	Upper wall temperature, $^{\circ}K$
$T_o$	Moving wall temperature, $^{\circ}K$
$\delta T$	Temperature difference between two successive cells
$u$	Mean velocity component in the x-direction, m/s
$U$	Moving wall velocity, m/s

<u>Symbol</u>	<u>Definition</u>
URF	Under-relaxation factor
u	Velocity fluctuation component in the x-direction, m/s
V	Mean velocity component in the y-direction, m/s
v	Velocity fluctuation component in the y-direction, m/s
VOL	Cell volume
X,Y	Dimensionless horizontal and vertical cartesian coordinates, x/d, y/d respectively
x,y	Horizontal and vertical cartesian coordinates

### Greek Letters

$\beta$	Coefficient of volumetric expansion, $1/^\circ\text{K}$
$\epsilon$	Dissipation rate of turbulence kinetic energy $\frac{c_D K^{3/2}}{l}$
$\kappa$	Constant in Van Driest's formula
$\lambda$	Thermal conductivity, $\text{W/m}^\circ\text{K}$
$\Gamma$	Exchange coefficient $\mu/\sigma$
$\mu$	Dynamic viscosity, $\text{kg/m-sec}$
$\nu$	Kinematic viscosity, $\text{m}^2/\text{s}$
$\rho$	Fluid density, $\text{kg/m}^3$
$\tau$	Shear stress, $\text{N/m}^2$
$\phi$	General variable
$\sigma$	Prandtl number
$\sum_i$	Summation over control volume sides

SymbolDefinitionSubscripts

E, W, N, S

East, west, north and south neighbouring nodes of p

e, w, n, s

East, west, north and south side boundaries of control volume

eff

Effective (molecular plus turbulent)

K

For kinetic-energy of turbulence

P

Centre node of control volume

t

Turbulent

x

Local value

W

Wall value

e

For energy-dissipation

Superscripts

—

Average value

n

n-th iteration

'

Previous iteration

## CHAPTER I

### INTRODUCTION

The transport of momentum, heat and mass are often affected by the gravitational field. Such is the case for recirculatory flows in enclosures, buoyant shear flows or warm jets submerged in cold temperature fluids.

In order to study the effects of buoyancy forces on the transport of momentum and heat, cavity flow was chosen. Its geometric simplicity and practical implications provided a good test for theoretical models and new numerical schemes.

One example of cavity flow may be found in the fast breeder nuclear reactor (Phoenix), where the reactor core is surrounded by a large vessel filled with hot liquid sodium and traversed at the bottom by a cold jet leaving the heat exchanger. The mixing layers of the cold jet create a turbulent recirculatory flow which is affected by buoyancy forces due to density changes induced by the temperature gradient.

The analytical study of this problem was carried out by Grand et al. [1] for laminar flow conditions, using water and liquid sodium, by solving numerically the Navier-Stokes and energy equations in the stream function and vorticity form. They presented the stream lines and the isotherms together with the Nusselt number for Reynolds numbers in the range of  $10^2$  to  $10^3$  and for ratios of the mixing convection parameter,  $Gr/Re^2$  between 0 and 1.

The objective of the present work was to study numerically the flow, heat transfer and turbulence characteristics of the cavity flow for high range of Reynolds number up to  $10^6$ . It also represents, to the author's knowledge, the first attempt to predict numerically the turbulent recirculatory flow affected by buoyancy forces in a rectangular cavity.

The numerical calculations were based on the development of the two equation model of turbulence in which the turbulent exchange coefficient (the turbulent viscosity) was determined from the solution of two transport equations for the kinetic energy of turbulence  $K$ , and the rate of dissipation of the kinetic energy of turbulence  $\epsilon$ .

A finite difference solution for the governing equations of motion in their primitive form (velocities and pressure), the energy equation and the transport equations for the turbulence quantities was obtained by developing a numerical technique suggested by Gosman et al. [2]. A hybrid central and upwind differentiating scheme based on the control volume integration approach was used.

A brief review of related literature in cavity flow problems and mathematical turbulence models is presented in chapter 2. The theoretical developments which led to the momentum equations, the energy equation and the transport equations for the turbulence quantities, together with the boundary conditions, are presented in chapter 3.

The numerical and computational procedures are discussed in chapters 4 and 5 respectively. The numerical results for the flow, heat transfer and turbulence characteristics are given in chapter 6.

Parameters studied include the Reynolds number  $Re$ , and the mixed convection parameter  $Gr/Re^2$  for Prandtl numbers of 3 and 0.01.

The numerical results are compared with available data published on the flow and heat transfer in cavity flow for low Reynolds numbers. It should be noted, however, that limited data appear to exist for cavity flow at high Reynolds numbers.

CHAPTER 2SURVEY OF LITERATURE2.1 STEADY FLOWS IN RECTANGULAR CAVITIES

One example of a closed streamline problem is the fluid motion generated in a rectangular cavity by the translation of the upper or lower wall. This problem has attracted several investigators because its geometric simplicity is appropriate for testing the theoretical models and new numerical schemes.

Cavity flows driven by shear in the absence of buoyancy forces have been studied for a wide range of Reynolds numbers. Analytical studies for high Reynolds numbers were carried out by Batchelor [3] and Squire [4]. Batchelor's analysis assumed that the flow inside the cavity can be considered as an inviscid core of constant vorticity with a thin layer along the boundaries. He also showed that the separated region has a fixed size at high Reynolds numbers; in other words, the size of the primary eddy is independent of the Reynolds number.

Numerical solutions of the Navier-Stokes equations have been reported by Donovan [5] and Burggraf [6]. They studied the problem of a square cavity and provided a comparison with Batchelor's model. The computations which were carried out at Reynolds number of 400 showed that the flow consists of

three eddies; one primary eddy occupying most of the cavity and two secondary eddies at the upstream and downstream corners of the cavity.

Furthermore, the results obtained analytically and experimentally by Pan and Acrivos [7] and Weiss and Florsheim [8] have provided some information about the flow configuration inside rectangular cavities for Reynolds numbers greater than 400. Their results showed that the size of the primary eddy is dependent on Reynolds number up to a value of at least 2700. The upstream corner eddy increases in size up to a value of 500 and then shrinks continuously.

The nature of the eddies formed in the cavity depends also on the aspect ratio (cavity height to width ratio). Visual studies by Mills [9] and Pan and Acrivos [7], for a cavity in which the upper wall is moving, investigated the behaviour of the eddies for different aspect ratios. The downstream corner eddy becomes larger with increasing aspect ratio. For an aspect ratio of two, the downstream corner eddy grows until it occupies the entire lower portion of the cavity. The relative position of the pair of eddies depends on the Reynolds number.

One of the main problems in computational fluid mechanics is that the grid size must decrease as the Reynolds number increases so that numerical stability is obtained. Greenspan [10] considered the cavity flow problem numerically, using the

generalized Newton's method with over relaxation to speed the convergence. He obtained a convergent solution for Reynolds number up to  $10^5$  and for a mesh size of  $1/20^*$  and  $1/50$ . Greenspan did not observe any secondary eddies when he employed a mesh size of  $1/20$  for any of the Reynolds numbers he assumed. This mesh size was found to be large. However, at mesh spacing of  $1/50$ , the flow configuration, which he obtained at Reynolds number of  $10^4$ , contains a downstream secondary eddy, whereas at Reynolds number of  $10^5$  no secondary eddies were observed.

The Imperial College group at London [11, 12 and 13] have conducted a series of investigations relating to the cavity flow driven by shear in the absence of buoyancy forces. These series of studies employed an unequal mesh spacing with decreasing mesh size towards the wall so that the variations near the wall could be predicted accurately. They also used a unidirectional differentiating technique on the vorticity so that the differences were always backwards with reference to the direction of flow and thus accelerated the convergence. These new features were not present in the previous investigations.

Studies on cavity flows driven by the combined effects of shear, induced by the moving top wall, and buoyancy forces, induced by the temperature difference between the top and bottom walls, have been carried out by Torrance et al [14] for Prandtl number of one and Reynolds number of 100 with

---

\* The notation  $1/20$  means that the ratio of mesh size to cavity dimension is 1:20.

different values of Grashof number. Their results showed that, in the absence of buoyancy forces, for aspect ratios of  $1/2$  and  $1$ , only a single primary eddy appears with a small corner eddy, whereas for an aspect ratio of  $2$ , a secondary eddy appears within the lower portion of the cavity with the existence of a corner eddy. They also found that the buoyancy forces tended to diminish the strength of the primary eddy.

Grand et al [1] have studied the problem for the two different Prandtl numbers of water and liquid sodium. They numerically solved the Navier-Stokes equations for laminar flow. Velocity and temperature distributions were obtained for Reynolds numbers ranging from  $10^2$  to  $2.5 \times 10^3$  and mixed-convection parameter ranging from  $0$  to  $1$ . They found that both secondary eddies are enhanced due to the buoyancy forces in the case of liquid sodium but, for water, only the downstream corner eddy is enhanced while the upstream one disappears.

Another investigation was carried out by Nallasamy and Prasad [15] for a wide range of Reynolds numbers from  $0$  to  $5 \times 10^4$ . They solved the full Navier-Stokes and energy equations numerically using a finite-difference technique. They observed the tendency of the secondary eddies to shrink in size with increasing Reynolds number, ending with only the primary eddy at high Reynolds numbers. The tendency of the centre of the primary eddy to move towards the centre of the cavity with increasing Reynolds number was also observed.

Summarizing the previous works on the cavity flow, results have been obtained by solving analytically and numerically the Navier-Stokes and energy equations for laminar flow. To the author's knowledge, no study has been carried out for turbulent flow affected by buoyancy forces in rectangular cavities.

## 2.2 MATHEMATICAL MODELS OF TURBULENCE

### 2.2.1 The Basis of Constructing a Turbulence Model

The momentum equation for turbulent flow (the Reynolds equation) can be written as follows:

$$\frac{\partial}{\partial t}(\rho U_i) + \frac{\partial}{\partial x_j}(\rho U_i U_j) - \frac{\partial}{\partial x_j}(\mu \frac{\partial U_i}{\partial x_j} - \rho \overline{u_i u_j}) + \frac{\partial P}{\partial x_i} = 0$$

This equation may be solved directly without correlating the fluctuating terms (Reynolds stresses  $-\rho \overline{u_i u_j}$ ). At present, this equation cannot be solved numerically, since the important details of turbulence are small scale in character. For example, eddies responsible for the decay of turbulence are typically about 0.1 mm. Consequently, in order to solve the equations numerically, about  $10^5$  discrete points may be needed, which would exceed the storage capacity of any existing computer. Therefore, the time-averaged effects of the turbulence are usually considered, rather than their macroscopic details.

Since there is no direct way of knowing the magnitude of these terms, it is necessary to approximate or 'model' their effects in terms of quantities that can be determined. Hence, a 'turbulence model' refers to a set of equations which, when numerically solved with the mean flow equations, provides a solution for turbulent flow problems.

The concept of a turbulence model was first formulated by Boussinesq [16]. As in Stokes's law for laminar flow ( $\tau_{ij} = \mu \frac{\partial U_i}{\partial x_j}$ ), he suggested that the turbulent shear stress ( $\tau_{ij} = -\rho \overline{u_i u_j}$ ) was equal to the product of the mean velocity gradient and a turbulent viscosity  $\mu_t$ . Hence,

$$\tau_{ij} = -\rho \overline{u_i u_j} = \mu_t \left( \frac{\partial U_i}{\partial x_j} + \frac{\partial U_j}{\partial x_i} \right)$$

where the turbulent viscosity  $\mu_t$  is not a fluid property as is  $\mu$ , but its value depends on the structure of turbulence at the point of interest.

The introduction of the concept of turbulent viscosity  $\mu_t$  was the basis for constructing a turbulence model. Further development involved its expression in terms of calculable quantities. This was accomplished by using different approaches.

### 2.2.2 Algebraic Turbulence Models

The first attempt to express the turbulent viscosity algebraically as a function of known quantities was attributed to Prandtl in 1925 [17], where an important advance in

modelling a turbulent flow was made by the introduction of a hypothesis which has become known as Prandtl's mixing-length theory. In this hypothesis, the turbulent viscosity is described by the following formula:

$$\mu_t = \rho \ell_m^2 \left| \frac{\partial U}{\partial y} \right|$$

where  $\ell_m$  has been prescribed algebraically.

One of the interesting contributions in describing the mixing-length was the proposal of Von-Kármán in 1930 [16]. He suggested that the mixing-length  $\ell_m$  is proportional to the ratio of the first to the second derivatives of the mean velocity, i.e.

$$\ell_m \propto \left| \frac{\partial U}{\partial y} \right| / \left| \frac{\partial^2 U}{\partial y^2} \right|$$

This proposal eliminated the need to prescribe the mixing-length profile, but in many cases where  $\frac{\partial^2 U}{\partial y^2} = 0$ , at the inflection points of the velocity profile, the formula gives infinite mixing-length, and therefore the turbulent shear stress cannot be computed for the above-mentioned condition.

A large amount of experimental data has been reported by Escudier [18] in the boundary layers near a wall. He concluded that, except in the semi-laminar region close to the wall, the mixing-length distribution could be described

by the following formula,

$$\ell_m = \kappa y$$

where  $\kappa = .435$ , and  $y$  is the perpendicular distance between the wall and the point of interest.

In the semi-laminar region, Van Driest [19] suggested that the effective viscosity is given by the sum of the laminar and turbulent viscosities, thus :

$$\mu_{\text{eff}} = \mu + \rho \ell_m^2 \left| \frac{\partial U}{\partial y} \right|$$

where  $\ell_m$  is described by the following algebraic equation

$$\ell_m = \kappa y \left[ 1 - \exp. - \frac{y \tau_w^{1/2} \rho^{1/2}}{A \mu} \right] \quad (2.1)$$

with  $A = 26.0$ .

Modifications to Van Driest's hypothesis were necessary for Van Driest's mixing-length formula to satisfy different cases. Among these modifications, Patankar and Spalding [20] proposed that the local shear stress  $\tau_+$  should appear in the formula of  $\ell_m$  instead of the shear stress at the wall  $\tau_w$ , thus:

$$\ell_m = \kappa y \left[ 1 - \exp. - y_+ \tau_+^{1/2} / A \right] \quad (2.2)$$

This formula gave a better correlation with the experimental results which they obtained.

In the same manner as the treatment of the momentum exchange coefficient, the mixing-length hypothesis was extended so that it could deal with the turbulent exchange coefficient of scalar quantities [16]. For a scalar quantity  $\phi$ , the turbulent diffusion flux may be expressed as:

$$J_{\phi} = -\Gamma_{\phi,t} \text{grad } \phi \quad (2.3)$$

where the turbulent exchange coefficient  $\Gamma_{\phi,t}$  is given by:

$$\Gamma_{\phi,t} = \rho \ell_{m,\phi} \ell_m \left| \frac{\partial U}{\partial y} \right| \quad (2.4)$$

and  $\ell_{m,\phi}$  is the mixing-length scale of the scalar quantity

### 2.2.3 Differential Turbulence Models

The expression of the turbulent viscosity through algebraic formulae did not fully describe the turbulent phenomena in most cases, because the algebraic formulae do not take into account the convective and diffusive transport of the turbulence properties. Hence, the turbulent viscosity is described using a differential transport equation, as conjectured by Kolmogorov [21].

### 2.2.3.1 One equation model of turbulence

Kolmogorov [21] proposed that, instead of relating the turbulence velocity to the mean velocity gradient, a better representation would be to relate it to the kinetic energy of turbulence  $K$  [16]. Thus the turbulence velocity may be expressed as:

$$V_t \propto \sqrt{K}$$

where  $K = \frac{1}{2} \langle u_i^2 \rangle$ , and the turbulent viscosity becomes

$$\mu_t = \rho V_t l_m = \rho \sqrt{K} l_m$$

The kinetic-energy of turbulence  $K$  is determined from the solution of the differential transport equation, but the mixing-length  $l_m$  still has to be prescribed algebraically.

Instead of solving the differential equation for the turbulence properties (i.e.  $K, l$ , etc.) to obtain the turbulent viscosity and hence the Reynolds stress, the turbulent stress can be obtained directly by solving a differential equation for the transport of the shear stress itself. The first model of this kind was that developed by Bradshaw et al [22]. The model is based on the hypothesis that the turbulent shear stress is proportional to the kinetic energy of turbulence  $K$  as follows:

$$\tau_t \propto \rho K$$

where  $K$  and hence  $\tau_t$  are determined from the differential transport equation. The length scale, which appeared in the equation for  $K$ , was described algebraically. Lack of experimental data did not allow them to simulate the  $\tau$ -equation. Nee and Kovaszny [23] developed a transport equation in which the turbulent viscosity is the dependent variable instead of  $K$ . In so doing, the transport effects on the turbulent viscosity were considered, but the assumed length scale profile was not universal.

In order to account for the transport effects on the length scale, the latter must be described through a differential equation. Hence, to obtain a better prediction, it is necessary to consider two equation models.

### 2.2.3.2 Two equation models of turbulence

The two equation models of turbulence are models in which the kinetic energy of turbulence  $K$  and the length scale  $l$  are determined from transport equations where the convection and diffusion effects on  $K$  and  $l$  are considered.

The transport equation for the kinetic energy of turbulence is derived by multiplying the momentum equation for each component of velocity by its fluctuating value, time-averaging and summing the resulting equations. Following Launder and Spalding [16], the form of the equation describing the transport of  $K$  is written as:

$$\frac{DK}{Dt} = \frac{1}{\rho} \frac{\partial}{\partial x_k} \left( \frac{\mu_t}{\sigma_K} \frac{\partial K}{\partial x_k} \right) + \frac{\mu_t}{\rho} \left( \frac{\partial U_i}{\partial x_k} + \frac{\partial U_k}{\partial x_i} \right) \frac{\partial U_i}{\partial x_k} - \epsilon$$

where the various terms are interpreted as follows:

The term  $\frac{DK}{Dt}$  represents the change in the kinetic energy due

to convection. The term  $\frac{1}{\rho} \frac{\partial}{\partial x_k} \left( \frac{\mu_t}{\sigma_K} \frac{\partial K}{\partial x_k} \right)$  represents the

diffusion of the kinetic energy. The production of the

kinetic energy is expressed by the term  $\frac{\mu_t}{\rho} \left( \frac{\partial U_i}{\partial x_k} + \frac{\partial U_k}{\partial x_i} \right)$ , and

the term  $\epsilon$  gives the value of the dissipation of the kinetic energy.

The transport equation for the length scale  $\ell$  has been developed in a different form by several authors. Among them, Ng and Spalding [24] have determined the length scale from the solution of two transport equations for  $K\ell$  and  $\ell$ . Spalding [25] determined  $\ell$  from the solution of two transport equations for  $K/\ell^2$  and  $\ell$ .

One of the models, which has successfully predicted turbulent flow, is the  $K-\epsilon$  model developed by Jones and Launder [26]. In this model, the turbulent viscosity is determined from the solution of two transport equations, one for the turbulence kinetic energy  $K$  and the other for the dissipation rate of the turbulence kinetic energy  $\epsilon$ , through the following relation:

$$\mu_t = c'_\mu \rho K^{3/2} / \ell$$

where  $c'_\mu$  is a constant. The length scale of turbulence  $\ell$  is defined in terms of  $K$  and  $\epsilon$  as follows:

$$\ell = c_D K^{3/2} / \epsilon$$

The transport equation for  $\epsilon$  was first developed by Hanjalic [27]. It may be written as:

$$\frac{D\epsilon}{Dt} = \frac{1}{\rho} \frac{\partial}{\partial x_k} \left( \frac{\mu_t}{\sigma_\epsilon} \frac{\partial \epsilon}{\partial x_k} \right) + \frac{c_1 c_\mu}{\rho} \frac{\epsilon}{K} \left( \frac{\partial U_i}{\partial x_k} + \frac{\partial U_k}{\partial x_i} \right) \frac{\partial U_i}{\partial x_k} - c_2 \frac{\epsilon^2}{K}$$

The interpretation of this equation follows a similar argument to that used for  $K$ .

A similar transport equation for the mean-square fluctuation of a scalar property 'F', such as the square of temperature fluctuations may be derived by multiplying the equation for 'F' by its fluctuating quantity 'f'. Spalding [28] has adopted the following form:

$$\frac{Dq}{Dt} = \frac{1}{\rho} \frac{\partial}{\partial x_k} \left( \frac{\mu_t}{\sigma_q} \frac{\partial q}{\partial x_k} \right) + \frac{c_{q1}}{\rho} \mu_t \left( \frac{\partial F}{\partial x_k} \right)^2 - c_{q2} \frac{K^2}{\ell} q$$

where  $q$  represents the mean square fluctuation of  $F$ , i.e.  $\overline{f^2}$ .

Jones and Launder [26] have applied the "K- $\epsilon$  model" to predict the behaviour of boundary layers in accelerating flows where the boundary layers revert from turbulent to

laminar flow, a phenomenon called "laminarization". Their predictions were in close agreement with the experimental results. Launder and Spalding [29] predicted turbulent boundary layer flows as well as turbulent recirculatory flows using the "K- $\epsilon$  model". The obtained results were in close agreement with experimental data.

The model has also been used by Taminini [30] to predict the turbulent diffusion flame, while Plumb and Kennedy [31] have applied it to natural convection from a vertical isothermal surface. Their results were found to be in reasonable agreement with experiment.

Mujumdar and Li [32] used the model to predict a two-dimensional turbulent flow between parallel plates and their results were found to be in close agreement with experimental data. Salcudean and Guthrie [33] applied the model to describe the recirculatory flow in filling ladles. The model has also been used to predict three-dimensional flow in ducts of rectangular cross-section rotating about an axis normal to the longitudinal direction [34]. Agreement with experimental data was good for constant area ducts at low rotation, but for divergent ducts at high rotation, the results were not in good agreement with experimental data. Modifications to the forms of the K and  $\epsilon$  equations were necessary to account for the rotational effect.

The purpose of the present work was to investigate the effects of Reynolds number and buoyancy forces on turbulent recirculatory flows in square cavities. The flow is driven by the combined effects of the moving bottom wall and the temperature difference between the top and bottom walls. In performing the calculations, the K- $\epsilon$  turbulence model was developed to account for the buoyancy forces. The flow patterns, temperature distribution and turbulence characteristics are presented for the two different Prandtl numbers of water and liquid sodium for a wide range of Reynolds numbers, up to  $10^6$ , and mixed convection parameters from 0 to 2.

CHAPTER 3MATHEMATICAL FORMULATION3.1 INTRODUCTION

The governing equations for steady, incompressible and Newtonian flow with constant physical properties in a rectangular cavity, with the exception of the contribution of the temperature dependent density to the buoyancy forces, are presented in section 3.2. The equations are then represented in a standard form in section 3.3 to simplify the solution procedure. The boundary conditions for the resulting elliptical equations and the treatment of the near wall regions are given in sections 3.4 and 3.5 respectively.

3.2 GOVERNING EQUATIONS

The physical model is shown in Fig. 3.1. A two-dimensional rectangular cavity of width  $d$  and height  $h$  is considered. The top and bottom walls are maintained at a constant temperature  $T_1$  and  $T_0$  respectively, the vertical walls being insulated. The temperature  $T_1$  of the top wall is higher than  $T_0$  for all cases. The bottom wall is moving with a constant velocity  $U_0$  from left to right.

The conservation of momentum for a turbulent flow can be obtained from the Navier-Stokes equations by expressing the velocities and pressures as mean and fluctuating components; by time-averaging, the resulting equation (the Reynolds equation) excluding the body force will be:

$$\frac{\partial}{\partial t}(\rho U_i) + \frac{\partial}{\partial x_j}(\rho U_i U_j) - \frac{\partial}{\partial x_j}(\mu \frac{\partial U_i}{\partial x_j} - \rho \overline{u_i u_j}) + \frac{\partial P}{\partial x_i} = 0 \quad (3.1)$$

where  $-\rho \overline{u_i u_j}$  is the turbulent (Reynolds) stress, which express the superposition of the fluctuation on the mean motion.

It is assumed that the turbulent shear stress is related to the mean rate of strain via a turbulent viscosity  $\mu_t$ .

$$\text{i.e.} \quad -\rho \overline{u_i u_j} = \mu_t \left( \frac{\partial U_i}{\partial x_j} + \frac{\partial U_j}{\partial x_i} \right) \quad (3.2)$$

By substituting the turbulent stress, Eq. 3.2, into Eq. 3.1, the conservation of the momentum for a turbulent flow is obtained:

$$\frac{\partial}{\partial t}(\rho U_i) + \frac{\partial}{\partial x_j}(\rho U_i U_j) - \frac{\partial}{\partial x_j} \left( \mu \frac{\partial U_i}{\partial x_j} + \mu_t \frac{\partial U_i}{\partial x_j} + \mu_t \frac{\partial U_j}{\partial x_i} \right) + \frac{\partial P}{\partial x_i} = 0 \quad (3.3)$$

The following assumptions are made:

- (i) The flow is two-dimensional and steady,
- (ii) the fluid is incompressible and Newtonian,
- (iii) the physical properties are independent of the temperature, with the exception of the contribution of the temperature dependent density to the buoyancy forces.

Under the above assumptions and by considering cartesian coordinates due to the geometry of the system, the x and y momentum equations reduce respectively to:

$$\begin{aligned} \frac{\partial}{\partial x}(\rho U^2) + \frac{\partial}{\partial y}(\rho VU) - \mu_{\text{eff}} \left( \frac{\partial^2 U}{\partial x^2} + \frac{\partial^2 U}{\partial y^2} \right) - \mu_{\text{eff}} \frac{\partial^2 U}{\partial x^2} \\ - \mu_{\text{eff}} \frac{\partial^2 V}{\partial x \partial y} + \frac{\partial P}{\partial x} = 0 \end{aligned} \quad (3.4)$$

$$\begin{aligned} \frac{\partial}{\partial x}(\rho UV) + \frac{\partial}{\partial y}(\rho V^2) - \mu_{\text{eff}} \left( \frac{\partial^2 V}{\partial x^2} + \frac{\partial^2 V}{\partial y^2} \right) - \mu_{\text{eff}} \frac{\partial^2 V}{\partial y^2} \\ - \mu_{\text{eff}} \frac{\partial^2 U}{\partial x \partial y} + \frac{\partial P}{\partial y} = 0 \end{aligned} \quad (3.5)$$

where  $\mu_{\text{eff}}$  is the effective viscosity of the fluid and is taken as the sum of the molecular and turbulent contributions, i.e.,

$$\mu_{\text{eff}} = \mu + \mu_t \quad (3.6)$$

Following Jones and Launder [26], the turbulent viscosity  $\mu_t$  is determined by the local values of the density  $\rho$ , the kinetic energy of turbulence  $K$ , and the turbulence length scale  $\ell$ . Thus, for dimensional homogeneity:

$$\mu_t = c'_\mu \rho K^{1/2} \ell \quad (3.7)$$

where  $c'_\mu$  is a constant. The turbulence length scale is determined from the solution of the rate of dissipation of

the turbulence kinetic-energy  $\epsilon$ , which may be assumed proportional to  $K^{3/2}/l$ .

Thus, the turbulent viscosity may be recast as:

$$\mu_t = c_\mu \rho K^2 / \epsilon \quad (3.8)$$

where  $c_\mu$  is a constant.

In the present work two equations for  $K$  and  $\epsilon$  are solved to determine the turbulent viscosity.

An equation for  $K$  may be obtained from the Reynolds equation. Launder and Spalding [16] have shown that the transport equation of the kinetic energy of turbulence can be written as:

$$\frac{\partial}{\partial x}(\rho U K) + \frac{\partial}{\partial y}(\rho V K) - \frac{\mu_{eff}}{\sigma_K} \frac{\partial^2 K}{\partial x^2} - \frac{\mu_{eff}}{\sigma_K} \frac{\partial^2 K}{\partial y^2} - \mu_t G + c_D \rho \epsilon = 0 \quad (3.9)$$

where  $\sigma_K$  is the turbulent Prandtl number

$\mu_t G$  is the turbulence generation

$\epsilon$  is the dissipation of the turbulence kinetic energy.

The transport equation for the dissipation rate of the kinetic energy of turbulence  $\epsilon$ , can be written as:

$$\frac{\partial}{\partial x}(\rho U \epsilon) + \frac{\partial}{\partial y}(\rho V \epsilon) - \frac{\mu_{eff}}{\sigma_\epsilon} \frac{\partial^2 \epsilon}{\partial x^2} - \frac{\mu_{eff}}{\sigma_\epsilon} \frac{\partial^2 \epsilon}{\partial y^2} - c_1 \frac{\epsilon}{K} \mu_t G + c_2 \rho \frac{\epsilon^2}{K} = 0 \quad (3.10)$$

where  $c_1$ ,  $c_2$  and  $\sigma_e$  are empirical coefficients [26].

The temperature distribution is computed by solving the following equation for the transport of energy:

$$\frac{\partial}{\partial x}(\rho UT) + \frac{\partial}{\partial y}(\rho VT) - \frac{\mu_{\text{eff}}}{\sigma_{\text{eff}}} \frac{\partial^2 T}{\partial x^2} - \frac{\mu_{\text{eff}}}{\sigma_{\text{eff}}} \frac{\partial^2 T}{\partial y^2} = 0 \quad (3.11)$$

where  $\sigma_{\text{eff}}$  is the effective Prandtl number, which is related to the molecular and turbulent values as follows:

$$\frac{\mu_{\text{eff}}}{\sigma_{\text{eff}}} = \frac{\mu}{\sigma} + \frac{\mu_t}{\sigma_t} \quad (3.12)$$

#### The Contribution of Buoyancy Forces

The cavity flow is affected by the temperature difference between the top and bottom walls, which causes changes in density, thereby inducing buoyancy forces. These forces are included in the y-momentum equation by considering them as imposed body forces, and are expressed by the term  $\rho g \beta \delta T$  [17].

In a turbulent flow, the fluctuation of the temperature affects the transport of the turbulence energy and its dissipation rate. Due to these effects, a buoyancy term needs to be added to the equations of the kinetic-energy of turbulence and the energy dissipation.

The relation between the temperature fluctuation and the vertical velocity fluctuation, as suggested by Launder and Spalding [16], was used as follows:

$$\overline{vt} = c_4 (qK)^{1/2} \quad (3.13)$$

where  $q$  is the mean-square temperature fluctuation.

The transport equation for the mean-square temperature fluctuation is derived by multiplying the energy equation by the fluctuating quantity of the temperature  $t$ , and then time-averaging the resultant equation. Following Launder's suggestion [16], the equation for  $q$  can be derived as:

$$\begin{aligned} \frac{\partial}{\partial x}(\rho Uq) + \frac{\partial}{\partial y}(\rho Vq) - \frac{\mu_{\text{eff}}}{\sigma_q} \frac{\partial^2 q}{\partial x^2} - \frac{\mu_{\text{eff}}}{\sigma_q} \frac{\partial^2 q}{\partial y^2} \\ + c_{q1} \mu_t \left[ \left( \frac{\partial T}{\partial x} \right)^2 + \left( \frac{\partial T}{\partial y} \right)^2 \right] - c_{q2} \rho \frac{\epsilon}{K} q = 0 \end{aligned} \quad (3.14)$$

Therefore, the complete set of equations describing the turbulent flow with the influence of buoyancy forces may be summarized as:

Conservation of Mass:

$$\frac{\partial U}{\partial x} + \frac{\partial V}{\partial y} = 0 \quad (3.15)$$

This equation is not solved directly, but is used to generate the pressure equation.

Conservation of Momentum:

x-component:

$$\begin{aligned} \frac{\partial}{\partial x}(\rho U^2) + \frac{\partial}{\partial y}(\rho VU) - \mu_{\text{eff}} \frac{\partial^2 U}{\partial x^2} - \mu_{\text{eff}} \frac{\partial^2 U}{\partial y^2} - \mu_{\text{eff}} \frac{\partial^2 U}{\partial x^2} - \mu_{\text{eff}} \frac{\partial^2 V}{\partial x \partial y} \\ + \frac{\partial P}{\partial x} = 0 \end{aligned} \quad (3.16)$$

y-component:

$$\frac{\partial}{\partial x}(\rho UV) + \frac{\partial}{\partial y}(\rho V^2) - \mu_{\text{eff}} \frac{\partial^2 V}{\partial x^2} - \mu_{\text{eff}} \frac{\partial^2 V}{\partial y^2} - \mu_{\text{eff}} \frac{\partial^2 V}{\partial y^2} - \mu_{\text{eff}} \frac{\partial^2 U}{\partial x \partial y} + \frac{\partial P}{\partial y} + \rho g \beta \delta T = 0 \quad (3.17)$$

Conservation of Energy:

$$\frac{\partial}{\partial x}(\rho UT) + \frac{\partial}{\partial y}(\rho VT) - \frac{\mu_{\text{eff}}}{\sigma_{\text{eff}}} \frac{\partial^2 T}{\partial x^2} - \frac{\mu_{\text{eff}}}{\sigma_{\text{eff}}} \frac{\partial^2 T}{\partial y^2} = 0 \quad (3.18)$$

Kinetic Energy of Turbulence:

$$\frac{\partial}{\partial x}(\rho UK) + \frac{\partial}{\partial y}(\rho VK) - \frac{\mu_{\text{eff}}}{\sigma_K} \frac{\partial^2 K}{\partial x^2} - \frac{\mu_{\text{eff}}}{\sigma_K} \frac{\partial^2 K}{\partial y^2} - \mu_t G + c_D \rho \epsilon - \rho g \beta c_4 (qK)^{\frac{1}{2}} = 0 \quad (3.19)$$

Dissipation Rate of the Kinetic Energy of Turbulence:

$$\frac{\partial}{\partial x}(\rho U \epsilon) + \frac{\partial}{\partial y}(\rho V \epsilon) - \frac{\mu_{\text{eff}}}{\sigma_\epsilon} \frac{\partial^2 \epsilon}{\partial x^2} - \frac{\mu_{\text{eff}}}{\sigma_\epsilon} \frac{\partial^2 \epsilon}{\partial y^2} - c_1 \frac{\epsilon}{K} \mu_t G + c_2 \rho \frac{\epsilon^2}{K} - c_3 c_4 \rho g \beta \epsilon \left(\frac{q}{K}\right)^{\frac{1}{2}} = 0 \quad (3.20)$$

Mean-Square Temperature-Fluctuation:

$$\frac{\partial}{\partial x}(\rho Uq) + \frac{\partial}{\partial y}(\rho Vq) - \frac{\mu_{\text{eff}}}{\sigma_q} \frac{\partial^2 q}{\partial x^2} - \frac{\mu_{\text{eff}}}{\sigma_q} \frac{\partial^2 q}{\partial y^2} - c_{q1} \mu_t \left[ \left( \frac{\partial T}{\partial x} \right)^2 + \left( \frac{\partial T}{\partial y} \right)^2 \right] + c_{q2} \rho \frac{\epsilon}{K} q = 0 \quad (3.21)$$

Turbulent Viscosity Equation:

$$\mu_t = c_\mu \rho K^2 / \epsilon \quad (3.22)$$

where the  $\sigma$ 's represent the turbulent Prandtl numbers for the parameters in question and the  $c$ 's are the constants of the model.

Numerical values for  $c_D$ ,  $c_\mu$ ,  $c_1$ ,  $c_2$ ,  $\sigma_K$  and  $\sigma_\epsilon$  are those recommended by Jones and Launder [26], the values for  $c_3$  and  $c_4$  chosen were based upon experimental data [31] and the constants  $c_{q1}$ ,  $c_{q2}$  and  $\sigma_q$  are those used by Taminini [30]. The values of these constants are given in table 3.1.

3.3 GENERAL TRANSPORT EQUATION

The set of equations, Eq. (3.15) - Eq. (3.21), represent the governing equations to be solved numerically. Following Gosman et al. [2], these equations can be represented by a standard form so that a single solution algorithm may be applied. This form is given by:

$$\underbrace{\frac{\partial}{\partial x}(\rho U \phi) + \frac{\partial}{\partial y}(\rho V \phi)}_{\text{convection terms}} - \underbrace{\frac{\partial}{\partial x}(\Gamma \frac{\partial \phi}{\partial x}) - \frac{\partial}{\partial y}(\Gamma \frac{\partial \phi}{\partial y})}_{\text{diffusion terms}} = \underbrace{S_\phi}_{\text{source term}} \quad (3.23)$$

Eq. (3.23) represents the transport of a general variable  $\phi$ . The first two terms of this equation account for the convection transport due to the fluid motion, where  $U$  and  $V$  are the horizontal and vertical mean velocities. The third and fourth terms represent the diffusion transport of  $\phi$ , where  $\Gamma$  represents the turbulent exchange coefficient. The term on the right-hand side is the source term, and is specific for all equations.

The substitutions for the  $\phi$ ,  $\Gamma$  and  $S_\phi$  terms for each different equation are summarized in table 3.2.

Table 3.1

The Values of the Model Constants

$c_\mu$	$c_D$	$c_1$	$c_2$	$c_3$	$c_4$	$c_{q1}$	$c_{q2}$	$\sigma_K$	$\sigma_\epsilon$	$\sigma_q$
0.09	1.0	1.44	1.92	1.44	0.5	2.38	1.7	1.0	1.3	0.9

Table 3.2

General Form of the Transport Equation

$$\frac{\partial}{\partial x}(\rho U \phi) + \frac{\partial}{\partial y}(\rho V \phi) - \frac{\partial}{\partial x}(\Gamma \frac{\partial \phi}{\partial x}) - \frac{\partial}{\partial y}(\Gamma \frac{\partial \phi}{\partial y}) = S_{\phi}$$

Equation	$\phi$	$\Gamma_{\phi}$	$S_{\phi}$
x-Momentum	U	$\mu_{eff}$	$-\frac{\partial p}{\partial x} + \mu_{eff} \frac{\partial^2 U}{\partial x^2} + \mu_{eff} \frac{\partial^2 V}{\partial x \partial y}$
y-Momentum	V	$\mu_{eff}$	$-\frac{\partial p}{\partial y} + \mu_{eff} \frac{\partial^2 V}{\partial y^2} + \mu_{eff} \frac{\partial^2 U}{\partial x \partial y} - \rho g \beta \Delta T$
Energy	T	$\frac{\mu_t}{\sigma} + \frac{\mu_t}{\sigma_t}$	0
Turbulence kinetic energy	K	$\frac{\mu_{eff}}{\sigma_K}$	$\mu_t G - c_D \rho \epsilon + \rho g \beta \epsilon_4 (qK)^{1/2}$
Turbulence energy dissipation rate	$\epsilon$	$\frac{\mu_{eff}}{\sigma_{\epsilon}}$	$c_{1K}^{\epsilon} \mu_t G - c_2 \rho \epsilon^2 + c_3 c_4 \rho g \beta \epsilon (\frac{q}{K})^{1/2}$
Mean square temperature fluctuation	q	$\frac{\mu_{eff}}{\sigma_q}$	$c_{q1}^{\epsilon} \mu_t \left[ \left( \frac{\partial T}{\partial x} \right)^2 + \left( \frac{\partial T}{\partial y} \right)^2 \right] - c_{q2}^{\epsilon} \rho \frac{\epsilon}{K} q$

where  $G = 2 \left[ \left( \frac{\partial U}{\partial x} \right)^2 + \left( \frac{\partial V}{\partial y} \right)^2 \right] + \left( \frac{\partial U}{\partial y} + \frac{\partial V}{\partial x} \right)^2$

### 3.4 BOUNDARY CONDITIONS

The applicable boundary conditions are specified as follows (see Fig. 3.1):

$U = U_0$ ; $V = 0$	on the moving wall
$U = 0$ ; $V = 0$	on the stationary walls
$T = T_0$ and $T = T_1$	on the lower and upper walls respectively
$\partial T / \partial n = 0$ .	on the vertical sides

### 3.5 NEAR WALL REGIONS

Far from the solid walls, the velocity and temperature gradients are usually not very steep, a moderately finite difference grid gives accurate solutions. However, close to the solid walls, the gradients of the velocity and temperature are much steeper, and therefore a fine grid is needed to obtain accurate results.

#### 3.5.1 Modification of the Momentum Transport Equation

Close to the walls, the momentum transport processes have been modelled through the wall function method [29].

In this method, the nearest-to-wall point  $p$ , as shown in Fig. 3.2, should be sufficiently remote from  $W$ , which lies on the wall, so that the term  $(\rho K^2 l / \mu)_p$  will be much greater than unity. Consequently, the viscous effect will be entirely overwhelmed by the turbulent effect. It is then assumed that

a logarithmic velocity profile prevails in the region between the wall and the node  $p$ , the expression being:

$$\frac{U_p}{(\tau/\rho)_W^{1/2}} = \frac{1}{\kappa} \ln \left( \frac{E y_p (\tau/\rho)_W^{1/2}}{\mu} \right) \quad (3.24)$$

where the subscript  $p$  indicates that the values are those at grid node  $p$ ,  $y_p$  is the distance from the wall, and  $\kappa$  and  $E$  are the log-law constants. Furthermore, in the uniform-shear stress layers, the convection and diffusion can be neglected. It may then be shown from Eq. (3.19) that:

$$\tau_p = \tau_W = c_\mu^{1/2} \rho K \quad (3.25)$$

From Eqs. (3.24) and (3.25), the shear stress can be related to the velocity and the kinetic energy of turbulence through the relation:

$$\tau_p = \frac{\rho \kappa c_\mu^{1/2} K_p^{1/2} U_p}{\ln \left( \frac{E y_p c_\mu^{1/2} \rho K_p^{1/2}}{\mu} \right)} \quad (3.26)$$

### 3.5.2 Modification of the Energy Transport Equation

Following Patankar and Spalding [20], the heat flux near the wall can be expressed as a function of the wall shear stress as follows:

$$(Q/A)_W = \frac{c_p \sqrt{\tau_W \rho} (T_w - T)}{\sigma_t (U_+ + p)} \quad (3.27)$$

where  $\sigma_t$  is the turbulent Prandtl number,

$$U_+ = U/\sqrt{\tau_w/\rho}$$

and  $p$  is a constant.

The value recommended by Spalding and Jayatillaka [35] has been used in this work.

$$\text{i.e. } p = 9.24 \left( \frac{\sigma}{\sigma_t} \right)^{0.75} \quad (3.28)$$

The heat flux can be related to the kinetic energy of turbulence as follows:

$$K = (\tau_w/\rho)/c_\mu^{1/2} \quad (3.29)$$

and hence,

$$\sqrt{\tau_w \rho} = c_\mu^{1/4} \rho K^{1/2}$$

Therefore,

$$(Q/A)_w = \frac{c_\mu^{1/4} c_p \rho K^{1/2} (T_w - T)}{\sigma_t (U_+ + p)} \quad (3.30)$$

### 3.5.3 Modification of the Transport of Dissipation Rate Equation

The rate of dissipation of the kinetic energy of turbulence near the wall  $\epsilon_p$  is fixed according to the hypothesis that the length scale varies linearly with the distance from the wall. Following [2], it is assumed that  $\epsilon_p$  varies according to the following relation:

$$\epsilon_p = \sqrt{(\tau_w/\rho)^3/\kappa Y_p} \quad (3.31)$$

From Eq. (3.29) ,  $\tau_w/\rho = K c_\mu^{1/2}$

Therefore, the expression for  $\epsilon_p$  becomes:

$$\epsilon_p = c_\mu^{3/4} K_p^{3/2}/\kappa Y_p \quad (3.32)$$

#### 3.5.4 Modification of the Transport of the Mean Square Temperature Fluctuation Equation

In the near-wall regions, the generation and dissipation terms in the transport equation for the mean square temperature fluctuation far outweigh the other terms. Thus, from Eq. (3.21), it can be shown that:

$$q = \frac{c_{q1}}{c_{q2}} \frac{K_p \mu t}{\rho \epsilon_p} \left[ \left( \frac{\partial T}{\partial x} \right)^2 + \left( \frac{\partial T}{\partial y} \right)^2 \right] \quad (3.33)$$

CHAPTER 4THE FINITE DIFFERENCE CALCULATION PROCEDURE4.1 INTRODUCTION

In this chapter, the finite difference procedure for the general transport equation, Eq. (3.23), is presented. The finite-difference equations are derived using the control volume integration technique.

The calculation procedure for the general terms is stated in section 4.2, while the source terms are presented in section 4.3. The stability of the final set of algebraic equations in the iterative solution procedure is discussed in section 4.4. Finally, the pressure equation is derived in section 4.5.

4.2 DERIVATION OF THE GENERAL TERMS4.2.1 The Grid Network

In deriving the finite difference equation, the cavity is represented by a rectangular grid network, as shown in Fig. 4.1. The continuous lines are the grid lines and the intersections of the latter are the nodal points. The dotted lines, which lie mid-way between the grid nodes, form the control volume.

The fluid properties ( $\rho$  and  $\mu$ ) and the quantities ( $P$ ,  $T$ ,  $K$ ,  $\epsilon$  and  $q$ ) are computed at each nodal point, while the components of the velocity vector  $U$  and  $V$  are calculated

at the control volume boundaries. Each variable will therefore be at the centre of its control volume.

The physical boundaries (cavity walls) are chosen to coincide with the control volume boundaries, in order to facilitate application of the boundary conditions.

#### 4.2.2 The Derivation Procedure

Since the variables and the control volume have been specified, the transport equation, Eq. (3.23), can be integrated over the corresponding control volume, within which the fluid properties are assumed constant. Thus,

$$\iint_{VOL} \left[ \frac{\partial}{\partial x} (\rho U \phi) + \frac{\partial}{\partial y} (\rho V \phi) - \frac{\partial}{\partial x} \left( \Gamma \frac{\partial \phi}{\partial x} \right) - \frac{\partial}{\partial y} \left( \Gamma \frac{\partial \phi}{\partial y} \right) \right] d(VOL) = \iint_{VOL} S_{\phi} d(VOL)$$

Using Gauss's theorem, the above equation can be written as:

$$\int_S^n \left[ (\rho U \phi - \Gamma \frac{\partial \phi}{\partial x})_e - (\rho U \phi - \Gamma \frac{\partial \phi}{\partial x})_w \right] dy + \int_W^e \left[ (\rho V \phi - \Gamma \frac{\partial \phi}{\partial y})_n - (\rho V \phi - \Gamma \frac{\partial \phi}{\partial y})_s \right] dx - \iint_{VOL} S_{\phi} d(VOL) = 0$$

or, in short form,

$$F_e - F_w + F_n - F_s = \iint_{VOL} S_{\phi} d(VOL) \quad (4.1)$$

where the subscripts e, w, n and s refer to the east, west, north and south boundaries respectively, and

$$F_e = \int_s^n (\rho U \phi - \Gamma \frac{\partial \phi}{\partial x})_e dy$$

$$F_w = \int_s^n (\rho U \phi - \Gamma \frac{\partial \phi}{\partial x})_w dy$$

$$F_n = \int_w^e (\rho V \phi - \Gamma \frac{\partial \phi}{\partial y})_n dx$$

$$F_s = \int_w^e (\rho V \phi - \Gamma \frac{\partial \phi}{\partial y})_s dx$$

The last four equations represent the total flux into the control volume from the east, west, north and south boundaries.

If the transport across the control volume boundary is regarded as one-dimensional, then the flux solution may be expressed as follows [2]:

$$F_s = \rho_s V_s A_s \left[ f_s \phi_s + (1 - f_s) \phi_p \right]$$

where

$$f_s = \exp. (Pe)_s / \left[ \exp(Pe)_s - 1 \right]$$

$$(Pe)_s = \rho_s V_s \Delta y_{ps} / \Gamma_s$$

$$\rho_s = (\rho_s + \rho_p) / 2$$

and

$$\Gamma_s = (\Gamma_s + \Gamma_p) / 2$$

In order to save computing time, the exponential terms are approximated in a simple algebraic form as follows:

For any  $x$ ,

$$\frac{e^x}{e^x - 1} = \begin{cases} \frac{1}{2} \left(1 + \frac{2}{x}\right) & |x| < 2 \\ 1 & x > 2 \\ 0 & x < -2 \end{cases}$$

Using this approximation, the expression for  $f_s$  becomes,

$$f_s = \begin{cases} \frac{1}{2} \left[1 + 2(\text{Pe})_s^{-1}\right] & |(\text{Pe})_s| < 2 \\ 1 & (\text{Pe})_s > 2 \\ 0 & (\text{Pe})_s < -2 \end{cases}$$

By letting  $a_s = \rho_s V_s A_s f_s$

$$c_s = \rho_s V_s A_s$$

$$\text{and } D_s = \Gamma_s A_s / \Delta y_{ps}$$

then  $(\text{Pe})_s$  becomes  $c_s / D_s$ , and the expression for the flux term  $F_s$  is given by:

$$F_s = a_s (\phi_s - \phi_p) + c_s \phi_p \quad (4.2)$$

where

$$a_s = \begin{cases} c_s/2 + D_s & |c_s/2| < D_s \\ c_s & c_s/2 > D_s \\ 0 & c_s/2 < -D_s \end{cases} \quad (4.3)$$

From the definitions of the  $c$ 's and  $D$ 's, it is clear that they represent the convection and diffusion transfer respectively. Consequently, the parameter  $Pe$ , the local Peclet number, is the ratio of the convection to diffusion transfer rate. The  $F$ 's represent the fluxes across the boundaries into or out of the control volume. They are equal to the weighted sum of the convection and diffusion terms, (see Eq. (4.2)).

The three expressions for  $a_s$  in Eq. (4.3) can be represented in one expression as:

$$a_s = \max(|c_s/2|, D_s) + \frac{1}{2} c_s \quad (4.4)$$

Similarly, by following the above procedure, expressions for  $F_e$ ,  $F_w$  and  $F_n$  can be written as:

$$\begin{aligned} F_e &= a_e (\phi_p - \phi_E) + c_e \phi_p \\ F_w &= a_w (\phi_W - \phi_p) + c_w \phi_p \\ F_n &= a_n (\phi_p - \phi_N) + c_n \phi_p \end{aligned} \quad (4.5)$$

with

$$\begin{aligned} a_e &= \max(|c_e/2|, D_e) - \frac{1}{2} c_e \\ a_w &= \max(|c_w/2|, D_w) + \frac{1}{2} c_w \\ a_n &= \max(|c_n/2|, D_n) - \frac{1}{2} c_n \end{aligned}$$

Substitution of the expressions  $F_s$ ,  $F_e$ ,  $F_w$  and  $F_n$ , from Eqs.(4.2) and (4.5), into the conservation equation for the control volume, Eq.(4.1), gives:

$$\phi_p [(a_e + a_w + a_n + a_s) + (c_e - c_w + c_n - c_s)] - (a_e \phi_E + a_w \phi_W + a_n \phi_N + a_s \phi_S) - \iint_{VOL} s_\phi d(VOL) = 0$$

The term  $(c_e - c_w + c_n - c_s)$  represents the net accumulation of mass and, to fulfil continuity conditions, it must be equal to zero. Therefore:

$$\sum_i a_i \phi_i - \phi_p \sum_i a_i + s_{\phi V} = 0 \quad (4.6)$$

where  $\sum_i$  denotes  $\sum_{i=e,w,n,s}$  and  $s_{\phi V} = \iint_{VOL} s_\phi d(VOL)$

the integral of the source term over the control volume.

#### 4.3 THE CALCULATION OF THE SOURCE TERM

The source term for the transport equation of each of the variables is expressed linearly as follows:

$$s_{\phi V} = \iint_{VOL} s_\phi d(VOL) = Sp_1 \phi_p + Su_1 \quad (4.7)$$

where  $Sp_1$  and  $Su_1$  take the following forms:

1. The Transport of U-Momentum Equation

$$Sp_1 = 0$$

$$Su_1 = \iint_{VOL} s_U d(VOL)$$

$$= \iint_{VOL} \left( -\frac{\partial P}{\partial x} + \mu_{eff} \frac{\partial^2 U}{\partial x^2} + \mu_{eff} \frac{\partial^2 V}{\partial x \partial y} \right) dx dy$$

$$= P \Big|_e^w \Delta y + \left( \mu_{eff} \frac{\Delta U}{\Delta x} \right) \Big|_w^e \frac{VOL}{\Delta x} + \left( \mu_{eff} \frac{\Delta V}{\Delta x} \right) \Big|_s^n \frac{VOL}{\Delta y}$$

2. The Transport of V-Momentum Equation

$$Sp_1 = 0$$

$$Su_1 = \iint_{VOL} \left( -\frac{\partial P}{\partial y} + \mu_{eff} \frac{\partial^2 V}{\partial y^2} + \mu_{eff} \frac{\partial^2 U}{\partial x \partial y} + \rho g \beta \delta T \right) dx dy$$

$$= P \Big|_n^s \Delta x + \mu_{eff} \frac{\Delta V}{\Delta y} \Big|_s^n \frac{VOL}{\Delta y} + \left( \mu_{eff} \frac{\Delta U}{\Delta y} \right) \Big|_s^n \frac{VOL}{\Delta x}$$

$$+ \rho g \beta \cdot \delta T \cdot VOL$$

3. The Transport of Kinetic-Energy of Turbulence

$$Sp_1 = -\frac{c_\mu c_D \rho^2 K_p}{\mu_t} \cdot VOL - \rho g \beta c_4 (q/K)^{1/2} \cdot VOL$$

$$Su_1 = \mu_t G \cdot VOL$$

4. The Transport of Energy Dissipation

$$Sp_1 = -c_2 \frac{\rho \epsilon_p}{K_p} \cdot VOL - c_3 c_4 \rho g \beta (q/K)^{1/2} \cdot VOL$$

$$Su_1 = c_1 \frac{\mu_t G \epsilon_p}{K_p} \cdot VOL$$

### 5. The Transport of Mean-Square Temperature-Fluctuation

$$Sp_1 = -c_{q_2} \rho \frac{\epsilon}{K} \cdot \text{VOL}$$

$$Su_1 = c_{q_1} \mu_t \left( \frac{\partial^2 T}{\partial x^2} + \frac{\partial^2 T}{\partial y^2} \right) \cdot \text{VOL}$$

Substituting the general form for the source term, Eq. (4.7), into Eq. (4.6), yields:

$$\sum_i a_i \phi_i - \phi_p \sum_i a_i + Sp_1 \phi_p + Su_1 = 0$$

or

$$\phi_p \left( \sum_i a_i - Sp_1 \right) = \sum_i a_i \phi_i + Su_1 \quad (4.8)$$

#### 4.4 STABILITY OF THE SOLUTION PROCEDURE

The finite difference equations derived in the previous section, Eq. (4.8), are a set of non-linear algebraic equations. For each variable, the coefficients  $a_i$ ,  $Sp_1$  and  $Su_1$  are functions of the other variables. Hence, these equations are solved using an iterative technique, and the stability of the iterative solution is discussed in this section.

Consider a set of algebraic equations of the form:

$$X_i = \sum_{j, j \neq i} (a_{ij} X_j + b_i) \quad (4.9)$$

where  $X_i$  are unknown vectors. If the coefficients  $a_{ij}$  and  $b_i$  are constants, then Eq. (4.9) will be a set of linear algebraic equations which may be solved iteratively to yield stable convergent solutions if  $\sum_{j, j \neq i} |a_{ij}| \leq 1$  for each  $i$ ; and for at least one  $i$ ,  $\sum_{j, j \neq i} |a_{ij}| < 1$ . In the case where Eq. (4.9) is non-linear, i.e.  $a_{ij}$  and  $b_i$  are not constants, the above conditions are necessary, but they may not be sufficient for convergence [13].

Comparison of Eqs. (4.8) and (4.9) yields the following,

$$a_{ij} = \sum_i \frac{a_i}{\sum_j a_j - Sp_1}$$

Therefore, in order for Eq. (4.8) to satisfy the conditions for convergence, the following conditions must be met:

$$\sum_i \frac{a_i}{\sum_j a_j - Sp_1} \leq 1$$

or

$$\sum_i |a_i| \leq \sum_i a_i - Sp_1 \quad (4.10)$$

Since, from Eq. (4.3), the coefficients  $a_{ij}$  are always positive, then Eq. (4.10) will be satisfied if  $Sp_1 \leq 0$ . In the last

section it was shown that  $Sp_1$  is always zero or negative. The conditions for convergence will then be satisfied and the iterative procedure becomes stable. However, during the iteration procedure, the coefficients may equal zero. This will lead to singularities in the finite-difference equations. To avoid this, an additional false term,  $S_{\text{false}}$ , is added to Eq. (4.8), where

$$S_{\text{false}} = \max\left(\sum_i c_i, 0.0\right) \times (\phi_p' - \phi_p) \quad (4.11)$$

and  $\phi_p'$  is the value from the previous iteration. It should be noted that the false term will not affect the final results for a converging solution, because at convergence  $\phi_p' = \phi_p$ . Adding Eqs. (4.11) and (4.8) yields:

$$\phi_p \left(\sum_i a_i - Sp_1\right) = \sum_i a_i \phi_i + Su_1 + \max\left(\sum_i c_i, 0.0\right) (\phi_p' - \phi_p)$$

and the final form of the finite-difference equations becomes,

$$\phi_p Ap = \sum_i a_i \phi_i + Su \quad (4.12)$$

where  $Su = Su_1 + \max\left(\sum_i c_i, 0.0\right) \phi_p'$

$$Sp = Sp_1 - \max\left(\sum_i c_i, 0.0\right)$$

and  $Ap = \sum_i a_i - Sp$

Since  $S_p$  is always negative, the iteration procedure for the final form of the finite-difference equations will be stable.

#### 4.5 DERIVATION OF THE PRESSURE EQUATION

In this section, the pressure equation is derived by the use of the continuity equation.

To satisfy the mass conservation in each control volume, the net accumulation of mass inside each control volume is calculated. The local pressure is adjusted to modify the fluid flow velocities in order to conserve the mass in the control volume.

The procedure involves the definition of a new dependent variable called the pressure correction  $\Delta P$ , so that  $P = P' + \Delta P$  where  $P'$  is the estimated value of pressure resulting from the previous iteration, and  $P$  is the actual local pressure.

An equation containing the pressure correction term  $\Delta P$  can be obtained by substituting  $P' + \Delta P$  for  $P$  in the source term of the U-momentum equation, and then subtracting the latter from the U'-equation resulting from the estimated value of  $P$ , i.e.  $P'$ . This gives

$$\Delta p (U_p - U'_p) = \sum_i a_i (U_i - U'_i) + \Delta y (\Delta P_w - \Delta P_e)$$

For converging results,  $U_i = -U'_i$  ( $i = E, W, N, S$ ) it follows that:

$$U_p = U'_p + (\Delta P_w - \Delta P_e) DU_p \quad (4.13)$$

where  $DU_p = \Delta y / \Delta p$

$$\text{Similarly, } V_p = V'_p + (\Delta P_s - \Delta P_n) DV_p \quad (4.14)$$

where  $DV_p = \Delta x / \Delta p$

In the same manner, the expressions for all the surrounding nodes become:

$$\begin{aligned} U_E &= U'_E + (\Delta P_p - \Delta P_E) DU_E \\ U_W &= U'_W + (\Delta P_W - \Delta P_p) DU_W \\ V_N &= V'_N + (\Delta P_p - \Delta P_N) DV_N \\ V_S &= V'_S + (\Delta P_S - \Delta P_p) DV_S \end{aligned} \quad (4.15)$$

From the continuity equation, it follows that:

$$(\rho UA)_W - (\rho UA)_E + (\rho VA)_S - (\rho VA)_N = 0 \quad (4.16)$$

Substituting Eq. (4.15) into Eq. (4.16) yields:

$$\begin{aligned} & [(\rho ADU)_E + (\rho ADU)_W + (\rho ADV)_N + (\rho ADV)_S] \Delta P_p \\ &= (\rho ADU)_E \Delta P_E + (\rho ADU)_W \Delta P_W + (\rho ADV)_N \Delta P_N \\ & \quad + (\rho ADV)_S \Delta P_S - \sum_i c_i = 0 \end{aligned} \quad (4.17)$$

where  $\sum_i c_i$  is the net mass accumulation.

The equation for  $\Delta P$ , Eq.(4.17), follows the general form of the algebraic equation, Eq.(4.12):

$$\phi_p \left( \sum_i a_i - S_p \right) = \sum_i a_i \phi_i + S_u \quad (4.12)$$

with  $\phi = \Delta P$  ;  $a = \rho ADU$  ;  $S_p = 0$  and  $S_u = 0$ .

It can then be solved using the same algorithm.

Having obtained the solution for  $\Delta P$ , the velocity components can then be updated using Eqs.(4.13) and (4.14).

CHAPTER 5COMPUTATIONAL PROCEDURE5.1 INTRODUCTION

In this chapter, a discussion of the grid design is outlined in section 5.2, followed by a presentation of the method used for iterative solutions of the algebraic equations in section 5.3. The selection of the under-relaxation factor is examined in section 5.4. Finally, the construction of the computer program is discussed in section 5.5. A complete listing of the computer program with a sample output print-out is included in Appendix B.

5.2 GRID DESIGN

The accuracy of the solution and the convergence characteristics depend on the grid size and distribution for any numerical method including those which involve discrete domains.

Close to the walls, the gradients of the variables are relatively large. Consequently, a non-uniform grid, with decreasing mesh size towards the walls was used.

In most of the computer runs in the present work an  $18 \times 18$  grid system was employed.

5.3 SOLUTION OF THE ALGEBRAIC EQUATION

The finite-difference equation previously derived, Eq. (4.12), together with the boundary conditions, constitute,

as already stated, a system of coupled non-linear simultaneous algebraic equations. The solution procedure for these equations is discussed in this section.

If  $N_I$  and  $N_J$  are the number of grid lines in the horizontal and vertical directions respectively, there will be an  $N_I \times N_J$  grid mesh. Subtracting the physical boundaries, then the number of algebraic equations for each of the seven variables  $U$ ,  $V$ ,  $\Delta P$ ,  $T$ ,  $K$ ,  $\epsilon$  and  $q$  will be  $(N_I-2) \cdot (N_J-2)$ . If the entire solution for all the variables taken together is considered, then a total of  $7(N_I-2)(N_J-2)$  simultaneous equations need to be solved.

It is impractical and computationally expensive to solve these equations using matrix inversion methods because of the enormous size of the coefficient matrix. To simplify the problem, the variables should be solved separately, following the cyclic repetition of the following steps:

1. Initial values  $U'$ ,  $V'$ ,  $P'$ ,  $T'$ ,  $K'$ ,  $\epsilon'$  and  $q'$  are assumed for all the variables.
2. The turbulent viscosity,  $\mu_t$  is calculated.
3. The coefficients of the U-momentum equation are assembled according to the guessed values and then solved for  $U$ .
4. The coefficients of the V-momentum equation are assembled according to the guessed values and then solved for  $V$ .
5.  $\Delta P$  is calculated, followed by the calculation of  $P$  and then updated values of  $U$  and  $V$  according to Eqs. (4.13) and (4.14).

6. The coefficients of the energy equation are assembled and the solution of  $T$  is obtained. Similarly, the calculations of  $K$ ,  $\epsilon$  and  $q$  follow the same procedure.
7. The modified variables are used as improved guesses and steps 2 to 6 are repeated until convergence is achieved.

Using this iterative procedure (steps 2 - 6), only the equations for each variable need to be solved simultaneously and consequently the number of simultaneous equations to be solved is reduced from  $7(NI-2) \cdot (NJ-2)$  to  $(NI-2) \cdot (NJ-2)$ .

Now, in order to solve  $(NI-2) \cdot (NJ-2)$  simultaneous equations, matrix inversion techniques may be employed. However, as previously stated, this procedure is expensive because of the large amount of computing time required.

In the present study, the set of  $(NI-2) \cdot (NJ-2)$  simultaneous equations is solved using the tridiagonal matrix algorithm method (TDMA), in which a set of equations, each with three unknowns in a particular order (except the first and last equations, which have only two unknowns due to the specification of the boundary conditions), may be solved sequentially. The values at grid nodes along a vertical grid line  $i$  (values at  $N$ ,  $p$  and  $s$  for each point  $p$ ) are considered as unknown, whereas those at each  $E$  and  $W$  neighbours, using the values from the previous iteration, are taken to be known (see Fig.5.1). The tridiagonal matrix algorithm method is then applied to this grid line  $i$ .

Eq. (4.12) may be recalled as follows:

$$\underline{A_p} \phi_p = \underline{a_n} \phi_N + \underline{a_s} \phi_S + (\underline{a_e} \phi_E + \underline{a_w} \phi_W + Su) \quad (5.1)$$

with the underlined quantities assumed to be known. This will result in equations with three unknowns, except for the node adjacent to the two boundaries. By imposing the boundary conditions, there will be two unknowns instead of three per equation. Therefore, for each line there exist (NJ-2) equations with (NJ-2) unknowns which can be solved using the tridiagonal matrix algorithm.

In this way, it is possible to traverse all the vertical grid lines sequentially starting from left to right through the entire mesh representing the cavity. A large number of traverses is required to obtain exact solutions for all the  $\phi$  values. However, since the coefficients of the algebraic equation in a given iteration are only tentative and must be updated before the next iteration, then it is not essential to obtain an accurate solution. Consequently, two to five traverses are sufficient. In the present work, following the recommendation of Gosman et al. [2], three traverses were used for the variables U, V, T, K,  $\epsilon$  and q, whereas five traverses were used for  $\Delta P$ .

A detailed description of the TDMA is presented in Appendix A [36].

#### 5.4 UNDER-RELAXATION FACTOR

Divergence often occurs in the computation if the difference in magnitude of the variables between successive iterations is large. In order to avoid this, the under-relaxation numerical technique is applied.

Assuming that  $\phi_p^{n-1}$  and  $\phi_p^n$  are the values of  $\phi_p$  computed in the (n-1)th and n-th iterations respectively, then, from the under-relaxation method, the value actually used in the following iteration,  $\phi_p^n$ , is given by:

$$\phi_p^n = \text{URF} \cdot \phi_p^n + (1 - \text{URF}) \phi_p^{n-1} \quad (5.2)$$

where URF is the under-relaxation factor which is a real number between 0 and 1.

Since, for a value of URF equal to unity, one can see from Eq. (5.2) that  $\phi_p^n = \phi_p^n$  and for URF = 0,  $\phi_p^n = \phi_p^{n-1}$ , then, the under-relaxation factor adjusts the degree of advancement of the variable  $\phi$  in the iteration process.

The calculation of  $\phi_p^n$  and its modification using the under-relaxation factor takes a large amount of computer time, particularly for a grid mesh consisting of a large number of nodes. To avoid this,  $\phi_p^n$  is calculated directly as follows.

From chapter 4, the equation which needs to be solved is Eq. (4.12):

$$\phi_p^n = (\sum_i a_i \phi_i + Su) / Ap \quad (4.12)$$

Substitution of  $\phi_p^n$  from Eq. (4.12) into Eq. (5.2) gives:

$$\phi_p^n = (\sum_i a_i \phi_i + Su) (URF / Ap) + (1 - URF) \phi_p^{n-1}$$

and upon arranging, yields:

$$\phi_p = (\sum_i (a_i \phi_i) + Su_2) / Ap_2 \quad (5.3)$$

where  $Ap_2 = Ap / URF$

$$Su_2 = Su + (1 - URF) Ap_2 \phi_p^{n-1} \quad (5.4)$$

Eqs. (5.3) and (4.12) are of the same form. Therefore, by computing the coefficients  $a_i$ ,  $Su$  and  $Ap$ , and modifying them using Eq. (5.4), the  $\phi$ 's can be under-relaxed directly by solving the equation for  $\phi_p^n$  following the normal procedure.

#### 5.5 SUMMARY OF THE COMPUTER PROGRAM

A flow chart of the computational procedure is shown in Fig. 5.2. The computer program is structured as follows:

1. The grid distribution is set up.
2. Subroutine INIT computes all the geometric quantities for each of the (NI-2) (NJ-2) nodes and stores them in arrays. It then initializes all the variables.

3. Subroutine PROP calculates the turbulent viscosity based on the assumed values of the kinetic energy of turbulence and the dissipation rate.
4. The initial conditions and the prescribed non-iterative boundary conditions are computed.
5. A complete cycle of iteration is performed by calling subsequently the subroutines CALCU, CALCV, CALCP, CALCT; CALCTE, CALCED and CALCQE which calculate the updated distributions of the variables  $U$ ,  $V$ ,  $\Delta P$ ,  $T$ ,  $K$ ,  $\epsilon$  and  $q$  for all the nodes of the grid distribution.
6. Based on the updated values of the kinetic energy of turbulence and the dissipation rate, the turbulent viscosity is recalculated by calling the subroutine PROP.
7. The results are printed out after each iteration by calling the subroutine PRINT.

The iteration procedure terminates automatically if the computer time or the number of iterations exceeds the prescribed values. After the total number of iterations required (MAXIT) is performed, the mean Nusselt number is then calculated.

Since the solution procedure for all the variables follows the same steps (see Eq.5.3), only the procedure for the solution of the U-momentum equation, i.e. Subroutine CALCU is indicated in detail.

The subprogram CALCU computes the convective and diffusive terms, the TDMA coefficients, according to Eqs.(4.3)

and (4.5), and then computes the source terms  $S_p$  and  $S_u$  for the entire field. The boundary conditions are prescribed by calling the subprogram MODU. The coefficients are under-relaxed using the method prescribed in section 5.4. The line-by-line solution procedure using the TDMA is finally performed by calling the subprogram LISOLV.

The number of traverses of line-solution is represented as NSWPU in the flow chart shown in Fig. 5.3. The complete program is listed in Appendix B, together with the corresponding output listing. Additional information on some aspects of this program can be found in Ref. [2].

## CHAPTER 6

### DISCUSSION OF RESULTS

#### 6.1 INTRODUCTION

A numerical study of the flow, heat transfer and turbulence characteristics of a turbulent recirculatory flow affected by buoyancy forces in a square cavity, was performed using the finite difference equations derived in chapter 4. The solution was obtained using the numerical procedure described in chapter 5. The results obtained were for water ( $Pr = 3$ ) and liquid sodium ( $Pr = 0.01$ ). The Reynolds number is varied from  $10^2$  to  $10^6$ , while the mixed convection parameter is between 0 and 2. The aspect ratio ( $E = d/h$ ) of the cavity is taken to be unity.

The flow characteristics are presented in section 6.2 in the form of a velocity distribution. The distribution is given by vectors, which indicate the magnitude and direction of the nodal velocity. In section 6.3, the temperature fields are represented by isothermal lines. A discussion of the heat transfer characteristics is outlined in section 6.4. Finally, the turbulence characteristics are discussed in section 6.5.

#### 6.2 FLOW DISTRIBUTION

##### 6.2.1 The Effects of Reynolds Number

###### For Water of $Pr = 3$

The effects of Reynolds number on the velocity distribution are illustrated in Figs. 6.1a through 6.1c. At low Reynolds

numbers, as shown in Fig.6.1a for  $Re = 1.3 \times 10^2$ , the flow is characterized by three eddies, a primary eddy occupying the centre core, and two secondary eddies located at the upper corners. The formation of the secondary eddies is due to the adverse pressure gradient at the corners. The kinetic energy of the flow, which passes through the corners, is insufficient to overcome the adverse pressure. When the Reynolds number is increased, as shown in Fig.6.1b, the upstream corner eddy disappears at a value of  $Re = 1.3 \times 10^3$ . With further increase of the Reynolds number, the downstream corner eddy shrinks in size, and it disappears at Reynolds numbers greater than  $6 \times 10^4$ . Fig.6.1c shows that at  $Re = 10^5$ , the flow consists of one primary eddy, since the flow passing along the corners has a kinetic energy high enough to overcome the adverse pressure gradient and consequently prevents the appearance of the corner eddies.

The results of Nallasamy and Prasad [15] showed that the downstream secondary eddy vanishes at  $Re = 3 \times 10^4$ , while in the present results it disappears at Reynolds numbers greater than  $6 \times 10^4$ . The difference may be explained by the fact that turbulence is considered in the present computations and thus more momentum is diffused from the higher velocity fluid flowing along the cavity sides. As a result of this, the stream possesses insufficient kinetic energy to impede the formation of a secondary eddy.

The behaviour of the primary eddy centre was studied by tracing the location of this centre as a function of Reynolds number. As the Reynolds number increases, the centre of the primary eddy tends to move upstream towards the centre of the cavity as shown in Fig.6.2. The same tendency was observed by Nallasamy and Prasad [15]. Their results, as shown in Fig.6.2 by the dotted line, were obtained for a cavity with a moving top wall.

For Liquid Sodium of Pr = 0.01

For liquid sodium, the effects of Reynolds number on the flow patterns are illustrated in Figs.6.3a, b and c. At Reynolds number of  $10^2$ , the flow field consists of a primary eddy with two corner eddies. This is shown in Fig.6.3a. At the higher Reynolds number of  $5 \times 10^3$ , as shown in Fig.6.3b, the upstream corner eddy disappears with the existence of the downstream one. In Fig.6.3c, where  $Re = 10^6$ , the flow pattern shows only one primary eddy.

6.2.2 The Effects of Buoyancy Forces

For Water of Pr = 3

The effects of buoyancy forces on the flow patterns are illustrated in Figs.6.4a, b and c for Reynolds number of  $8.4 \times 10^4$ . In the absence of buoyancy forces, where  $Gr/Re^2 = 0$  as shown in Fig.6.4a, no secondary eddy appears, since at this Reynolds number, as indicated earlier, the flow consists of one primary eddy. The secondary eddy is present both for

$Gr/Re^2 = 1$  and for  $Gr/Re^2 = 2$  in Figs.6.4b and c, respectively.

Fluid from colder regions of the top wall will tend to flow downwards in the direction of the left wall (from A to B) and warm fluid from B will flow along the top wall (to A) enhancing the secondary eddy (Figs.6.4b and c). Computations indicated the presence of a secondary eddy up to  $Re = 2 \times 10^5$  for  $Gr/Re^2 = 1$  and up to  $Re = 10^6$  for  $Gr/Re^2 = 2$ .

For Liquid Sodium of  $Pr = 0.01$

The computations for  $Pr = 0.01$  showed that the effects of buoyancy forces are similar to that for  $Pr = 3$ .

The effects of buoyancy forces on the velocity distribution examined for  $Pr = 3$  and  $0.01$  were at high Reynolds numbers, at which values the upstream secondary eddy no longer exists. In order to investigate the effects of buoyancy forces at low Reynolds numbers, a hypothetical fluid with high viscosity was examined.

In the absence of buoyancy forces, as shown in Fig.6.5a, the flow consists of a primary eddy and two secondary eddies. With the influence of buoyancy forces, as shown in Fig.6.5b, the upstream corner eddy does not practically change, while the downstream one increases significantly and occupies most of the upper half of the cavity.

The effects of buoyancy forces on the movement of the centre of the primary eddy was observed. This was found to be a downwards movement of the centre.

### 6.3 TEMPERATURE DISTRIBUTION

#### 6.3.1 The Effects of Reynolds Number

For Water of  $Pr = 3$

The isotherms for  $Pr = 3$  are given for different Reynolds numbers in Figs. 6.6a and b. At low Reynolds number,  $Re = 1.3 \times 10^2$  as shown in Fig. 6.6a, the temperature distribution is affected by both conduction and convection with the effect of convection being relatively higher. As the Reynolds number increases to  $Re = 1.3 \times 10^3$ , the transport of heat by convection dominates and the development of a core of constant temperature is obtained. This is shown in Fig. 6.6b.

The temperature profiles along the vertical centre-line, horizontal centre-line, right side wall and left side wall are illustrated in Figs. 6.7a, b, c and d respectively. As shown in Fig. 6.7a, for low Reynolds numbers, a stratification of the temperature is observed, which reflects the predominance of conduction transfer. With increasing Reynolds number, the convection dominates and the stratification decreases until a core of constant temperature is obtained at high Reynolds numbers. Further increase of Reynolds number leads to a decrease of the core temperature.

The temperature profile along the horizontal centre-line is represented in Fig. 6.7b. It is also noted that, as the Reynolds number increases, the temperature decreases with

decreasing stratification. On the right and left side walls, the temperature profiles are illustrated in Figs. 6.7c and d. As expected, the temperature of the right side wall is lower than that of the left side wall.

For Liquid Sodium of  $Pr = 0.01$

For liquid sodium of  $Pr = 0.01$ , the Peclet number ( $Pe = Re \cdot Pr$ ) is small for small Reynolds numbers ( $Re < 10^3$ ) and the heat is transmitted mostly by conduction. This is shown in Fig. 6.8a for  $Re = 10^2$ ,  $5 \times 10^2$ , and  $10^3$  where the isotherms differ slightly from the case of pure conduction where they are horizontal.

At  $Re = 8 \times 10^3$ , as shown in Fig. 6.8b, the temperature field is affected by both conduction and convection. As the Reynolds number increases to  $Re = 5 \times 10^5$ , the convection effect dominates and a core of constant temperature is obtained, as shown in Fig. 6.8c.

6.3.2 The Effects of Buoyancy Forces

For Water of  $Pr = 3$

The temperature profiles along the horizontal centre-line and at the top wall are represented in Fig. 6.9a, for flows without the influence of buoyancy forces and for those with buoyancy at  $Gr/Re^2 = 1$  and  $Gr/Re^2 = 2$ . At the horizontal centre-line, the temperature rises with the influence of buoyancy due to decrease of the convection effect. The decrease in convection also causes an enhancement of the stratification

in the right hand side of the cavity with increasing  $Gr/Re^2$  ratio. The left hand side of the cavity exhibits less stratification with increasing  $Gr/Re^2$  ratio. This is due to the relatively lower temperature fluid flowing downwards as a result of the growing downstream secondary eddy.

In Fig.6.9b, the temperature profiles along the vertical centre-line and left and right walls are illustrated, indicating increase of temperature with buoyancy. It is also observed that the stratification increases and is more pronounced in the upper half of the cavity.

#### For Liquid Sodium of $Pr = 0.01$

The influence of the buoyancy forces on the temperature distribution corresponding to  $Re = 10^3$ , with and without the buoyancy forces, is represented in Fig.6.10. The continuous lines represent the case without buoyancy forces, while the dotted lines represent that with buoyancy forces. Since the circulation of the primary eddy is low due to the influence of the buoyancy forces, as stated in section 6.2, the convection transport of energy decreases. Therefore, the isotherms tend to be similar to those for pure conduction.

#### 6.4 THE HEAT TRANSFER CHARACTERISTICS

The variation of the mean Nusselt number,  $\overline{Nu}$ , along the top wall is plotted against the Reynolds number in Figs.6.11a and b. It is shown in Fig.6.11a, for liquid sodium ( $Pr = 0.01$ ), that the Nusselt number differs slightly from unity. The high

thermal conductivity of the liquid sodium causes the heat transfer at low Reynolds numbers to be unaffected by convection. However, for water ( $Pr = 3$ ), the mean Nusselt number is higher than unity and it increases with increasing Reynolds number. The variation of Nusselt number with Reynolds number is fitted by the following correlation,

$$\overline{Nu} = 1.29 Re^{0.313} \quad \text{for } 10^2 \leq Re \leq 2.5 \times 10^3.$$

This result agrees reasonably with the data obtained by Grand et al. [1] for this range of Reynolds numbers.

For Reynolds numbers in the range  $3 \times 10^3 - 8 \times 10^4$ , as shown in Fig. 6.11b, the variation of the Nusselt number is fitted by the following relation:

$$\overline{Nu} = 1.564 Re^{0.287} \quad \text{for } 3 \times 10^3 \leq Re \leq 8 \times 10^4$$

Further increase of Reynolds number does not significantly change the mean Nusselt number.

The influence of buoyancy forces is also illustrated in Fig. 6.11b. A decrease of the mean Nusselt number with the increase of the mixed-convection parameter,  $Gr/Re^2$ , is observed. There is an approximately 10% decrease in the Nusselt number for the ratio of  $Gr/Re^2 = 1$ , and about a 20% decrease for  $Gr/Re^2 = 2$ .

### 6.5 TURBULENCE CHARACTERISTICS

A discussion of the effect of Reynolds number and buoyancy forces on the turbulence parameters  $K$ ,  $\nu_{eff}$  and  $q$  is presented in this section.

The maximum turbulent kinetic energy versus Reynolds number is shown in Fig.6.12. Increasing Reynolds number gives rise to an increase in the turbulent kinetic energy because of the increased fluctuating velocities. In Fig.6.13, the maximum effective viscosity is plotted against the Reynolds number. It increases with increasing Reynolds number. The value of the maximum turbulent viscosity is equal to 10 times its molecular value at  $Re = 10^4$ , and it reaches  $0.5 \times 10^3$  times the molecular value at  $Re = 10^6$ . This leads to the importance of considering the flow in the cavity for high Reynolds numbers as a turbulent flow.

The effect of buoyancy forces on the turbulent kinetic energy is illustrated in Fig.6.14. The local values of  $K$  on two vertical lines with and without buoyancy effect is represented. The maximum value of the turbulent kinetic energy occurs at the moving wall and decreases with increasing distance from the moving wall. The buoyancy effect is represented by curves 1b and 2b at  $X = 0.8$  and  $X = 0.2$  from the left side wall respectively. It reduces the value of the turbulent kinetic energy because the buoyancy forces tend to dampen the fluctuating velocities. It may also be noted that the decrease of  $K$  values due to buoyancy downstream, as shown by curve 2b, exceeds that upstream, as shown by curve 1b.

The influence of buoyancy forces on the effective viscosity on two vertical lines is shown in Fig.6.15. Curves 1a, b represent the effective viscosity profiles in the upward moving stream at a distance of  $X = 0.8$  from the left side wall, without and with buoyancy effect respectively. Curve 1a indicates that the viscosity decreases with increasing distance from the moving wall. It then increases in the middle of the cavity and finally decreases at the top wall. The variation of the effective viscosity downstream at distance  $X = 0.21$  from the left side wall is represented by curves 2a, b without and with buoyancy force respectively. Curve 2a follows a similar variation to curve 1a. It is also shown that the buoyancy effect, represented by curves 1b and 2b, decreases the effective viscosity, since it decreases the kinetic energy of turbulence.

The local value of the mean square temperature fluctuation on two vertical lines is represented in Fig.6.16. Since the value of the mean square temperature fluctuation depends on the temperature gradient as well as the convection and diffusion transfer, it follows that near the wall, where high temperature gradients occur, higher values of the mean square temperature fluctuation are observed. The profiles of the two curves show an agreement with the observed temperature gradient in the fluid.

CHAPTER 7CONCLUSIONS AND SUGGESTIONS7.1 CONCLUSIONS

A turbulence model was derived based on the K- $\epsilon$  two equation model in order to study the effects of buoyancy forces on the transport of momentum and energy for a turbulent flow in a rectangular cavity. The results obtained lead to the following conclusions:

i) The turbulent viscosity obtained by employing the present model is significant for Reynolds numbers greater than  $10^3$ . Therefore, the use of the turbulence model to compute high Reynolds number cavity flows is fully justified.

ii) For low Reynolds numbers, the flow consists of a primary eddy and two secondary eddies. The upstream corner eddy first disappears at Reynolds numbers greater than  $1.3 \times 10^3$ , followed by the disappearance of the downstream eddy at Reynolds numbers greater than  $6 \times 10^4$ . This study observed the presence of the downstream secondary eddy for higher Reynolds numbers than those based on the Navier-Stokes equations.

iii) The buoyancy forces enhance the downstream secondary eddy. The present results indicated the presence of a secondary eddy up to  $Re = 10^6$  for  $Gr/Re^2 = 2$ .

iv) Stratification of the temperature distribution is obtained for low Reynolds numbers; with further increase of the Reynolds number, a core of constant temperature is observed.

v) The buoyancy forces increase the temperature on both vertical and horizontal centre-lines of the cavity for the range of  $Re = 10^4 - 10^6$ . The stratification is increased on the right side of the cavity and decreased on the left.

vi) The mean Nusselt number increases with increasing Reynolds number up to  $Re = 6 \times 10^4$ . The buoyancy forces act to decrease the mean Nusselt number.

vii) Turbulence characteristics show an increase of the turbulence kinetic energy and effective viscosity with increasing Reynolds numbers. The effective viscosity and turbulence kinetic energy are decreased by buoyancy effects. The square mean fluctuating temperature exhibits high values for high temperature gradients in the fluid. ✓

## 7.2 SUGGESTIONS FOR FURTHER RESEARCH

i) The results obtained in this work were for a cavity of an aspect ratio of 1; further study is suggested for different aspect ratios, to investigate the effect of the latter on the flow configuration.

ii) Further work is required in order to assess the values of the model constants for application to the flow of liquid sodium.

iii) The buoyancy affected turbulent flow has important applications, and further development of the present model could extend these considerably.

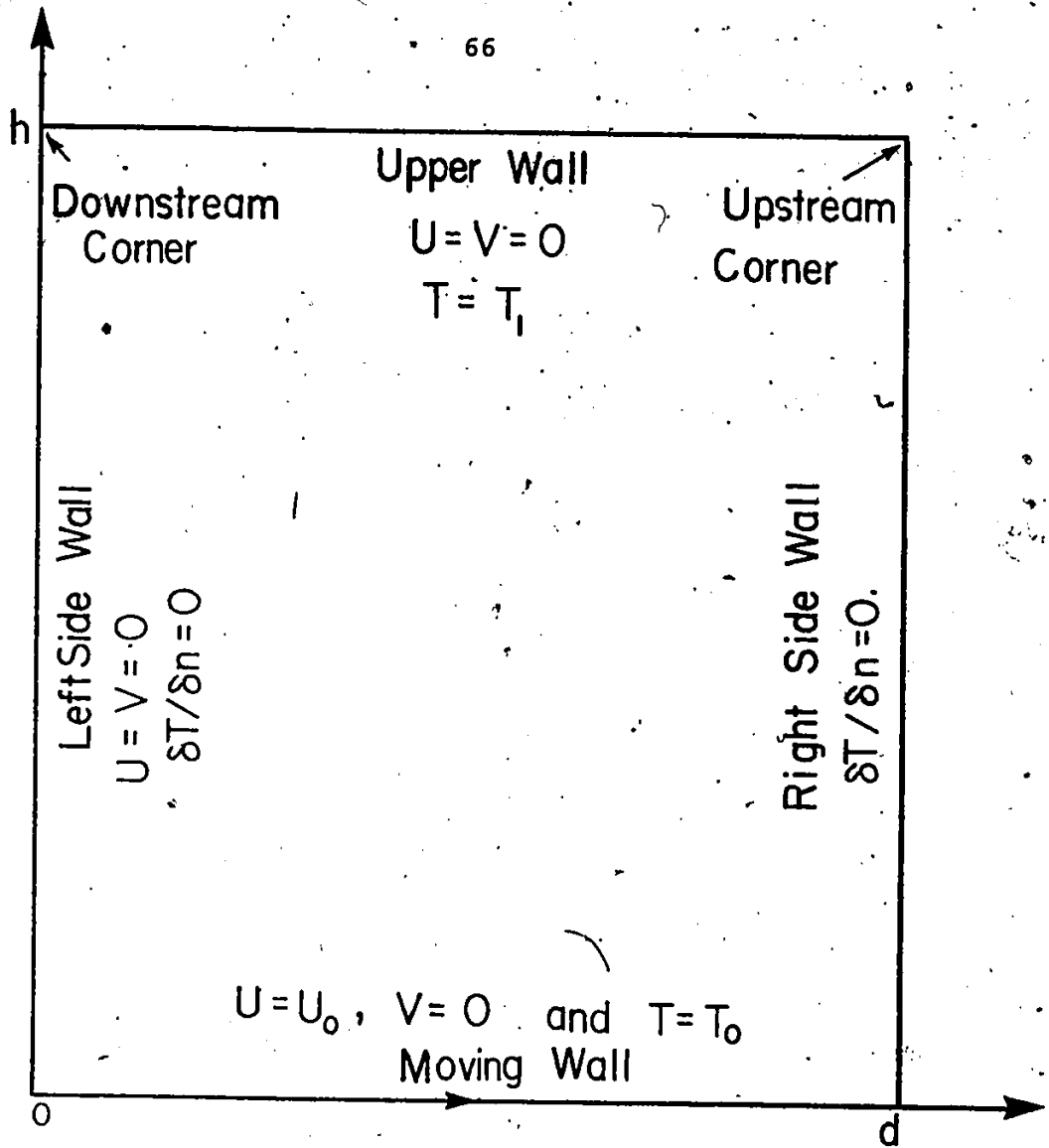


Fig.3.1 Physical Model

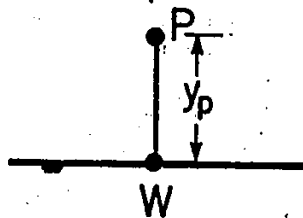


Fig.3.2 Near Wall Region

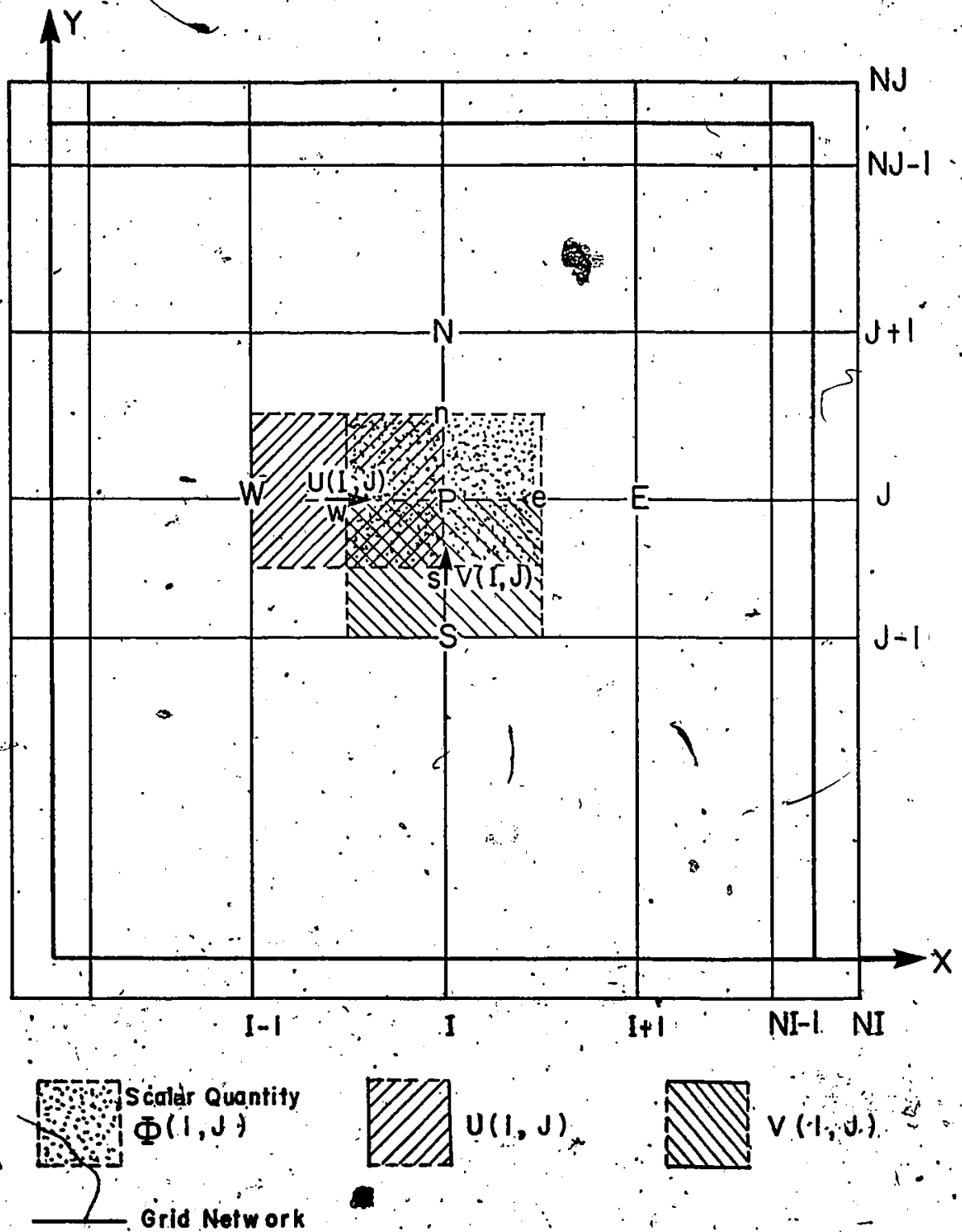


Fig.4.1 Grid Network

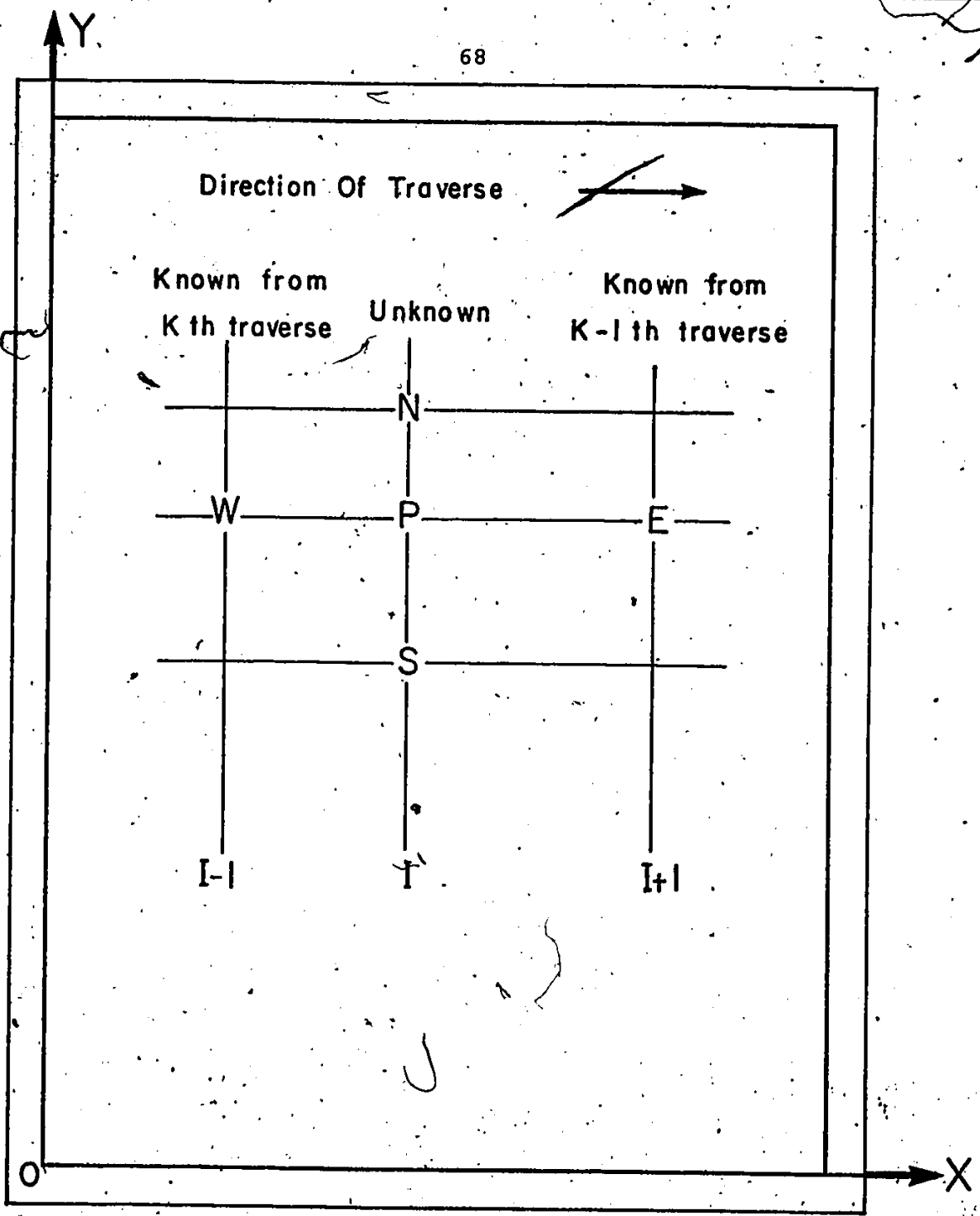


Fig.5.1 Line Iteration Procedure

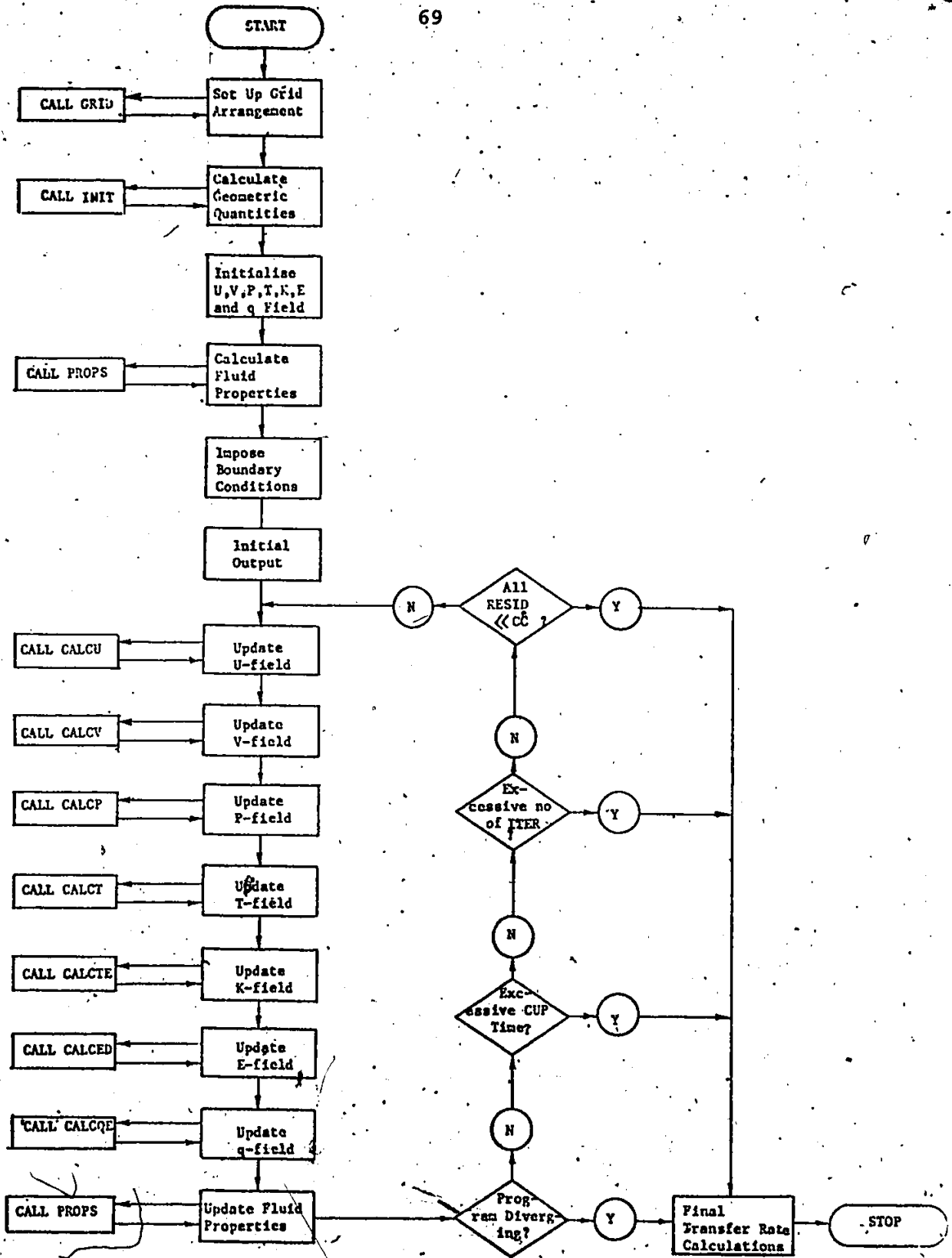


Fig.5.2 Computational Flow Chart: Main Program

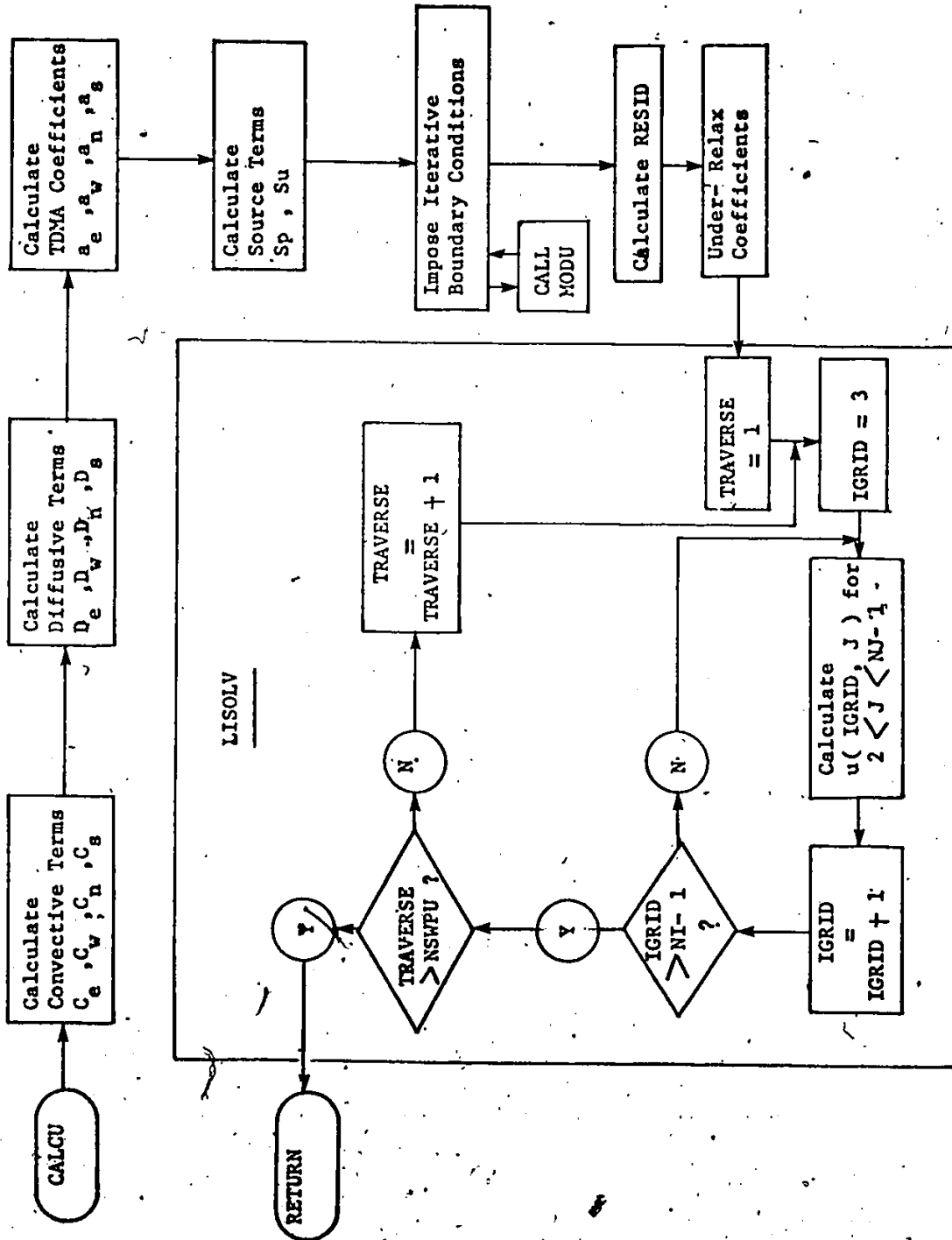


Fig.5.3 Computational Flow Chart: Subroutine CALCU

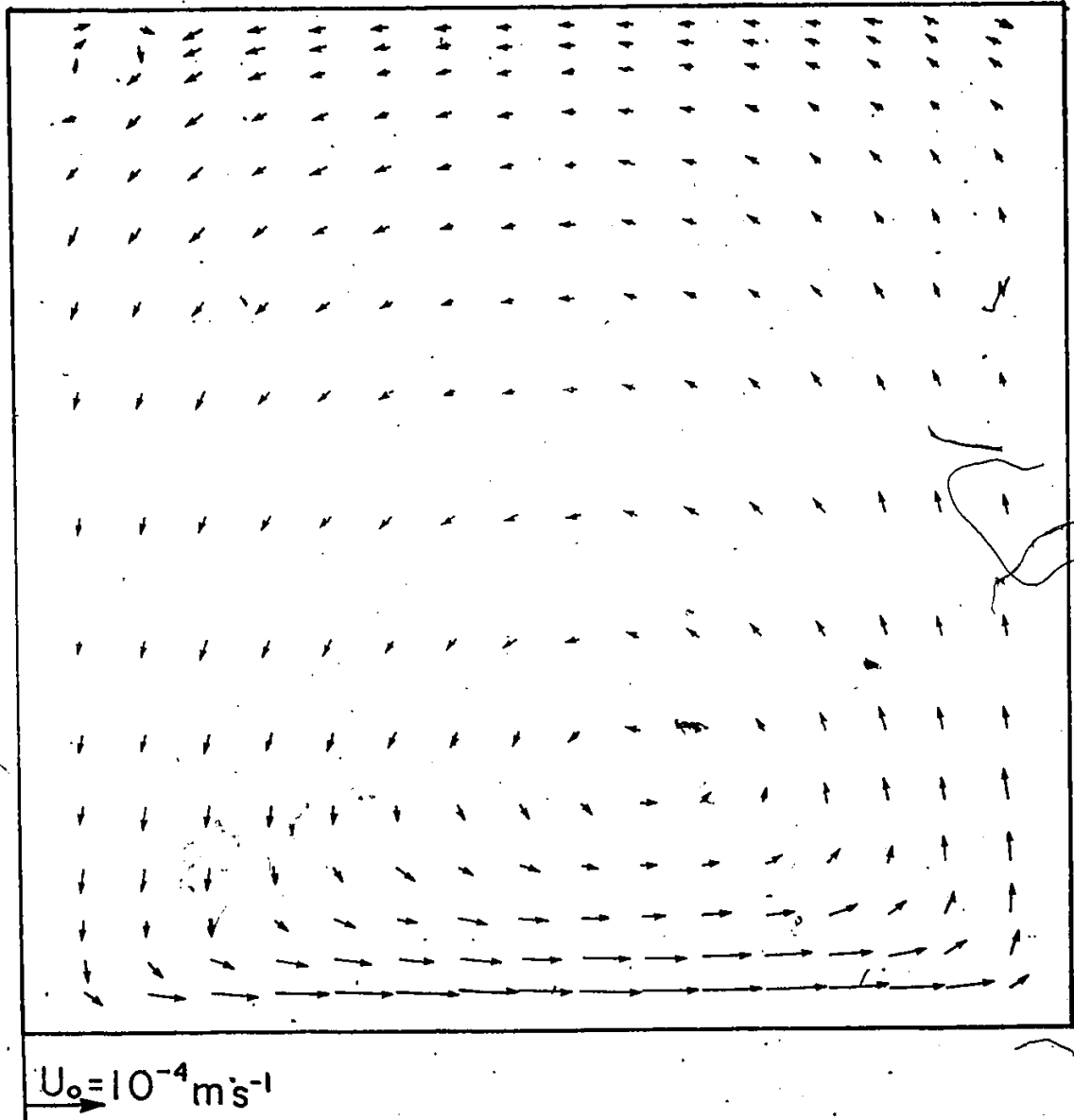
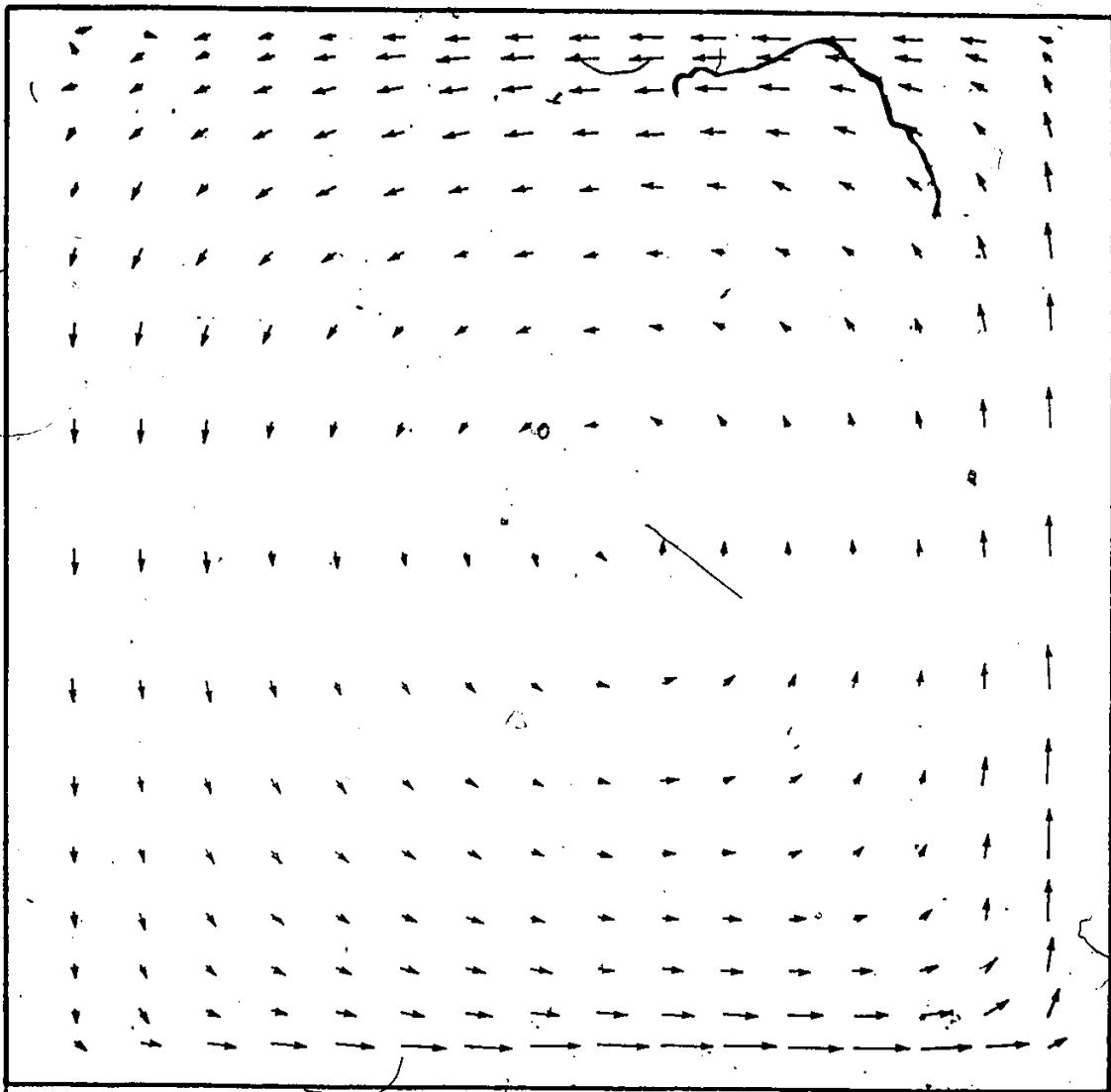


Fig. 6.1a Velocity Distribution

$$\text{Re} = 1.3 \times 10^2, \text{Pr} = 3, \text{Gr}/\text{Re}^2 = 0$$



$U_0 = 10^{-2} \text{ m s}^{-1}$

Fig.6.1b Velocity Distribution

$Re = 1.3 \times 10^3, Pr = 3, Gr/Re^2 = 0$

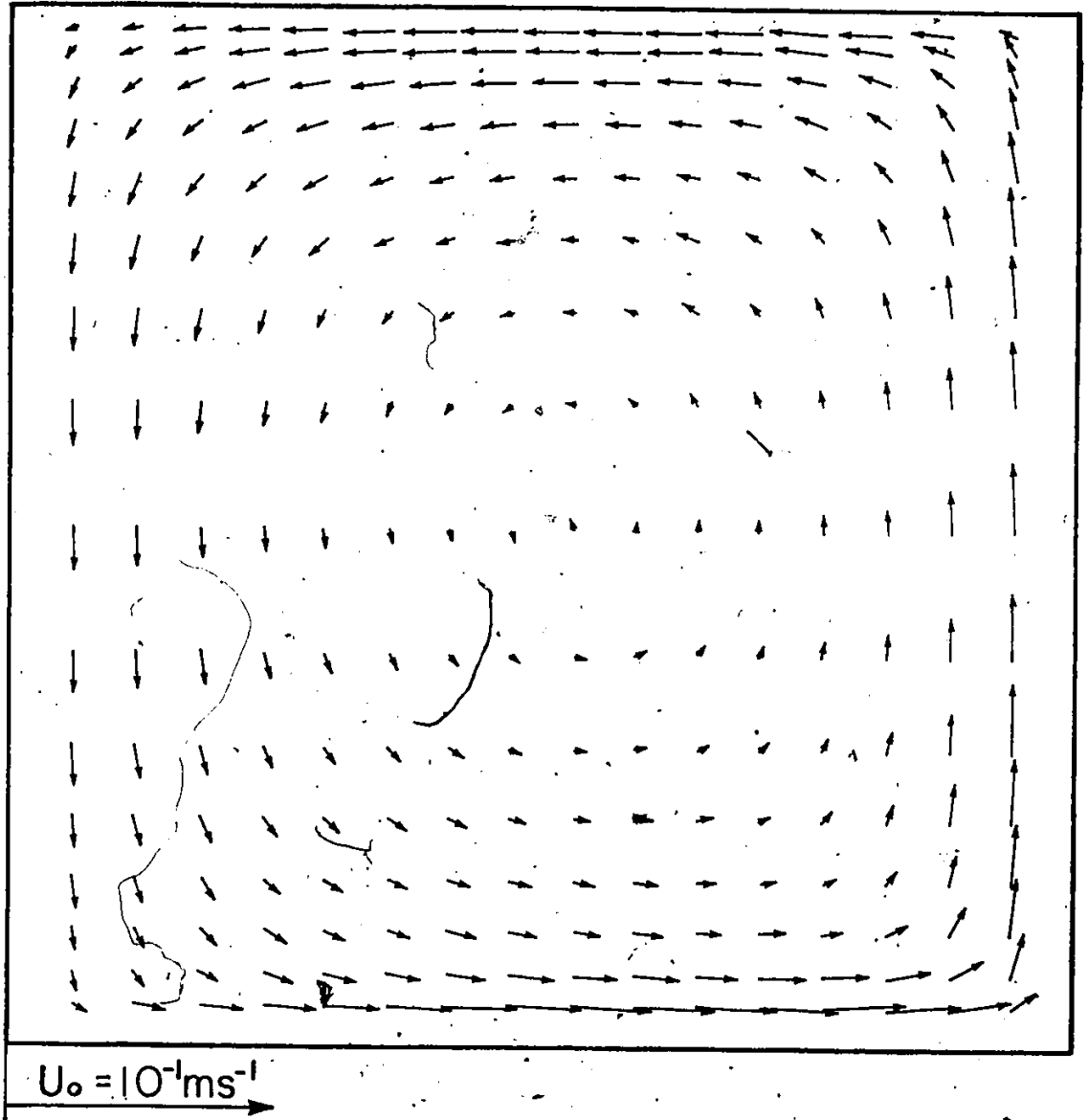


Fig.6.1c Velocity Distribution

$$\text{Re} = 10^5, \text{Pr} = 3, \text{Gr}/\text{Re}^2 = 0$$

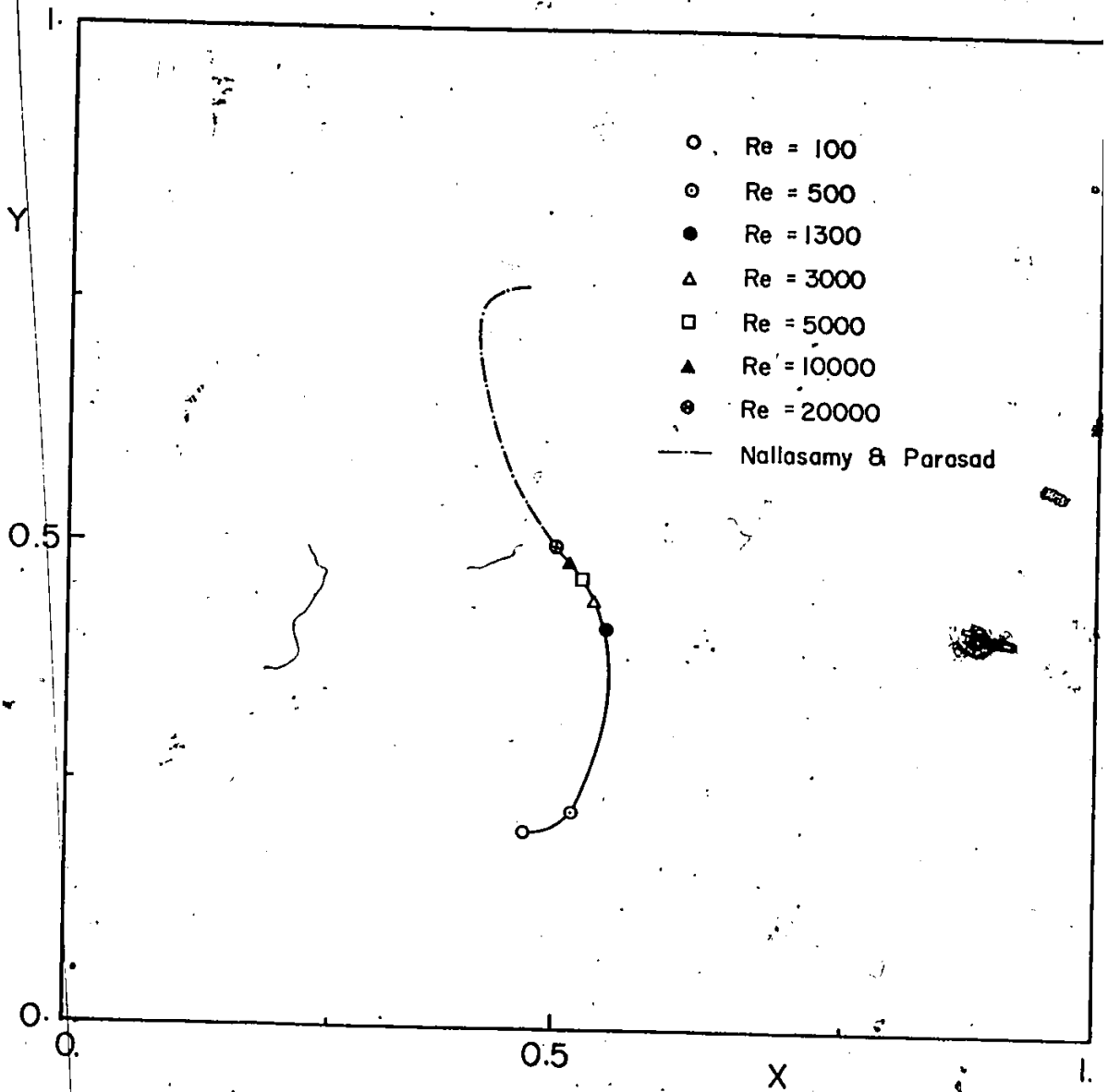


Fig.6.2 Movement of Primary Eddy Centre

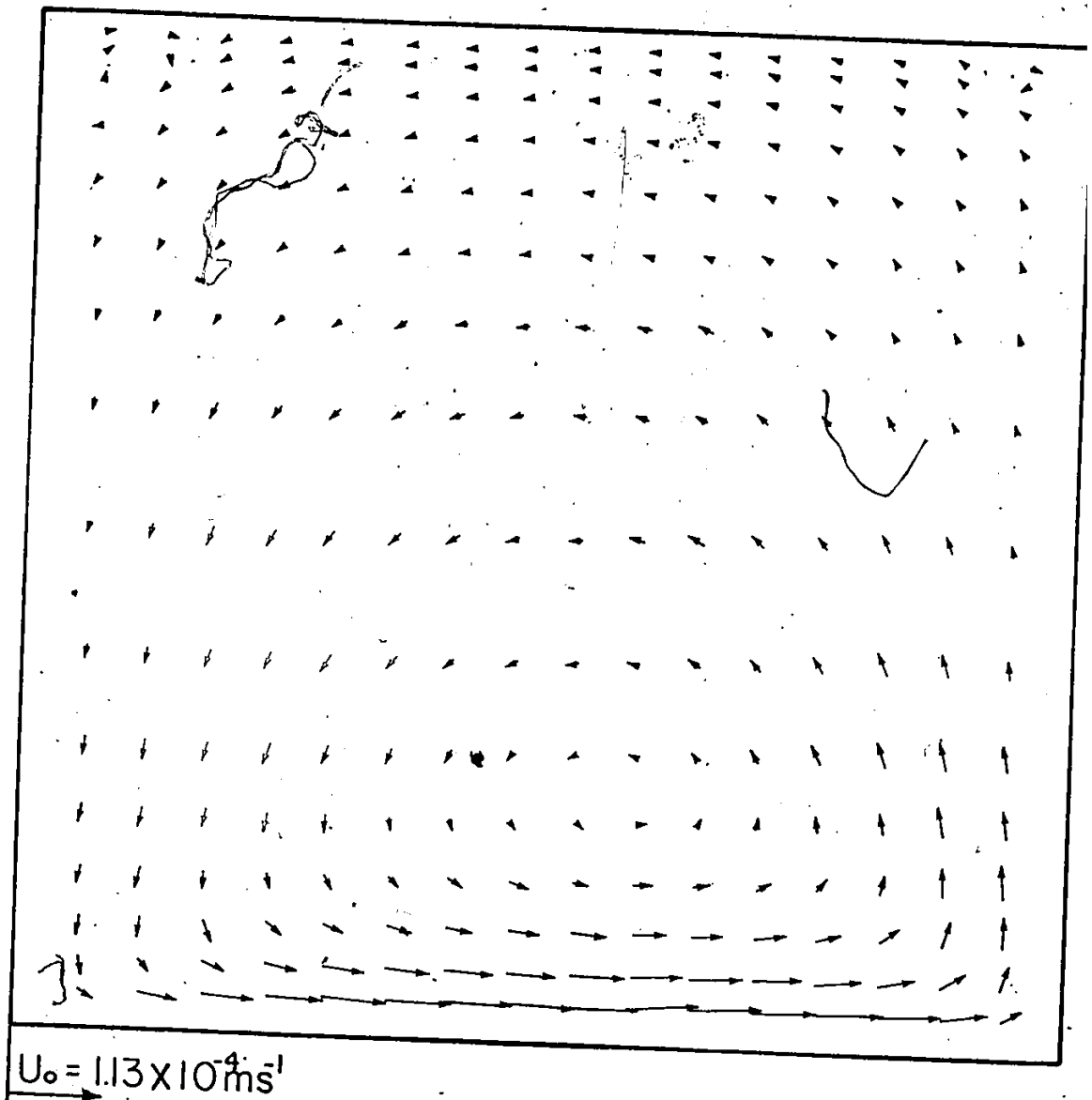


Fig. 6.3a Velocity Distribution

$$\text{Re} = 10^2, \text{Pr} = 0.01, \text{Gr}/\text{Re}^2 = 0$$

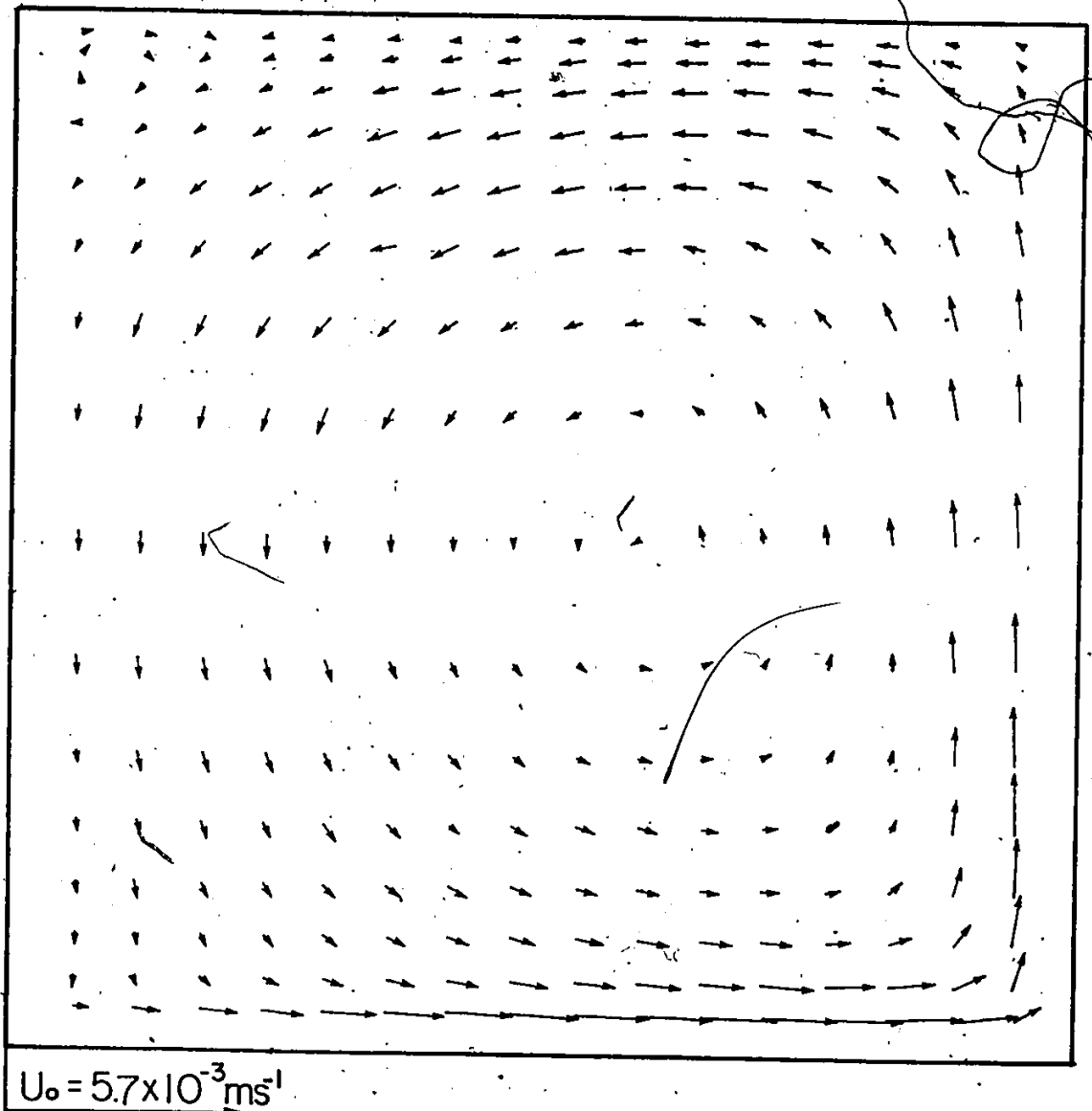


Fig. 6.3b Velocity Distribution

$$\text{Re} = 5 \times 10^3, \text{Pr} = 0.01, \text{Gr}/\text{Re}^2 = 0$$

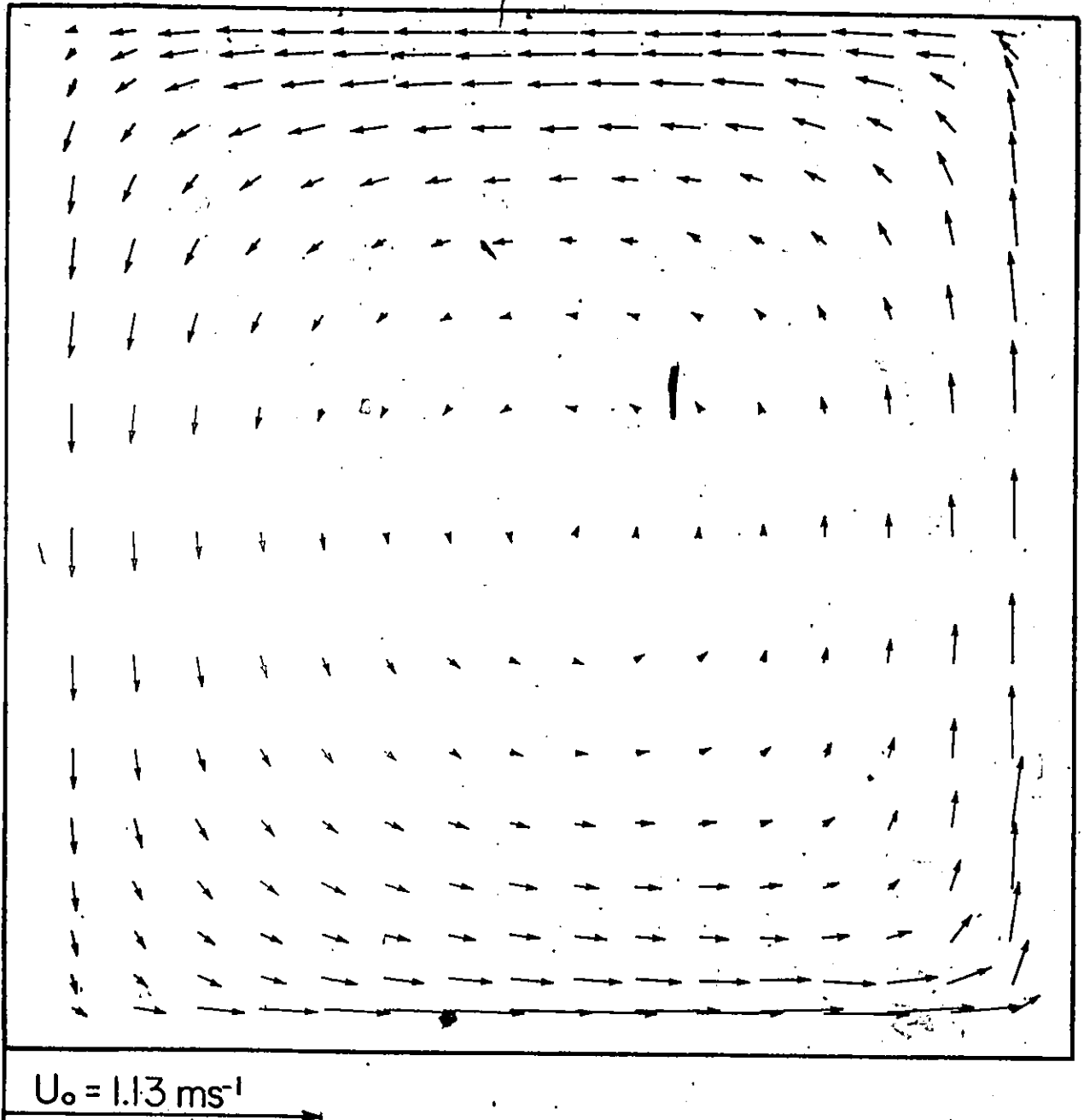


Fig.6.3c Velocity Distribution

$$\text{Re} = 10^6, \text{Pr} = 0.01, \text{Gr}/\text{Re}^2 = 0$$

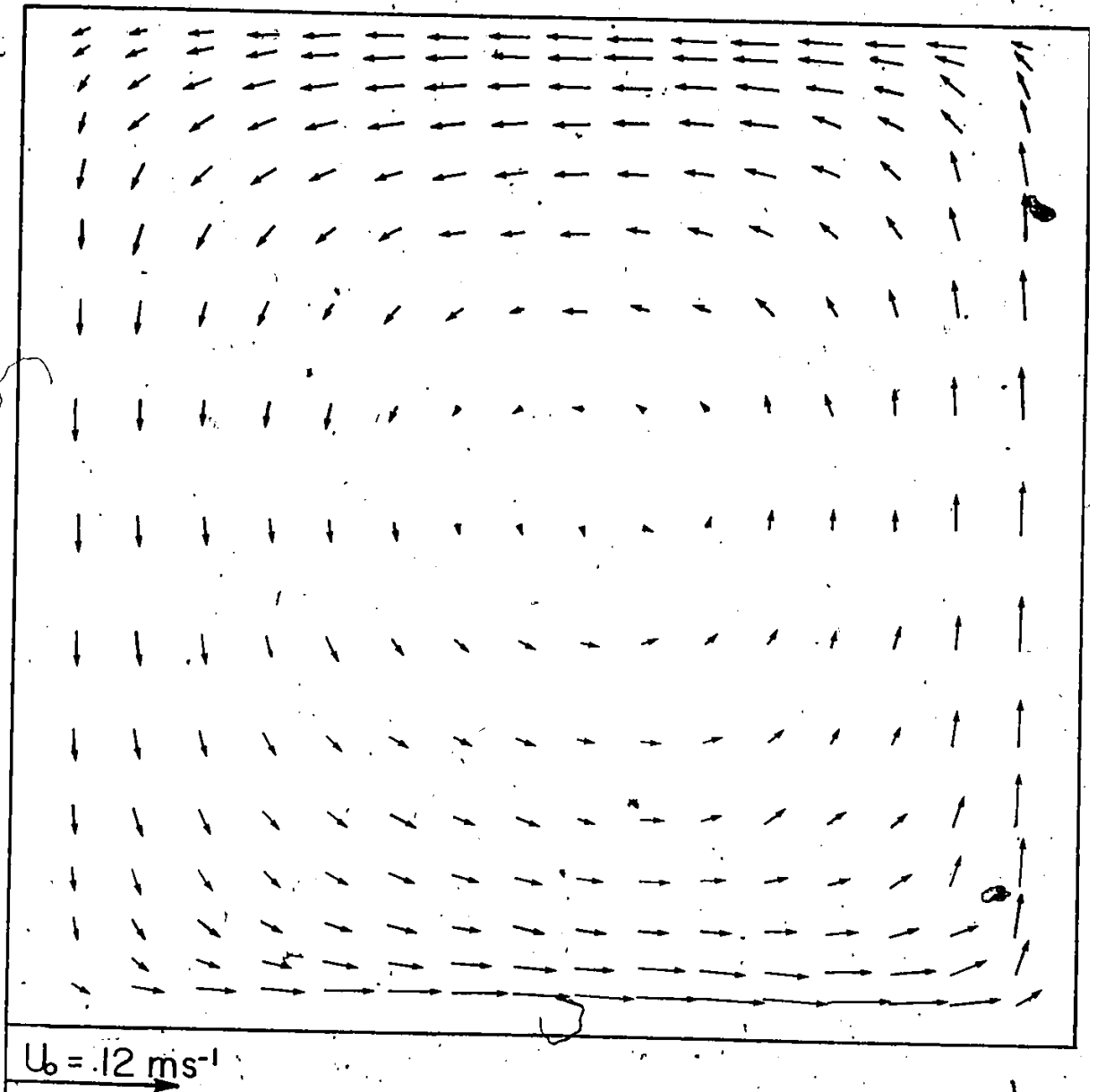


Fig. 6.4a Velocity Distribution

$$\text{Re} = 8.4 \times 10^4, \text{Pr} = 3, \text{Gr}/\text{Re}^2 = 6$$

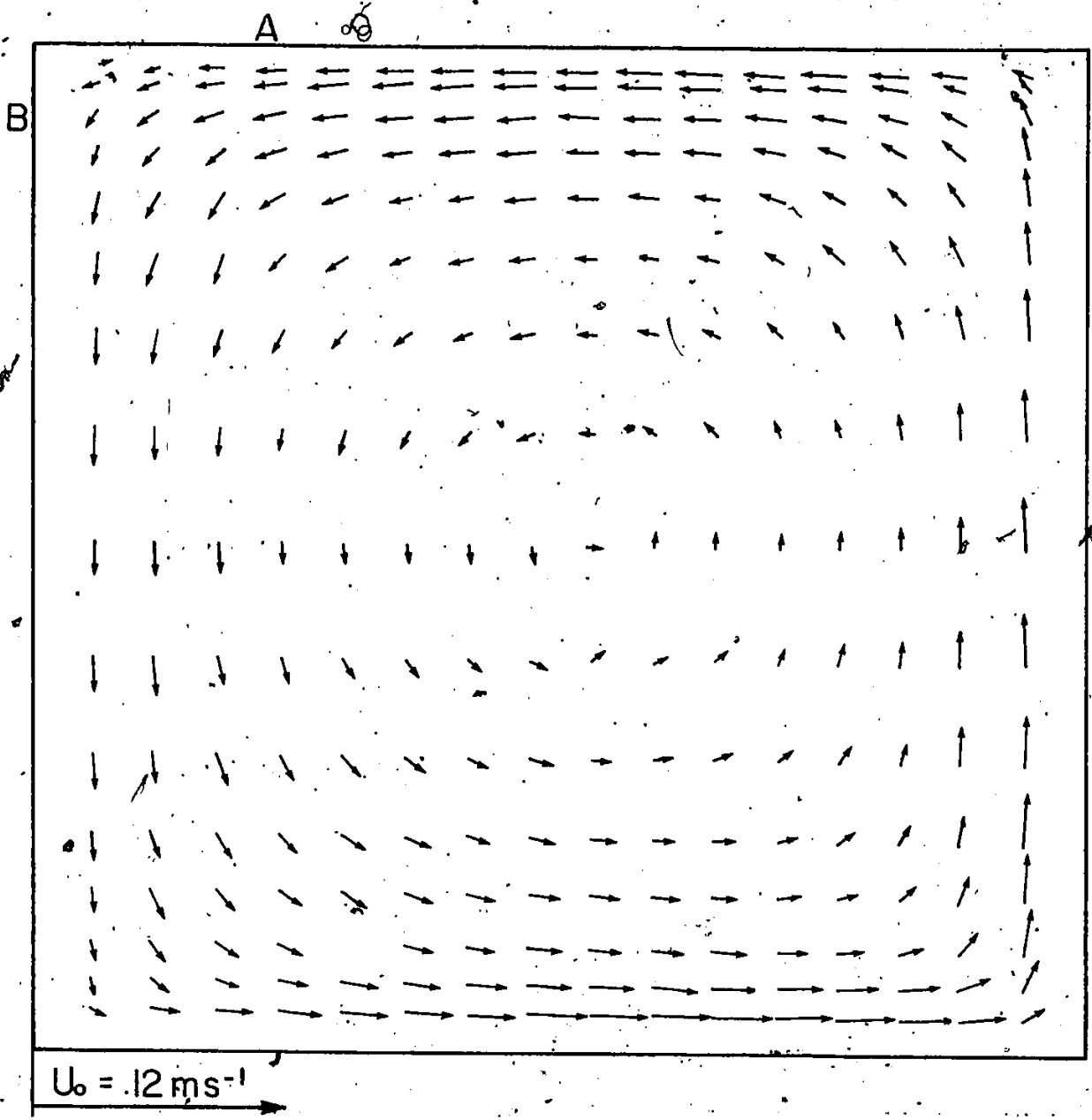


Fig. 6.4b. Velocity Distribution

$Re = 8.4 \times 10^4, Pr = 3, Gr/Re^2 = 1$

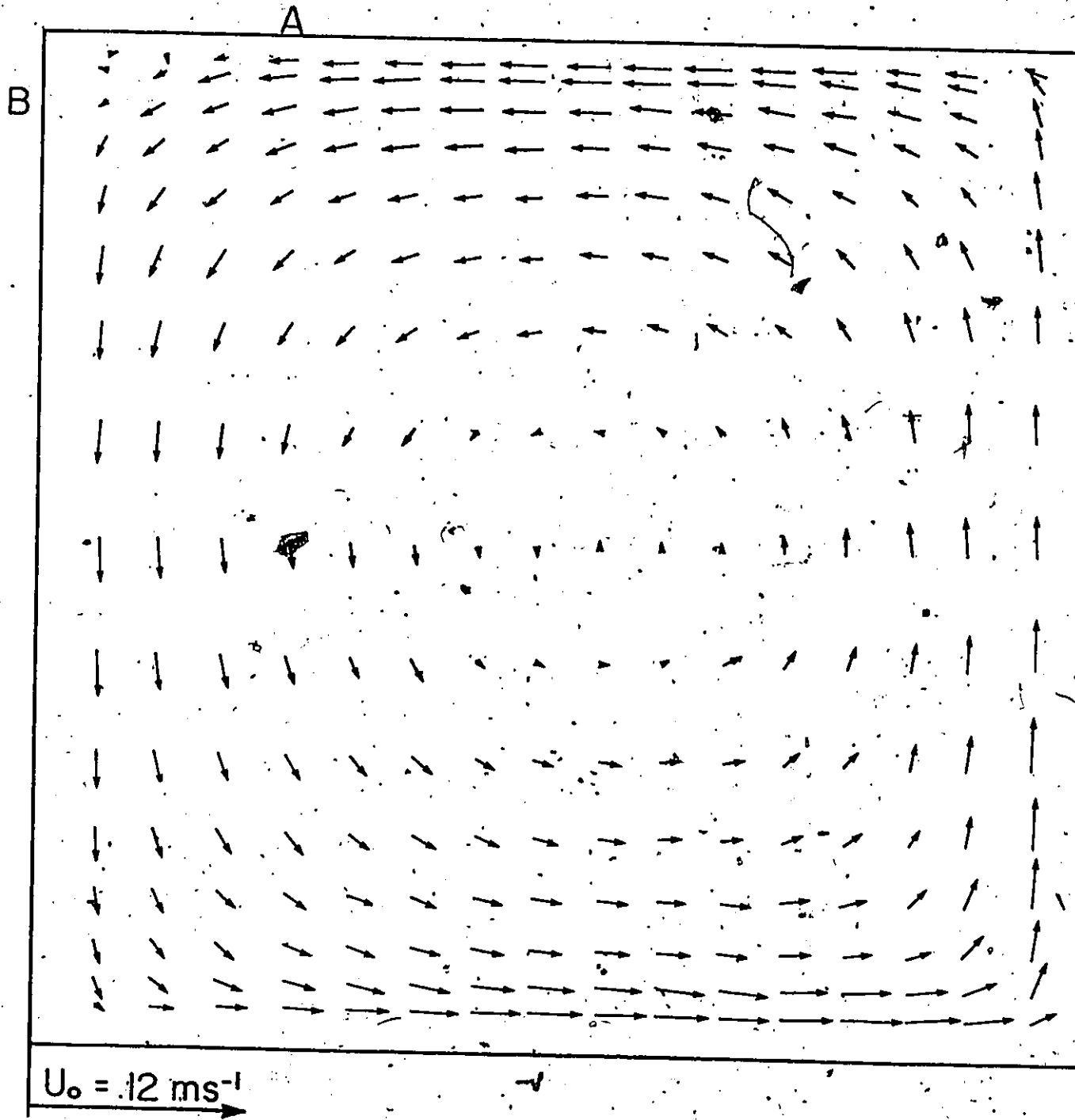


Fig. 6.4c Velocity Distribution

$$Re = 8.4 \times 10^4, Pr = 3, Gr/Re^2 = 2$$

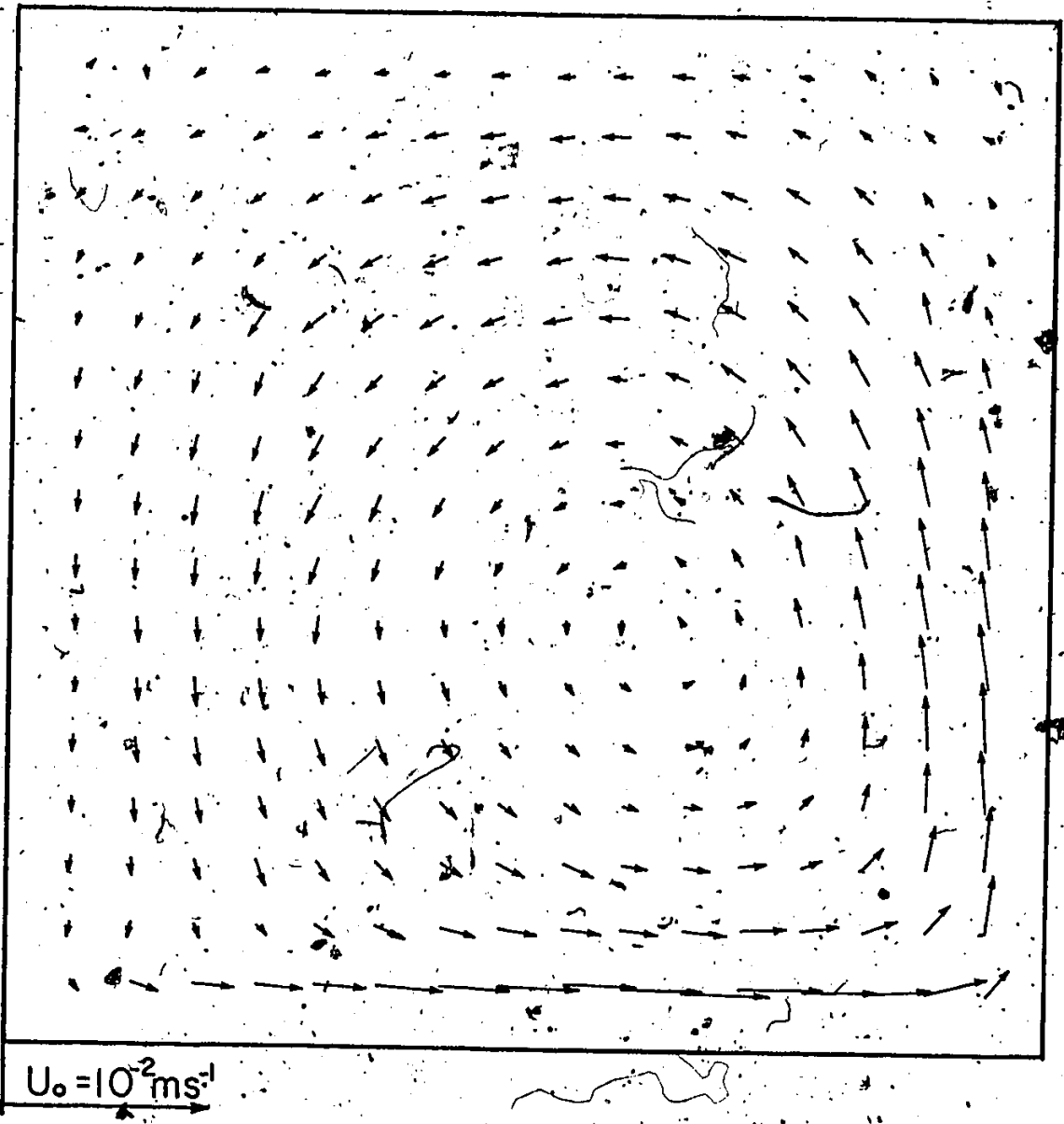


Fig. 6.5a Velocity Distribution

$Re = 10^3, Pr = 0.01, Gr/Re^2 = 6$

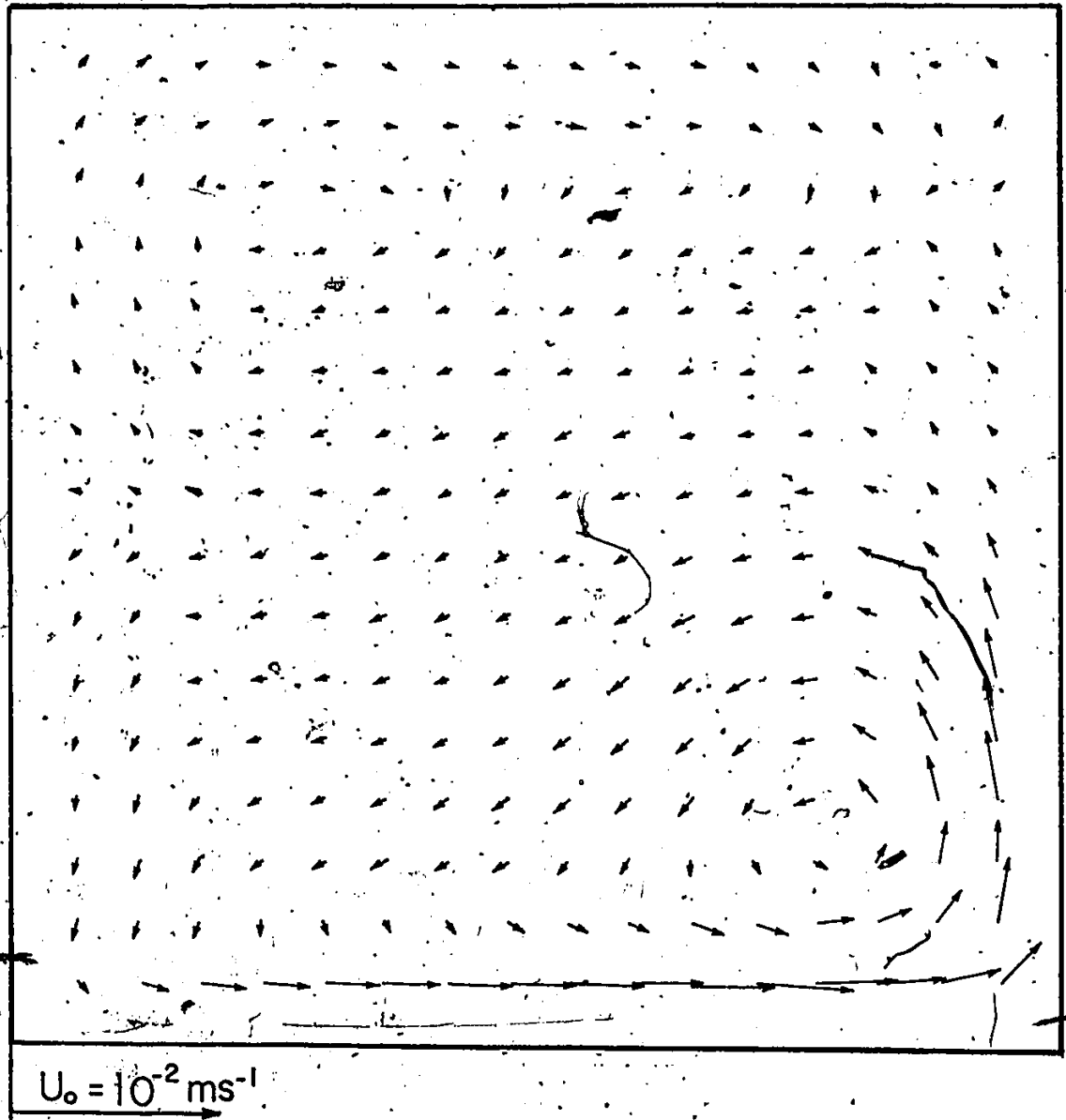
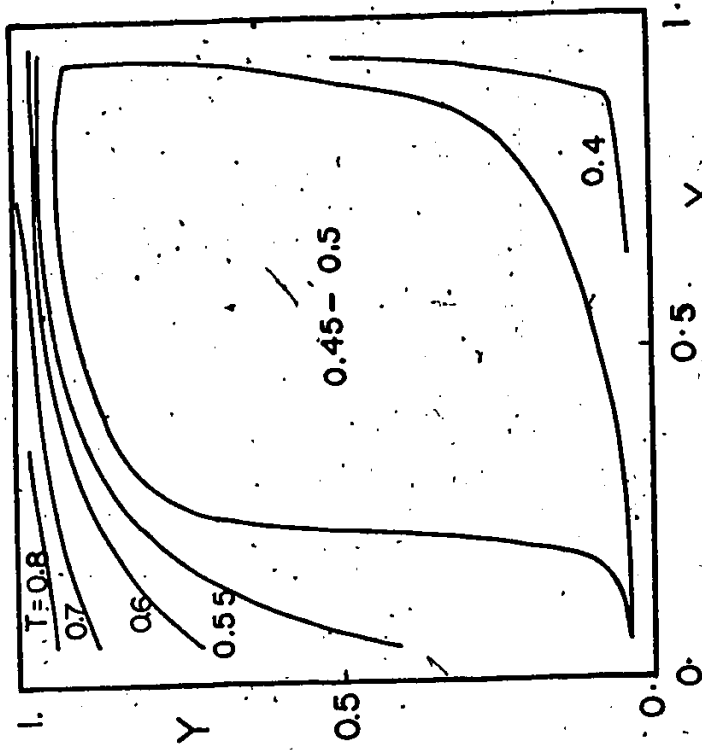
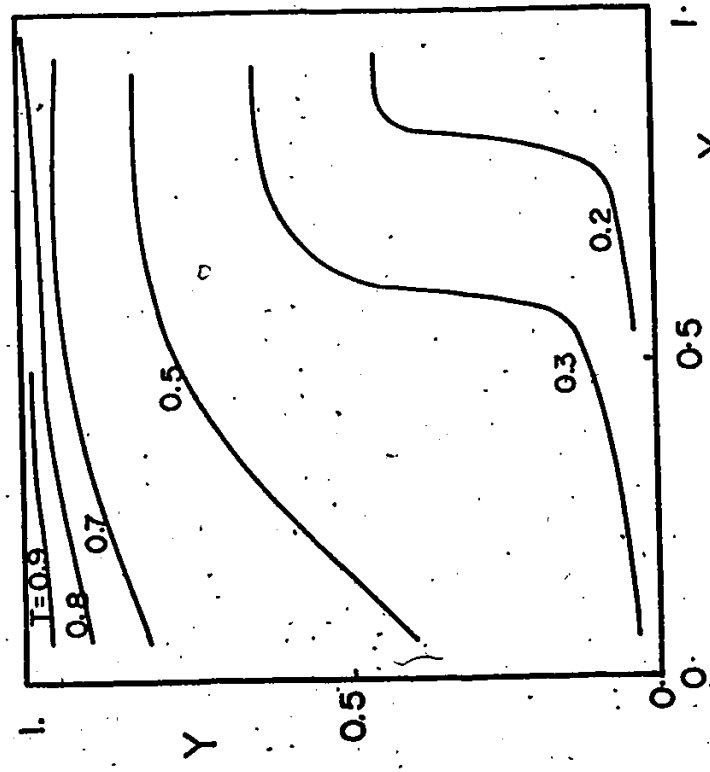


Fig. 6.5b Velocity Distribution

$$\text{Re} = 10^3, \text{Pr} = 0.01, \text{Gr}/\text{Re}^2 = 1$$



a.  $Re = 1.3 \times 10^2$



b.  $Re = 1.3 \times 10^3$

Fig. 6.6 Isotherms for  $Pr = 3$ ,  $Gr/Re^2 = 0$

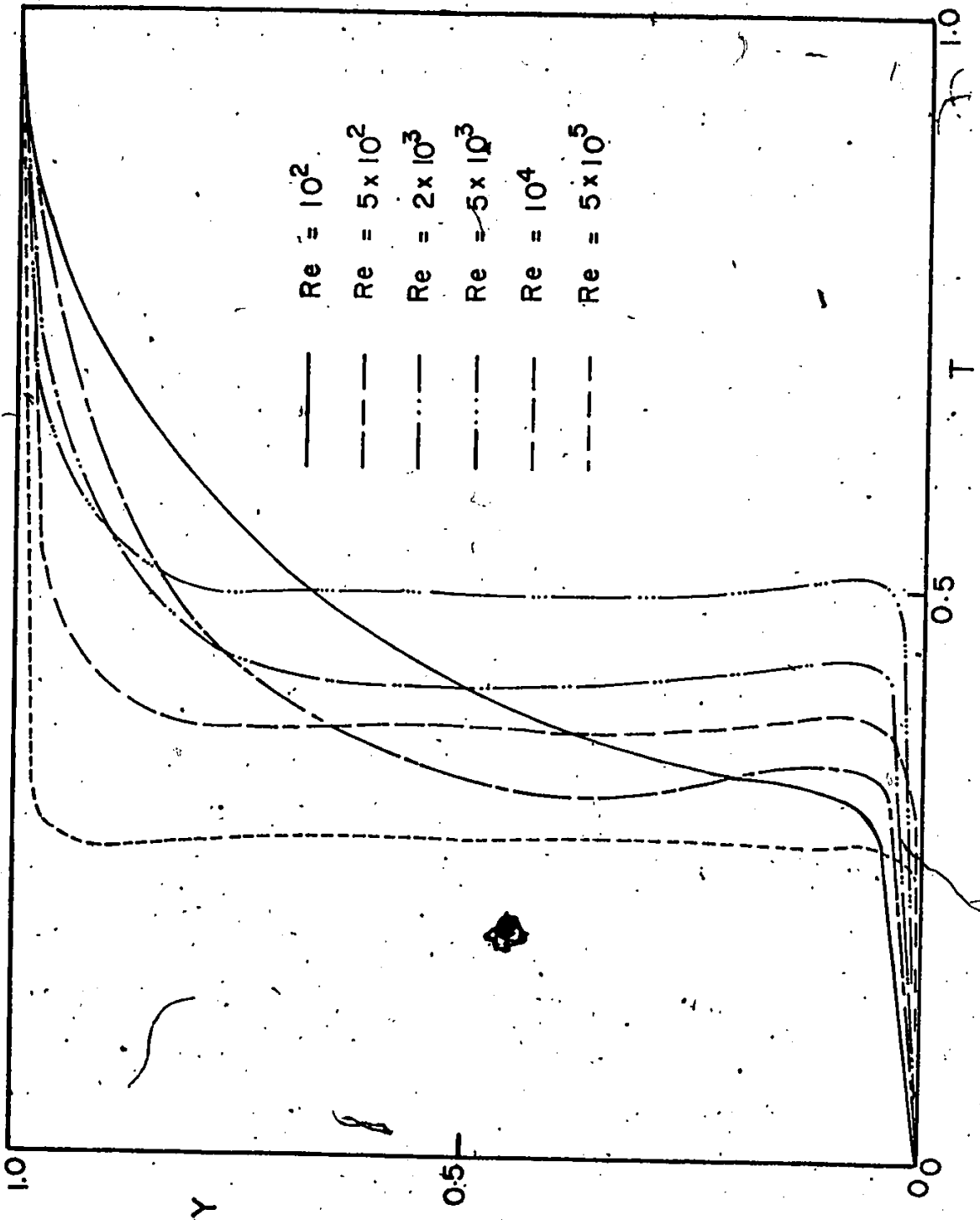


Fig.6.7a Vertical Centre-line Temperature Distribution, Pr = 3, Gr/Re<sup>2</sup> = 0

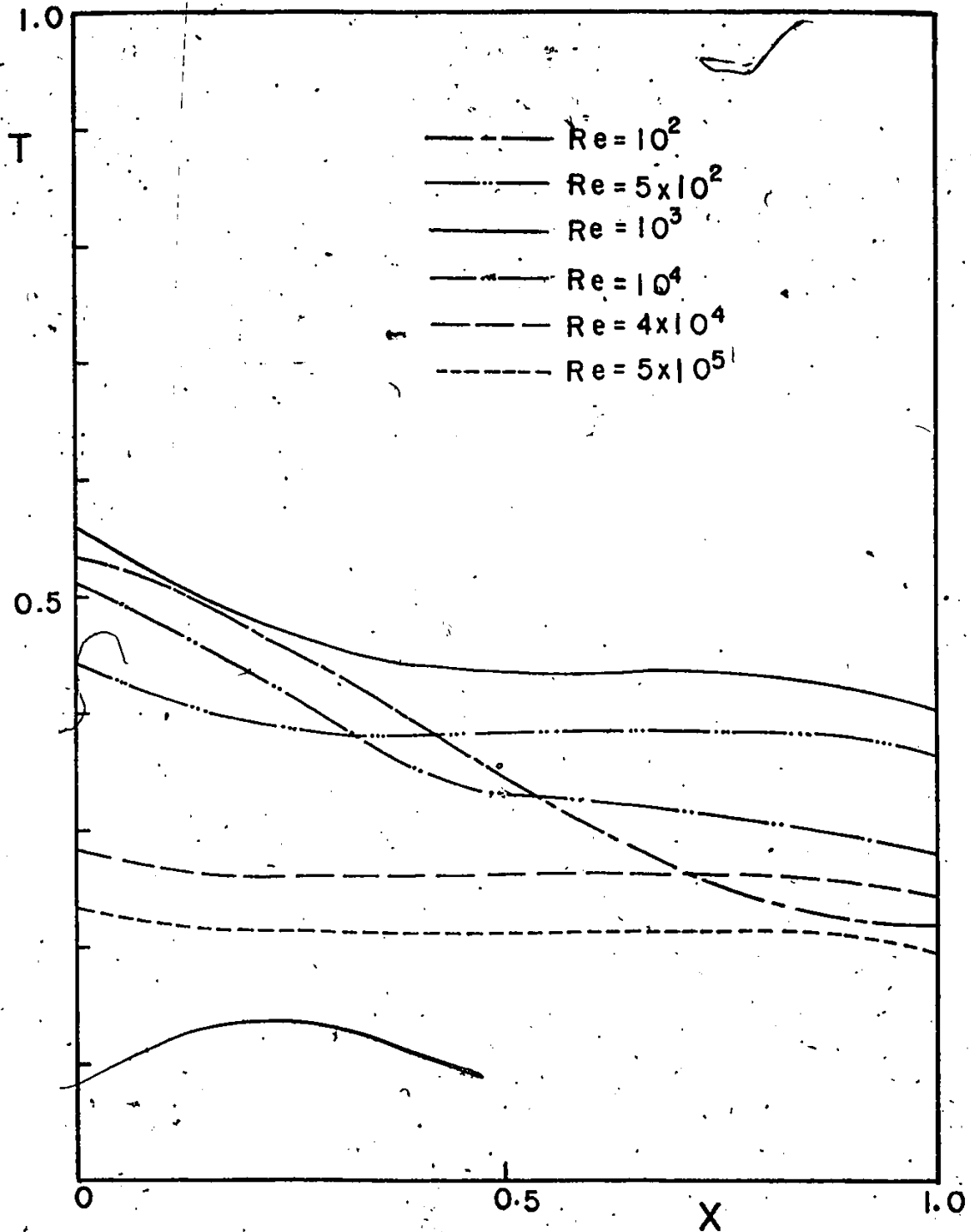


Fig.6.7b Horizontal Centre-line Temperature Distribution

$Pr = 3, Gr/Re^2 = .0$

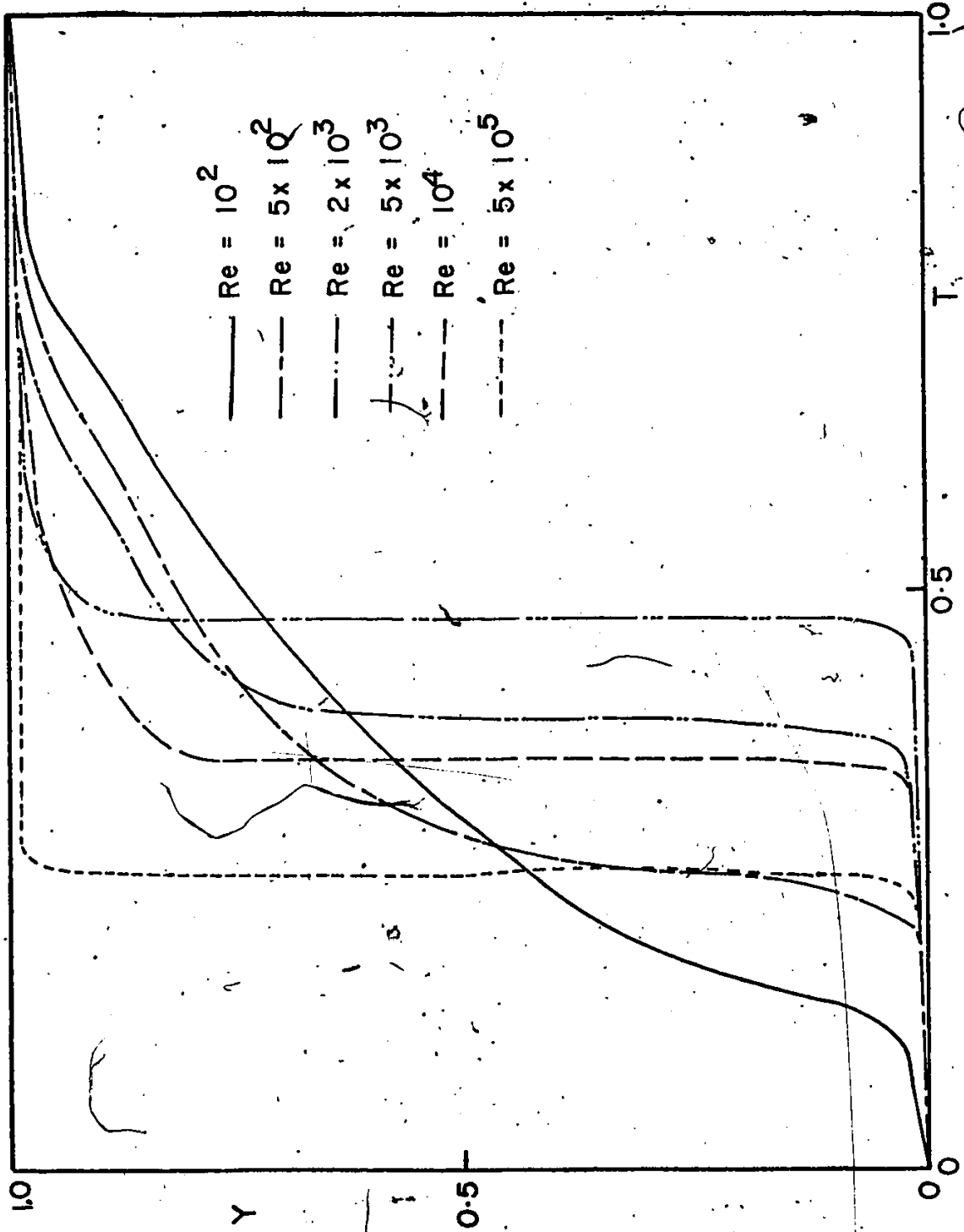


Fig.6.7c Right Side Wall Temperature Distribution,  $Pr = 3$ ,  $Gr/Re^2 = 0$

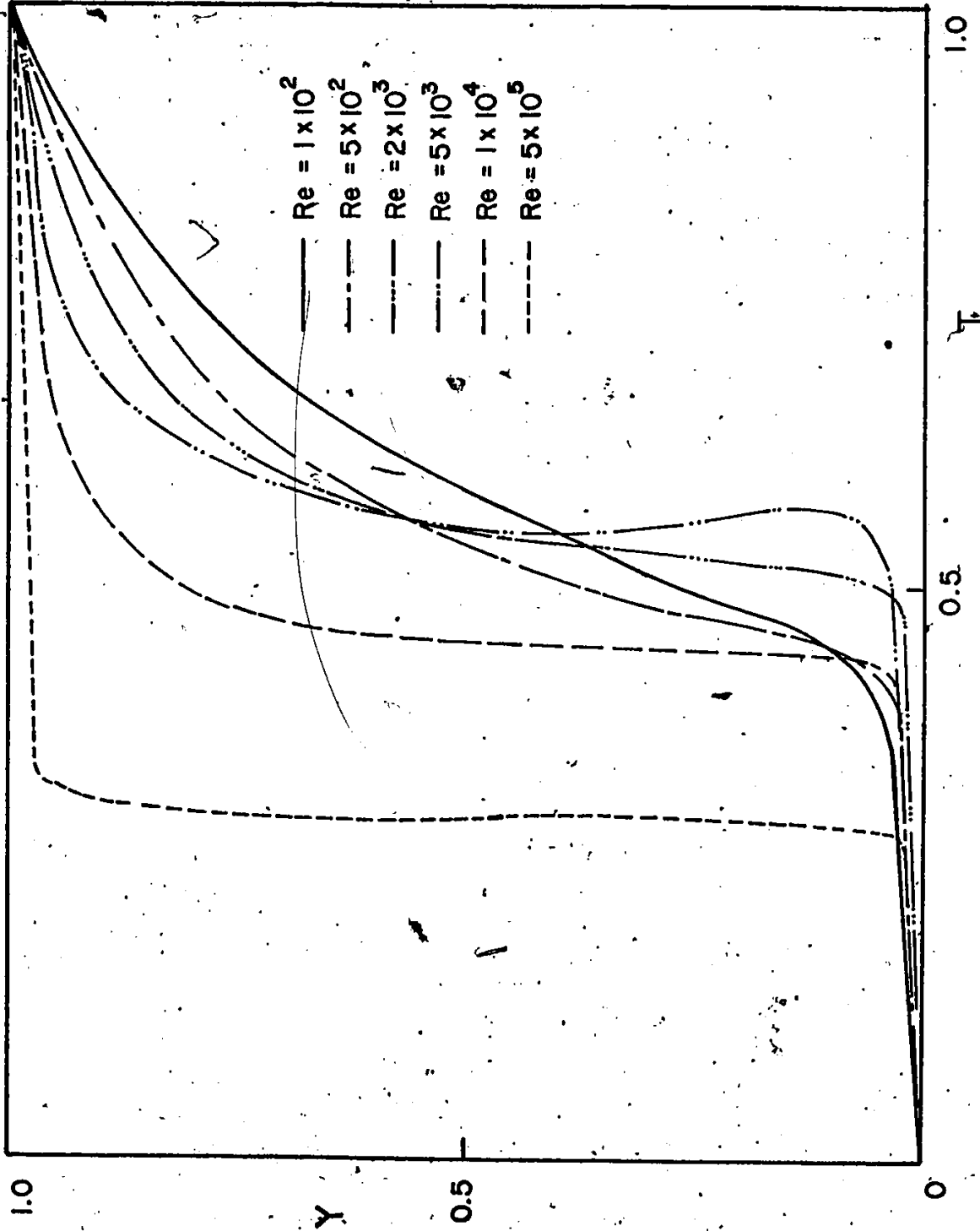


Fig. 6.7d Left Side Wall Temperature Distribution, Pr = 3, Gr/Re<sup>2</sup> = 0

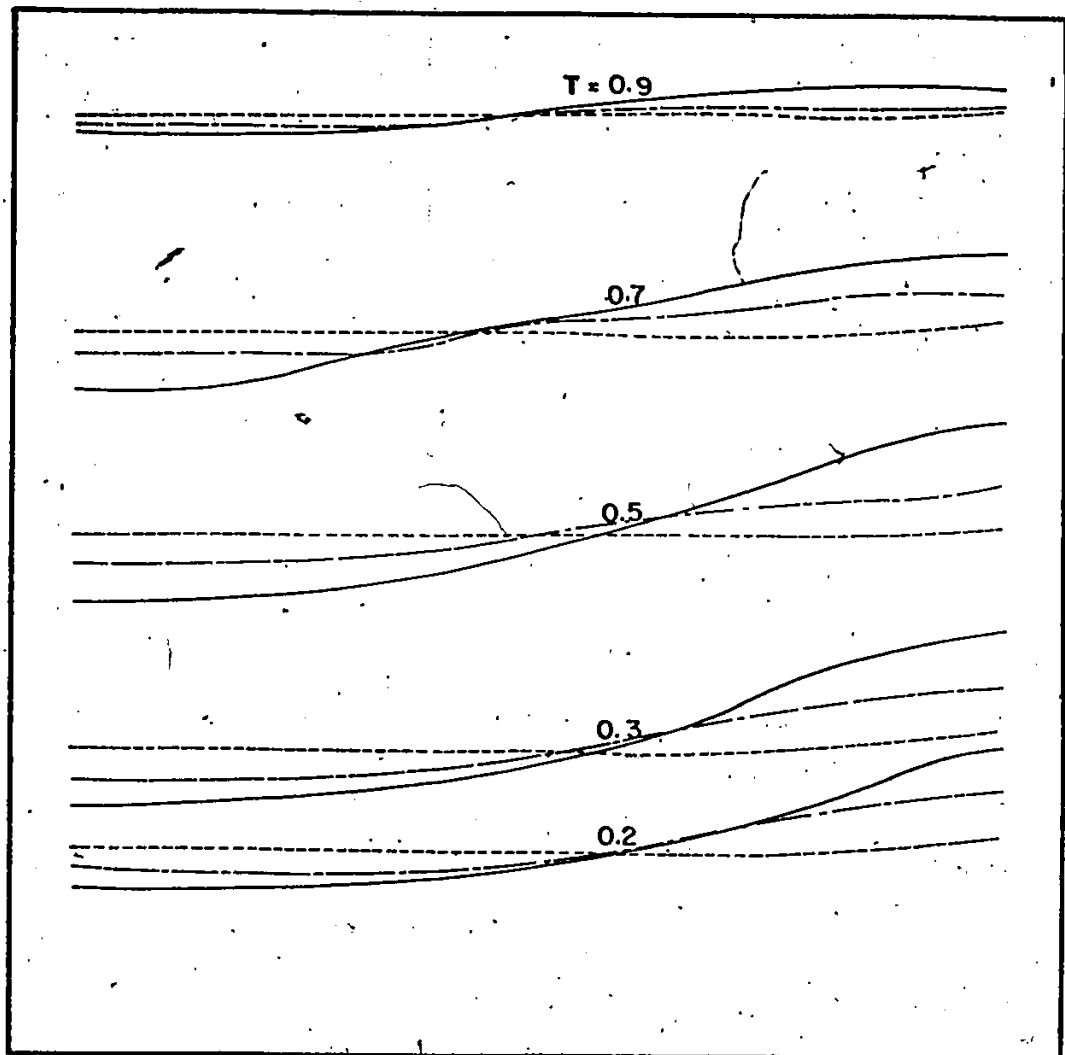


Fig. 6.8a Isotherms,  $Pr = 0.01$ ,  $Gr/Re^2 = 0$

---  $Re = 100$ , - - -  $Re = 500$ , —  $Re = 1000$

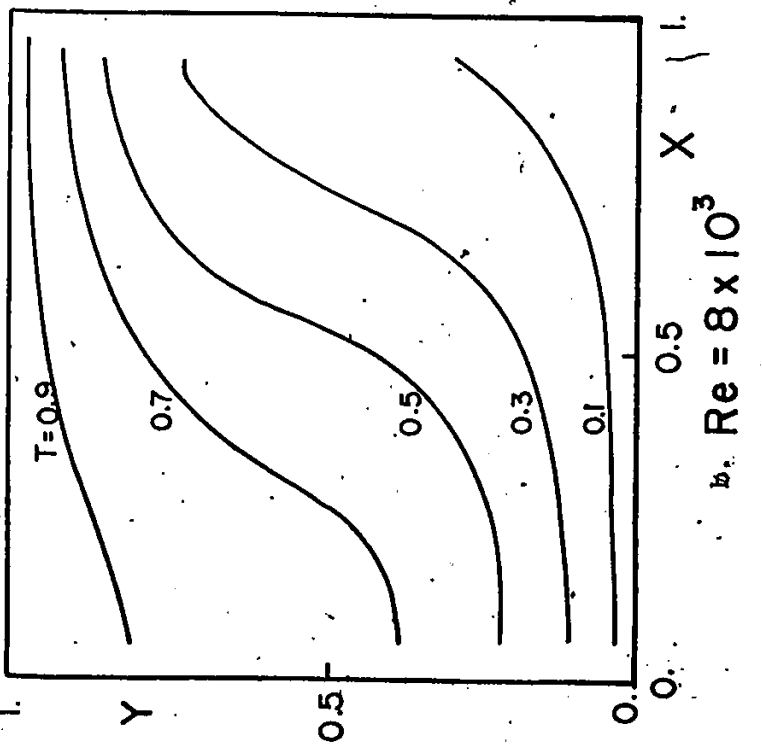
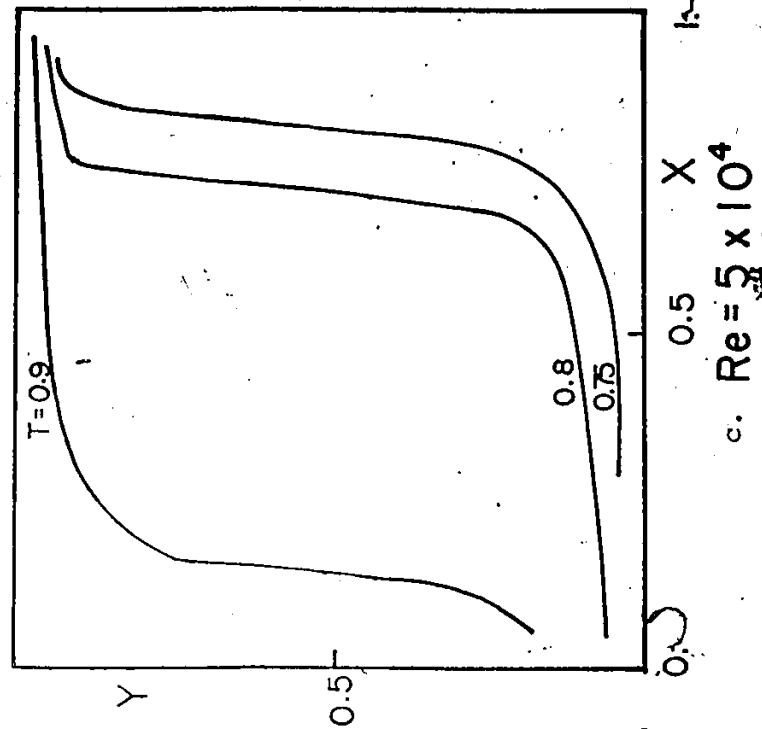


Fig. 6.8 Isotherms for  $Pr = 0.01$ ,  $Gr/Re^2 = 0$

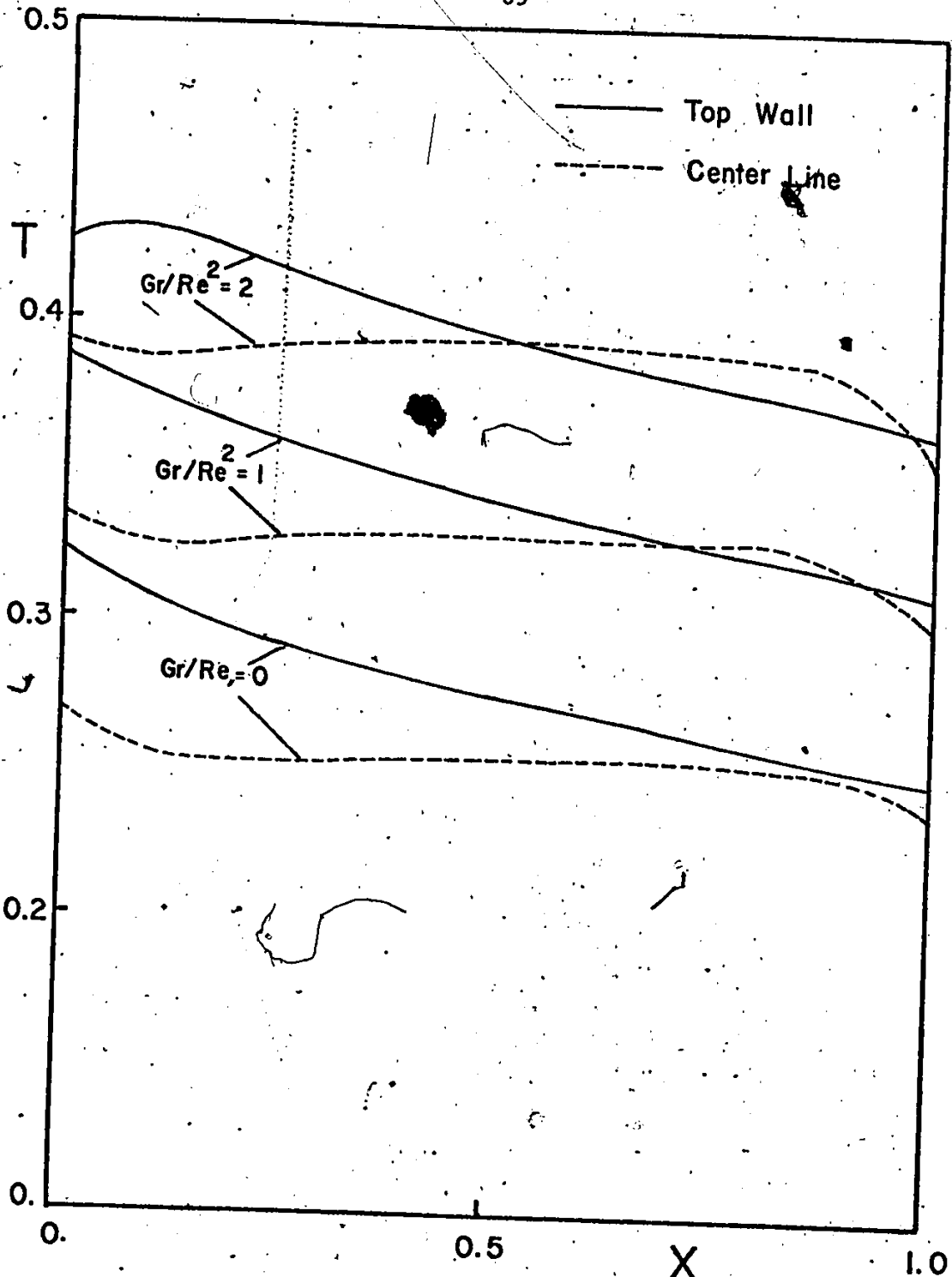


Fig.6.9a Horizontal Temperature Distribution

$Re = 2.7 \times 10^5, Pr = 3$

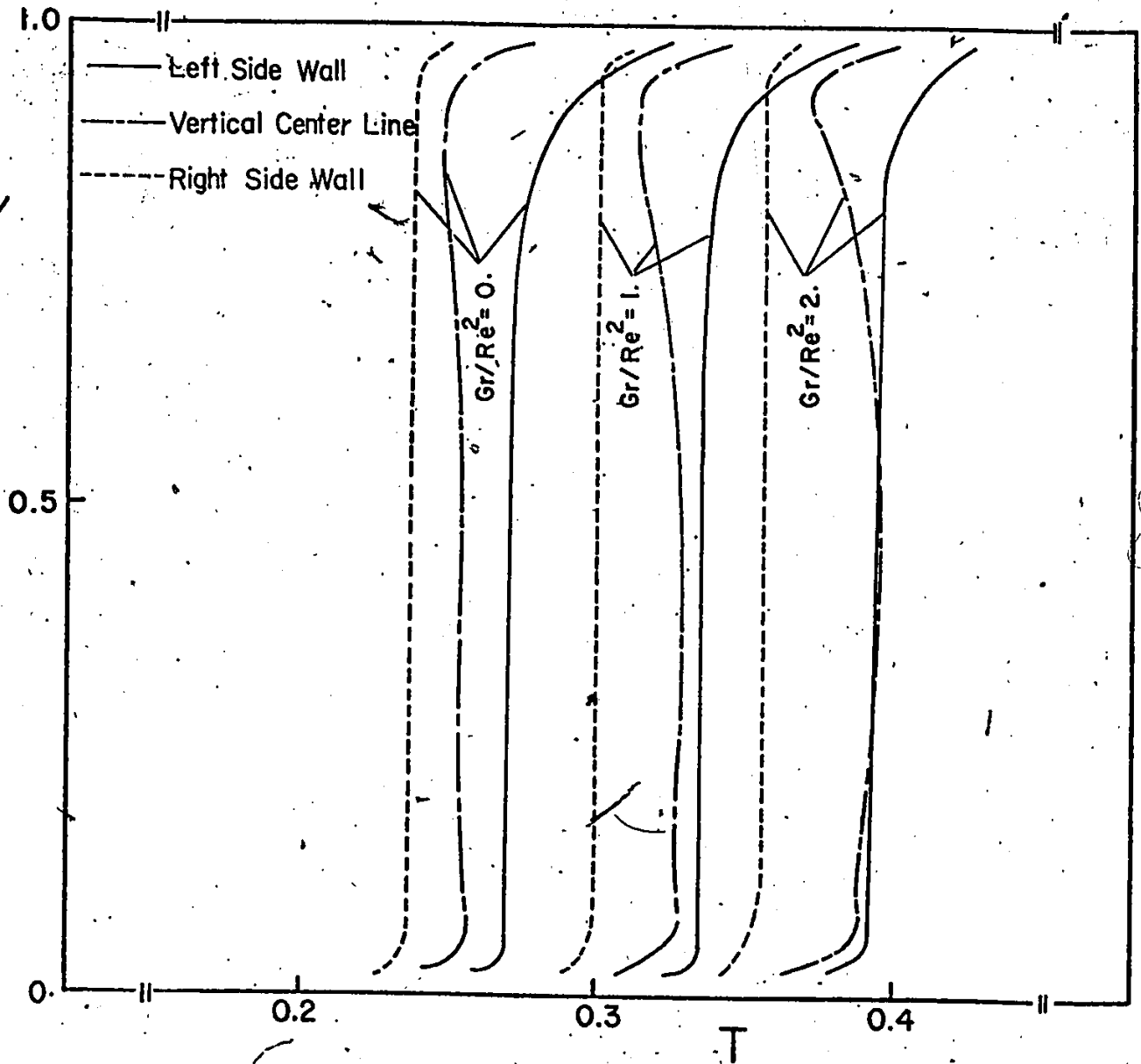


Fig. 6.9b Vertical Temperature Distribution

$$Re = 2.7 \times 10^5, Pr = 3$$

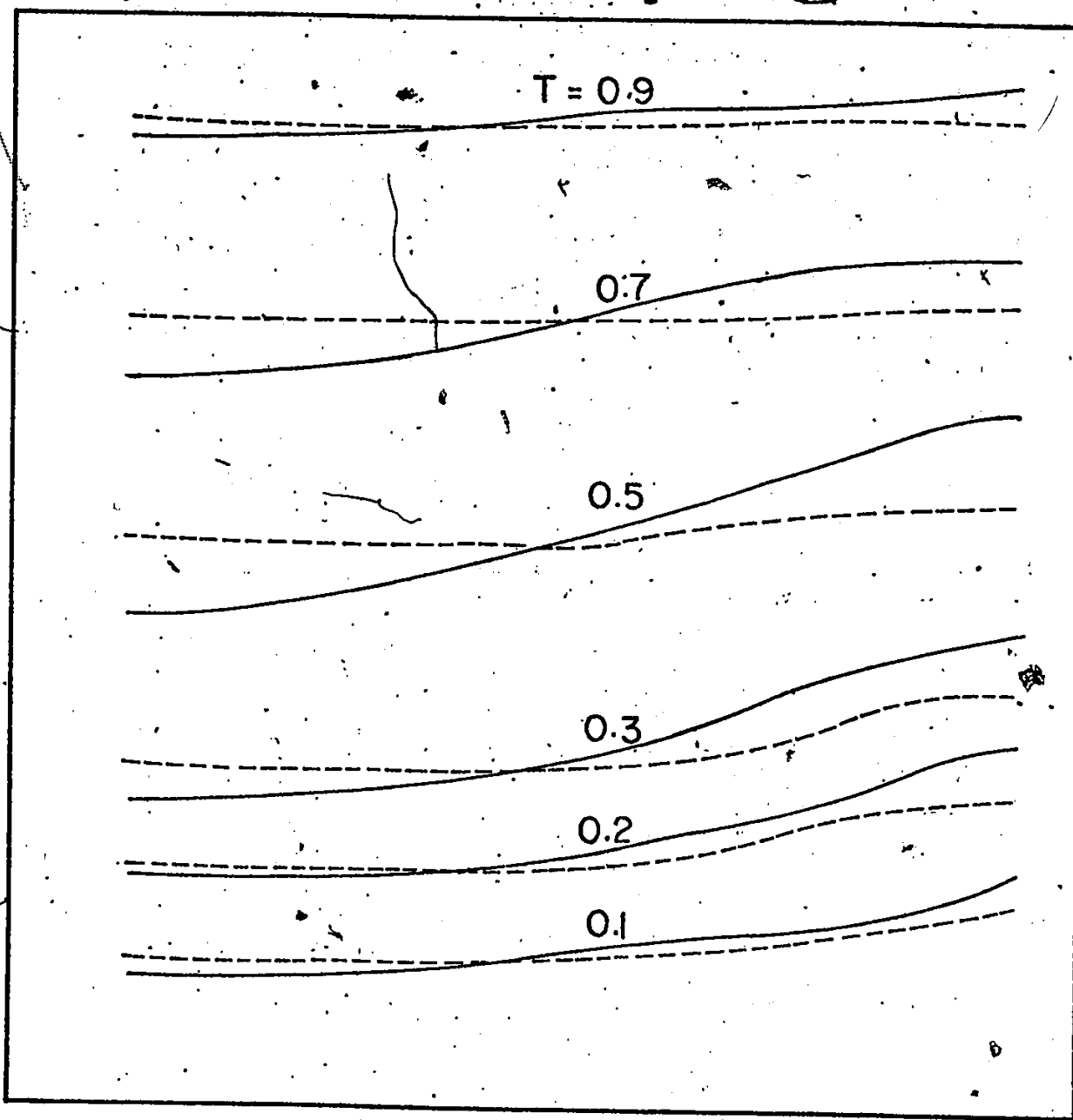
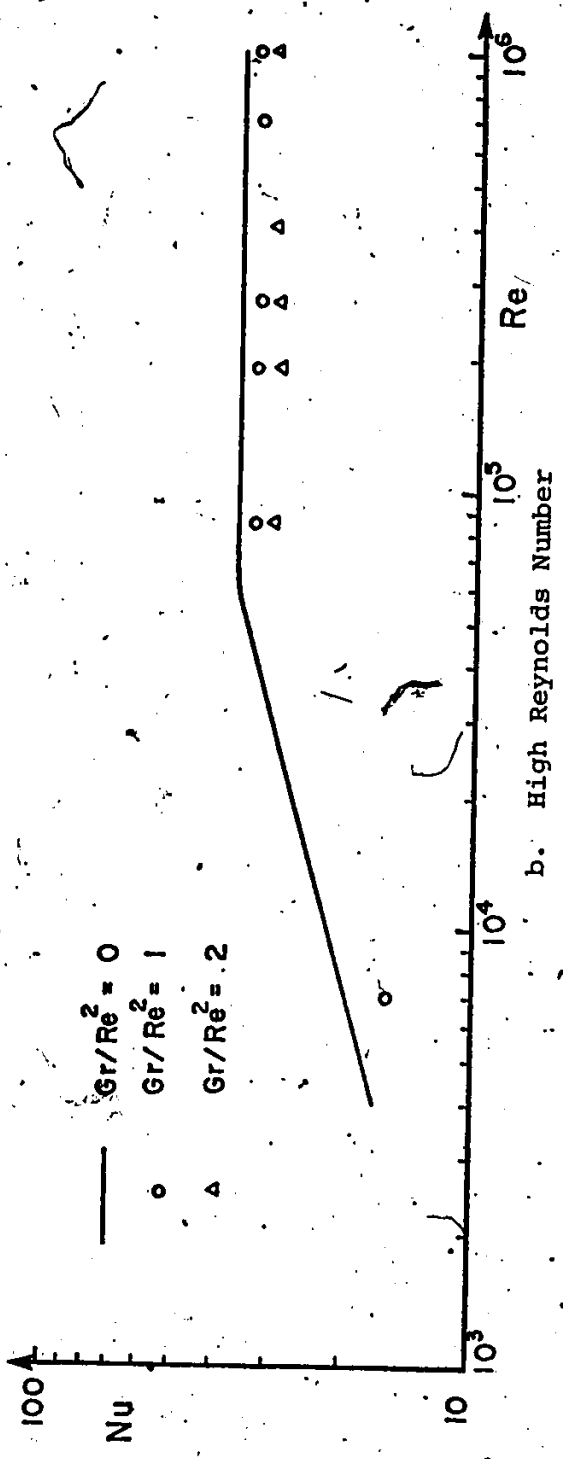
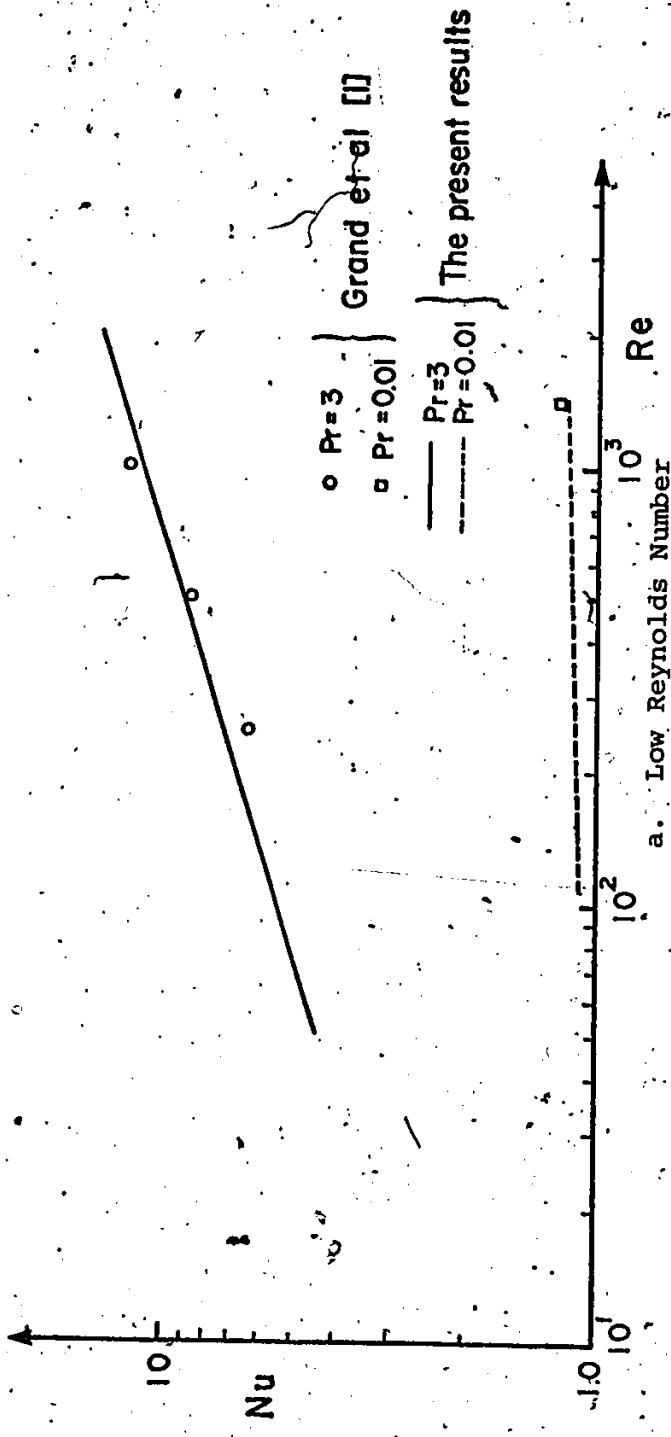


Fig.6.10. Isotherms,  $Pr = 0.01$ ,  $Re = 10^3$

—  $Gr/Re^2 = 0$ , - - -  $Gr/Re^2 = 1$



b. High Reynolds Number



a. Low Reynolds Number

Fig. 6.11 Mean Nusselt Number

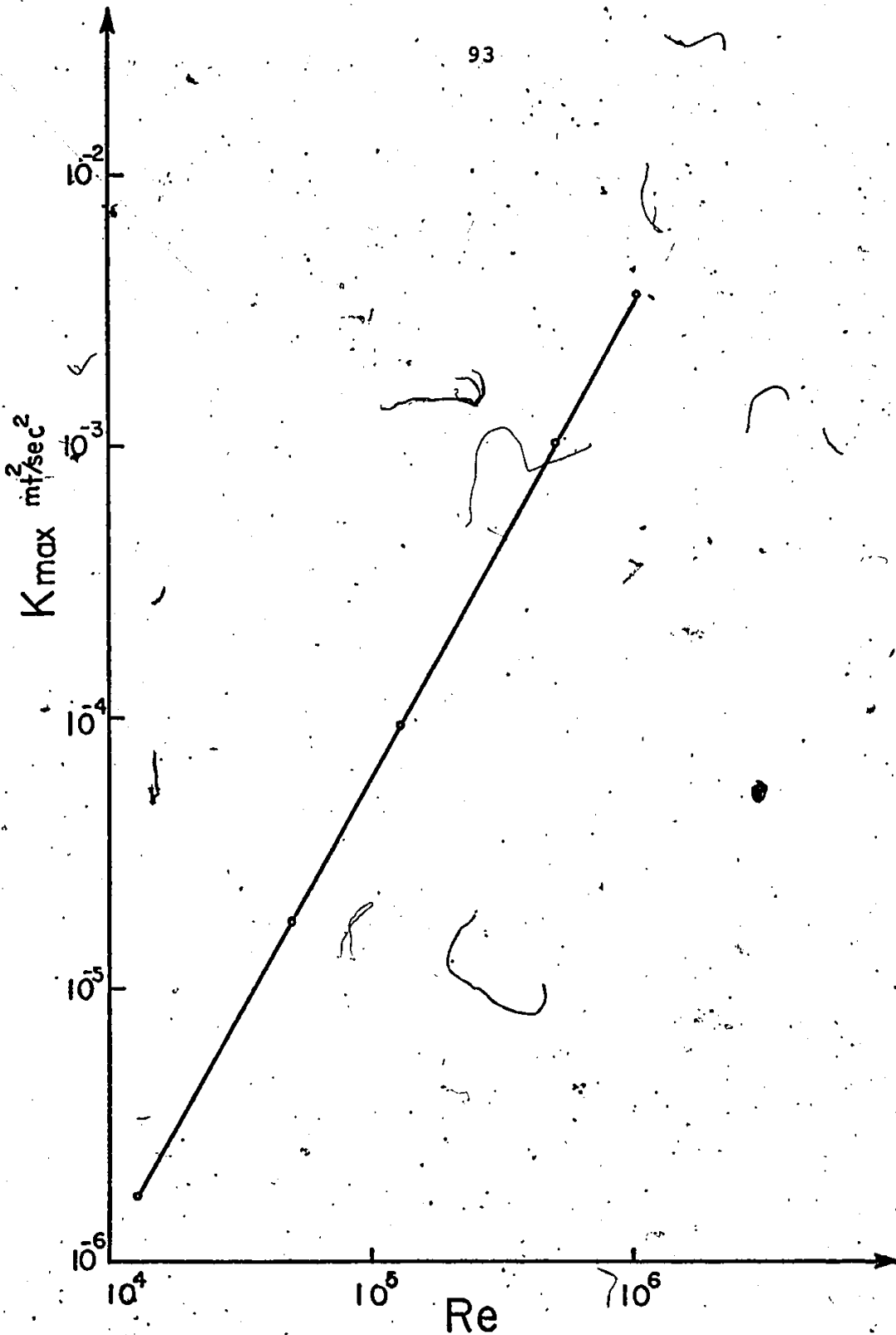


Fig.6.12 Variation of the Turbulence Kinetic Energy with Reynolds Number

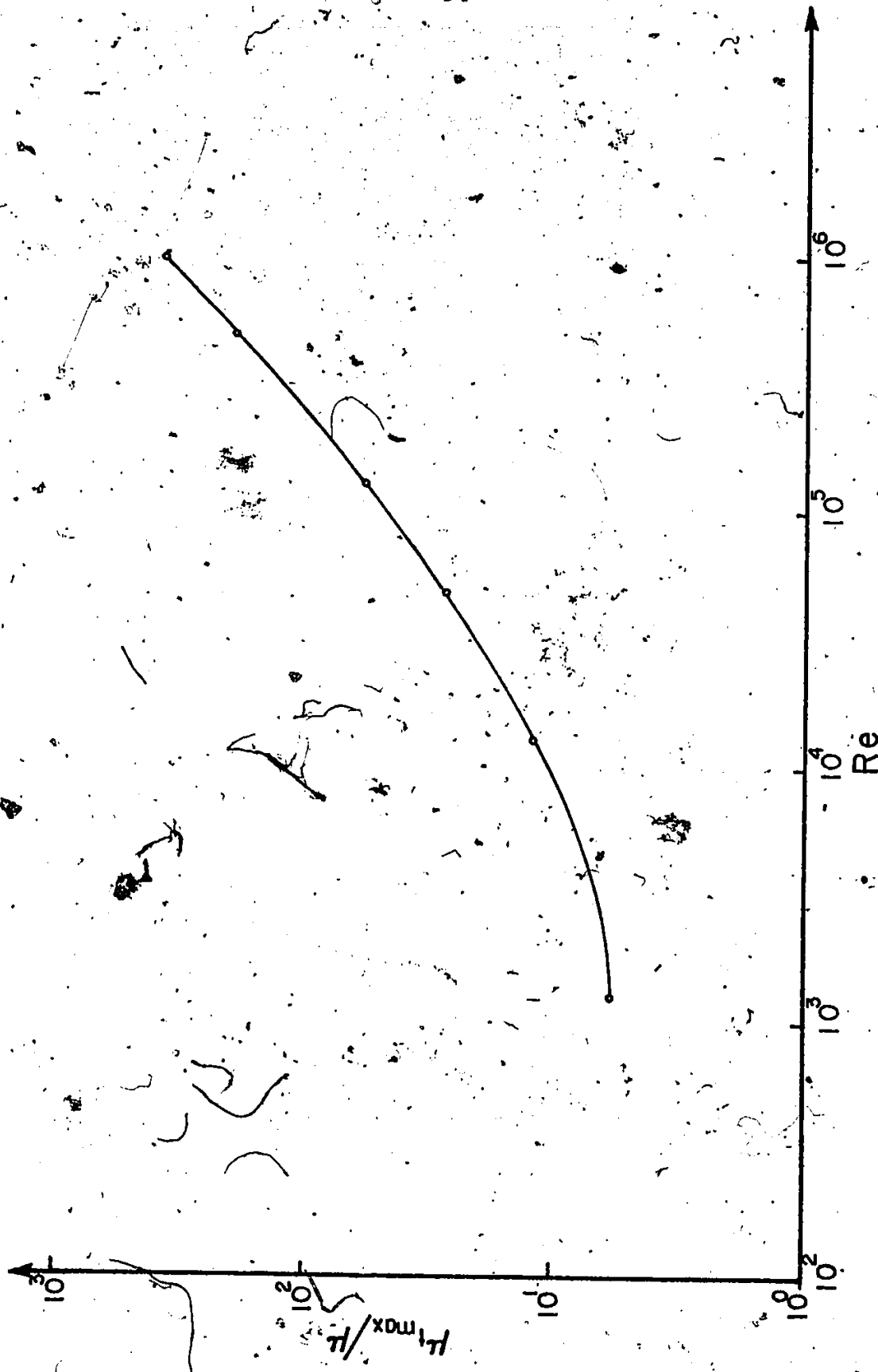


Fig.6.13 Variation of the Effective Viscosity with Reynolds Number

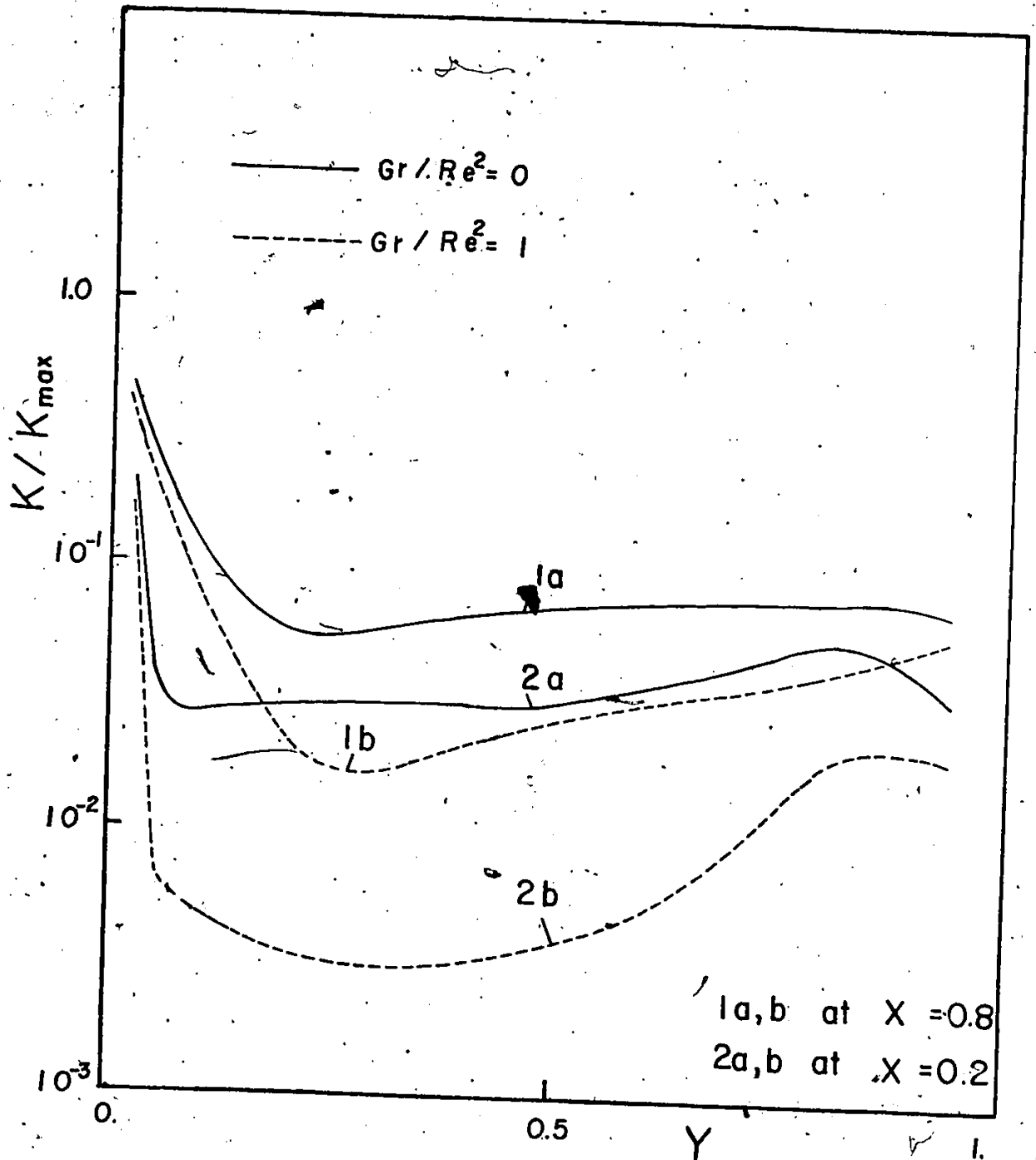


Fig.6.14 Vertical Turbulence Kinetic Energy Distribution

$Re = 8.4 \times 10^4$

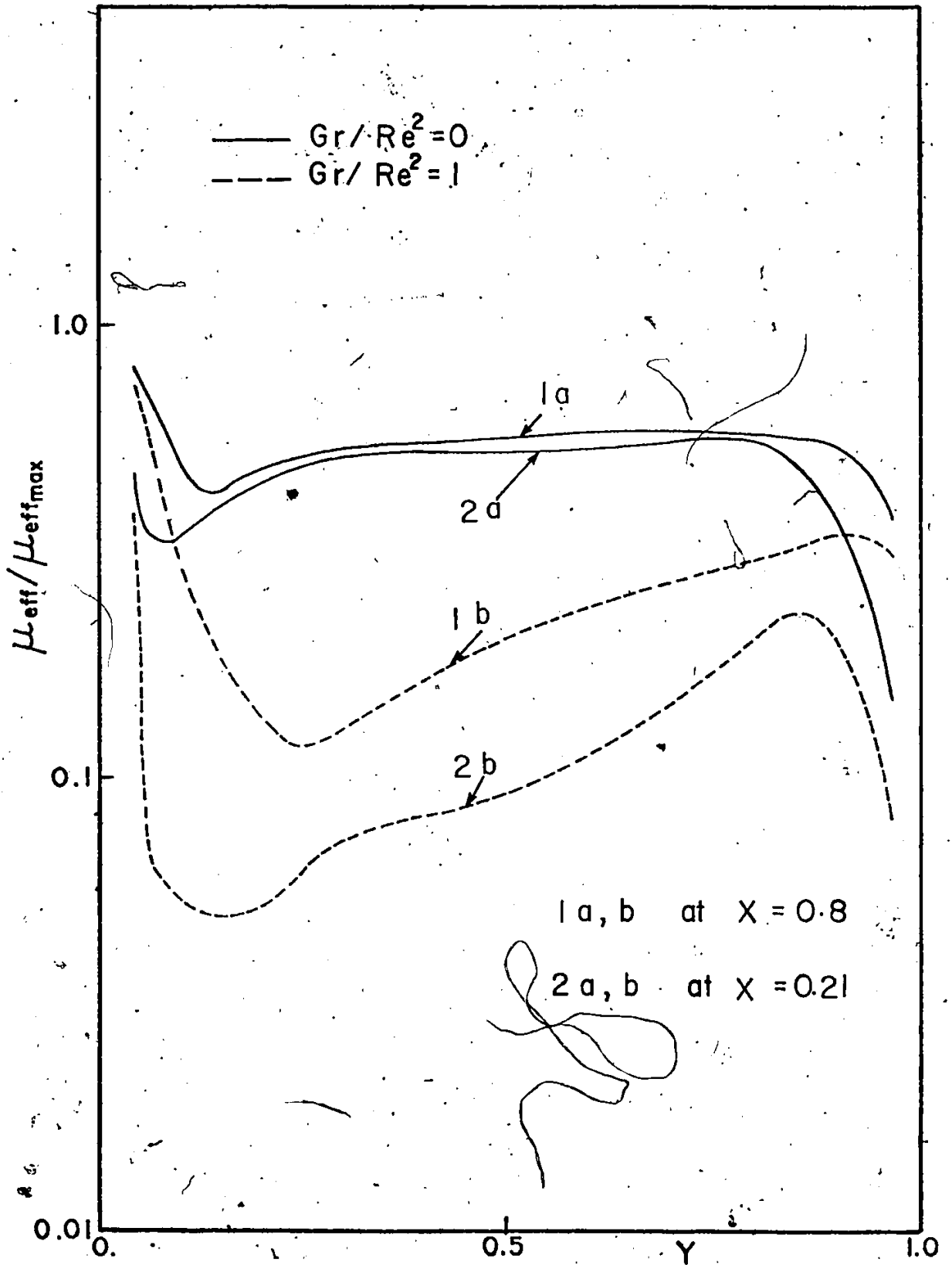


Fig.6.15 Vertical Effective Viscosity Distribution  
 $Re = 8.4 \times 10^4$

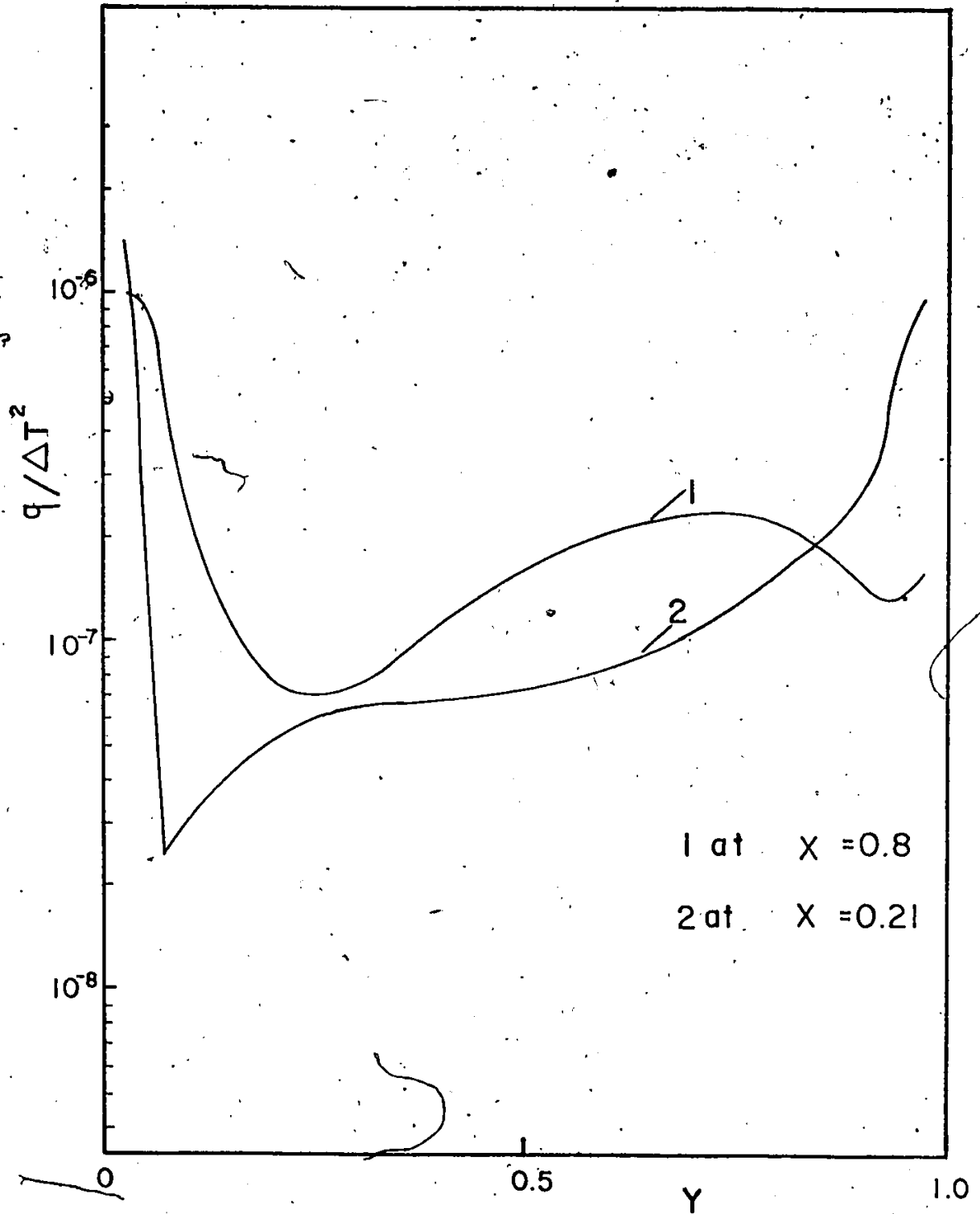


Fig.6.16 Vertical Distribution of the Mean Square Temperature Fluctuation,  $Re = 8.4 \times 10^4$

REFERENCES

1. D. Grand, A. Latrobe, P.H. Vernier, "Heat Transfer by Recirculating Flow with Body Forces in a Rectangular Cavity", a numerical study, Fifth International Heat Transfer Conference, Japan, Sept. 3-7, 1974, N.C. 5.6, pp. 197-201.
2. A.D. Gosman, "Flow Heat and Mass Transfer in Turbulent Recirculating Flows". Slide Panels of Lectures, Aug. 4-6, 1976, McGill University, Montreal.
3. G.K. Batchelor, "On Steady Laminar Flow with Closed Streamlines at Large Reynolds Numbers", J. Fluid Mech., 1, (1956), pp. 177-190.
4. H.B. Squire, "Note on the Motion Inside a Region of Recirculation", (1956), J. Roy. Aero. Soc. 60, pp. 203-205.
5. L.F. Donovan, N.A.S.A. Tech. Memo X-52767, 1970.
6. O.R. Burggraf, "Analytical and Numerical Studies of the Structure of Steady Separated Flows", J. Fluid Mech., 24, 113.
7. F. Pan and A. Acrivos, "Steady Flows in Rectangular Cavities", J. Fluid Mech., 28, 1967, pp. 643-655.
8. R.F. Weiss and B.H. Florsheim, "Flow in a Cavity at Low Reynolds Number" The Physics of Fluids, Vol. 8, No. 9 (1965), p. 1631.
9. R.D. Mills, "Numerical Solutions of the Viscous Flow Equations for a Class of Closed Flows", J. Roy. Aero. Soc., 69, 1965, pp. 714-718.
10. D. Greenspan, "Numerical Studies of Prototype Cavity Flow Problems", Computer J., 12, 1969, pp. 88-93.
11. A.K. Runchal, D.B. Spalding and M. Wolfshtein, "Numerical Solution of the Elliptic Equations for Transport of Vorticity, Heat and Matter in Two-Dimensional Flow", Phys. Fluid., 12, 1969, pp. 21-28.
12. A.K. Runchal and M. Wolfshtein, "Numerical Integration Procedure for the Steady State Navier-Stokes Equation", J. Mech. Engng. Sci., 11, 445.
13. A.D. Gosman, W.M. Pan, A.K. Runchal, D.B. Spalding and M. Wolfshtein, "Heat and Mass Transfer in Recirculating Flows", Academic Press, New York, 1969, pp. 159-167.

14. K. Torrance, R. Davis, K. Eike, P. Gill, D. Gutman, A. Hsui, S. Lyons and H. Zien, "Cavity Flows Driven by Buoyancy and Shear", J. Fluid Mech. 51 (1972), pp. 221-231.
15. M. Nallasamy and K. Krishna Prasad, "On Cavity Flow at High Reynolds Numbers", J. Fluid Mech., 79, 1977, pp. 391-414.
16. B.E. Launder and D.B. Spalding, "Mathematical Models of Turbulence", Academic Press, London, 1972.
17. H. Schlichting, "Boundary Layer Theory", 6th Ed., McGraw-Hill, 1968.
18. M.P. Escudier, "The Distribution of Mixing-Length in Turbulent Flows Near Walls", Imperial College, Heat Transfer Section Rep. TWF/TN/1, 1966.
19. E.R. Van Driest, "On Turbulent Flow Near a Wall", J. Aero. Sci., 23, 1956, pp. 1007.
20. S.V. Patankar and D.B. Spalding, "Heat and Mass Transfer in Boundary Layers", 2nd Edition, Intertext Books, London, 1970.
21. A.N. Kolmogorov, "Equations of Turbulent Motion of an Incompressible Turbulent Fluid", Izv. Akad. Nauk SSSR Ser Phys. VI, No. 1-2, 1942, pp. 56.
22. E. Bradshaw, D.H. Ferriss and N.P. Atwell, "Calculation of Boundary Layer Development Using the Turbulent Energy Equation", J. Fluid Mech., 28, 1967, pp. 593.
23. V.W. Nee and L.S.G. Kovaszny, "The Calculation of the Incompressible Turbulent Boundary Layer by a Simple Theory", Proc. of AFOSR/IFP Conf. on Computation of Turbulent Boundary Layers, Vol. I, Stanford University. Also, Physics of Fluids, 12, 1968, pp. 473.
24. K.H. NG and D.B. Spalding, "Some Applications of a Model of Turbulence to Boundary Layers Near Walls", Physics of Fluids, 15, 1972.
25. D.B. Spalding, "The Prediction of Two-Dimensional Steady Turbulent Flows", Imperial College, Heat Transfer Section Rep. EF/TN/A/16, 1970.
26. W.P. Jones and B.E. Launder, "The Prediction of Laminarization With Two-Equation Model of Turbulence", Int. J. Heat and Mass Transfer, 15, 1972, pp. 301.
27. K. Hanjalic, "Two-Dimensional Asymmetric Turbulent Flow in Ducts", Ph.D. Thesis, University of London.

28. D.B. Spalding, "Concentration Fluctuations in a Round Turbulent Free Jet", J. Chem. Eng. Sci., 26, 1971, pp. 95.
29. B.E. Launder and D.B. Spalding, "The Numerical Computation of Turbulent Flows", Comp. Math. Appl. Mech. Engg. 3, 1974, pp. 269-289.
30. F. Taminini, "On the Numerical Prediction of Turbulent Diffusion Flames", Presented at the Joint Meeting of the Central and Western States Section of the Combustion Institute, Southwest Research Institute, San Antonio, Tex., 1975, Apr. 21-22.
31. O.A. Plumb and L.A. Kennedy, "Application of a K- $\epsilon$  Turbulence Model to Natural Convection from a Vertical Isothermal Surface", Transactions of the ASME - Journal of Heat Transfer, Feb. 1977, pp. 79-85.
32. A.S. Mujumdar and Y.K. Li, Communication re: "The Numerical Prediction of Turbulent Flow and Heat Transfer in the Entrance Region of a Parallel Plate Duct", By Emery and Gesner, J. of Heat Transfer, Trans. ASME, Series C., Vol. 99, pp. 347-349.
33. M. Salcudean and R.I.L. Guthrie, "Turbulent Flow in Filling Ladles", Met. Transactions, 9B, Dec. 1978, pp. 673-680.
34. A.K. Mujumdar, V.S. Pratap and D.B. Spalding, "Numerical Computation of Flow in Rotating Ducts", J. of Fluids Engineering, Trans. of ASME, March 1977, pp. 148.
35. D.B. Spalding and C.L.V. Jayatilaka, "A Survey of the Theoretical and Experimental Information on the Resistance of the Laminar Sub-Layer to Heat and Mass Transfer", Proc. 2nd All Soviet Union Conf. on Heat and Mass Transfer, Minsk, USSR, 1964, 2, pp. 234-264 (in Russian); English Translation, ed. by C. Gayley, J.P. Hartnett and E.R.G. Eckert, Rand Corp., California, 1966.
36. S.D. Conte, "Elementary Numerical Analysis", McGraw-Hill, New York, 1965.

APPENDIX ATridiagonal Matrix Algorithm (TDMA)

Starting with Eq. (5.1):

$$\underline{A}_p \phi_p = \underline{a}_n \phi_N + \underline{a}_s \phi_S + (\underline{a}_e \phi_E + \underline{a}_w \phi_W + Su)$$

with the underlined quantities assumed known. This equation can be represented by a system of  $N_j - 2$  equations of the general form:

$$d_i \phi_i = a_i \phi_{i+1} + b_i \phi_{i-1} + c_i$$

or

$$-a_i \phi_{i+1} + d_i \phi_i - b_i \phi_{i-1} = c_i \quad (A.1)$$

where  $d_i = A_p$ ;  $a_i = a_n$ ;  $b_i = a_s$ ;

$$c_i = a_e \phi_E + a_w \phi_W + Su$$

and the values of  $\phi_1$  and  $\phi_{N_j}$  are specified.

The set of equations (A.1) can be written in the following matrix form:

$$P\phi = Q$$







$$\begin{aligned}
 T_2 C_2 &= c_2 + b_2 \phi_1 \\
 -B_3 C_2 + T_3 C_3 &= c_3 \\
 -B_4 C_3 + T_4 C_4 &= c_4 \\
 &\dots\dots\dots \\
 -B_j C_{j-1} + T_j C_j &= c_j \\
 &\dots\dots\dots \\
 -B_{Nj-1} C_{Nj-2} + T_{Nj-1} C_{Nj-1} &= c_{Nj-1} + a_{Nj-1} \phi_{Nj}
 \end{aligned}$$

with  $B_j = b_j$  as expressed in Eq. (A.3) and defining  $C_1 = \phi_1$ , the solution of C can be obtained directly. This yields the following, provided that  $T_j \neq 0$  :

$$C_j = (c_j + b_j c_{j-1}) / T_j \quad 2 \leq J \leq Nj-2$$

$$C_{Nj-1} = (c_{Nj-1} + b_{Nj-1} c_{Nj-2}) / T_{Nj-1} + a_{Nj-1} \phi_{Nj} / T_{Nj-1} \quad (A.6)$$

By defining  $A_{Nj-1} = a_{Nj-1} / T_{Nj-1}$ , the second term on the right-hand side of  $C_{Nj-1}$  becomes  $\phi_{Nj} A_{Nj-1}$ .

With all the C's defined as in Eq. (A.6), the  $\phi$ 's can be solved using Eq. (A.5), which gives:

$$\begin{bmatrix} 1 & -A_2 & & & & & \\ & 1 & -A_3 & & & & \\ & & \dots\dots & & & & \\ & & & 1 & -A_j & & \\ & & & & \dots\dots & & \\ & & & & & 1 & -A_{Nj-2} \\ & & & & & & 1 \end{bmatrix}
 \begin{bmatrix} \phi_2 \\ \phi_3 \\ \dots \\ \phi_j \\ \dots \\ \phi_{Nj-2} \\ \phi_{Nj-1} \end{bmatrix}
 =
 \begin{bmatrix} c_2 \\ c_3 \\ \dots \\ c_j \\ \dots \\ c_{Nj-2} \\ c_{Nj-1} \end{bmatrix}$$

Finally  $\phi$  is solved by back substitution, beginning with  $\phi_{Nj-1}$  giving,

$$\left. \begin{aligned} \phi_{Nj-1} &= c_{Nj-1} \\ \phi_{Nj-2} - A_{Nj-2} \phi_{Nj-1} &= c_{Nj-2} \\ \dots & \\ \phi_j - A_j \phi_{j+1} &= c_j \\ \dots & \\ \phi_2 - A_2 \phi_3 &= c_2 \end{aligned} \right\} \equiv \left\{ \begin{aligned} \phi_{Nj-1} &= c_{Nj-1} \\ \phi_{Nj-2} &= c_{Nj-2} + A_{Nj-2} \phi_{Nj-1} \\ \dots & \\ \phi_j &= c_j + A_j \phi_{j+1} \\ \dots & \\ \phi_2 &= c_2 + A_3 \phi_3 \end{aligned} \right.$$

with the C's defining as in Eq. (A.6), the  $\phi$ 's can be written as:

$$\phi_j = (c_j + b_j c_{j-1}) / T_j + A_j \phi_{j-1} \quad 2 \leq j \leq Nj-1$$

with

$$T_j = d_j - b_j A_{j-1} \quad 2 \leq j \leq Nj-1$$

$$A_j = a_j / T_j, \quad 2 \leq j \leq Nj-1$$

$$C_j = (c_j + b_j c_{j-1}) / T_j, \quad 2 \leq j \leq Nj-2$$

$$A_1 = 0 \quad ; \quad C_1 = \phi_1$$

Note that the calculation of the coefficients  $c_j$ ,  $A_j$  and  $T_j$  has to be calculated from  $j = 2$  to  $Nj-1$ , while the calculation of the  $\phi$ 's is from  $j = Nj-1$  to 2.



APPENDIX B

A Sample Computer Program

C\*\*\*\*\*  
C TUD-DIMENSIONAL(PLANE OR AXISYMMETRICAL) C  
C BASIC TEST CASE : C  
C C  
C PRIDITION OF A3TURBULENT RECIRCULATORY FLOW C  
C IN RECTANGULAR CAVITY AFFECTED BY BUOYANCY FORCES. C  
C\*\*\*\*\* C

1 DIMENSION HEDU(9), HEDV(9), HEDP(9), HEDT(9), HEDK(9), HEDD(9), HEDH(9)  
1 HEDA(9), HEDB(9), HEDQ(9), HEDR(9), HEDG(9), HEDE(9) 0340  
2 COMMON 0350  
1/UVEL/RESORU, NSUPU, URFU, DXEPU(32), DXPMU(32), SEUU(32) 0360  
1/VVEL/RESORV, NSUPV, URFV, DYNPV(32), DYPSV(32), SNSV(32), RCV(32) 0370  
1/PCOR/RESORH, NSUPP, URFP, DU(30,30), DV(30,30), IPREF, JPREF 0380  
1/TEN/RESORK, NSUPK, URFK 0390  
1/TDIS/RESORE, NSUPD, URFE 0400  
1/VAR/U(30,30), V(30,30), P(30,30), PP(30,30), TE(30,30), ED(30,30) 0410  
1/ALL/IT, JT, NI, NJ, NIMI, NJMI, GREAT 0420  
3 COMMON 0430  
1/GEOM/INDCOS, X(32), Y(32), DXEP(32), DXPM(32), DYNP(32), DYPS(32), 0440  
1 SNS(32), SEH(32), XU(32), YV(32), R(32), RV(32) 0450  
1/FLUPR/URFVIS, VISCOS, DENSIT, PRANDT, DEN(30,30), VIS(30,30), 0480  
2 VISD(30,30)  
1/PROB1/UIN, TEIN, EDIN, FLOWIN, ALANDA,  
2 RSMALL, RLARGE, AL1, AL2, JSTEP, ISTEP, JSTP1, JSTM1, ISTP1, ISTH1,  
3 NITER, US  
1/TURB/GEN(30,30), CD, CHU, C1, C2, CAPP, ELDG, PRED, PRTE 0490  
1/WALLF/YPLUSN(30,30), XPLUSU(30,30), TAUN(30,30), TAUW(30,30)  
1/COEF/AP(30,30), AN(30,30), AS(30,30), AE(30,30), AU(30,30), SU(30,30), 0510  
1 SP(30,30)

4 COMMON  
1/SUS/SU1(30,30), SU2(30,30), SU3(30,30), SU4(30,30)  
1/SUSP/SUKD(30,30), SPKD(30,30)  
1/TEMP/T(30,30), GAMH(30,30), RESORT, NSUPT, URFT, PRANDL, PFUN,  
2 TWALLN, TIN, GANQ(30,30), TBTOTN  
1/INSTF/OE(30,30), PROE, CB1, CQ2, RESQE, URFO, BETA, GRAVITY, C3, C4, NSWPB,  
1 SUDE(30,30), GENB(30,30), SPOE(30,30), RESORB  
1/AREA1/INCT  
1/FINAL/ALNUUL(32), ALNUUL(32), ALNUUT(32), ALNUWT(32),  
2 VAVR(30,30), RA(30,30), ANGLE(30,30), UAVR(30,30), FENRG(30,30)



1060  
1050  
1070

INCALD=.TRUE.  
INCALK=.TRUE.  
INPRO=.TRUE.  
INCT=.TRUE.  
INCALQ=.TRUE.  
INCALR=.TRUE.  
INCALG=.TRUE.  
INCAFE=.TRUE.

1080

C-----FLUID PROPERTIES

DENSIT=974.  
VISCOS=3.72E-4  
PRANDL=2.33  
TK=0.16  
CPP=1002.3  
BETA=6.72E-4  
NU=VISCOS/DENSIT

1110

C-----TURBULENCE CONSTANTS

CMU=0.09  
CD=1.00  
C1=1.44  
C2=1.92  
C3=1.44  
C4=0.5  
CAPPA=.4187  
ELOG=9.793  
PRED=1.3  
PRTE=1.0  
PRANDT=0.9  
PFUN=PRANDL/PRANDT  
PFUN=9.24\*PFUN\*0.75

1200

C-----BOUNDARY VALUES

UIN=0.1E-9  
TURBIN=.03  
TEIN=1.E-6  
QEIN=0.001\*TURBIN  
ALANDA=0.005  
EPIN=1.E-4

1230

1250

38  
39  
40  
41  
42  
43  
44  
45

46  
47  
48  
49  
50  
51  
52

53  
54  
55  
56  
57  
58  
59  
60  
61  
62  
63  
64  
65

66  
67  
68  
69  
70  
71

```

C-----PRESSURE CALCULATION
C
C
72 JREF=9
73 IPREF=9
74 TIN=350.
C
C-----PROGRAM CONTROL AND MONITOR
C
75 MAXIT=75
76 IMON=4
77 JMON=4
78 URFU=0.5
79 URFV=0.5
80 URFP=1.0
81 URFT=1.0
82 URFE=0.7
83 URFK=0.7
84 URFQ=0.7
85 URFVIS=0.7
86 TWALEN=400.
87 TBOTON=300.
88 INDPRI=100
89 SDRMAX=0.01
90 GRAVITY=-9.806
C
CHAPTER 2 2 2 2 2 INITIAL OPERATIONS 2 2 2 2 2 2 2 2
C
C-----CALCULATE GEOMETRICAL QUANTITIES AND SET VARIABLES TO ZERO
C
91 CALL INIT
C-----SPECIFY INLET CONDITIONS
C
92 US=500.*NU/X(INI)
93 U(2,2)=UIN
94 DO 202 I=2,NI
95 DO 202 J=2,NJM1
96 T(I,J)=TIN
97 T(2,1)=TBOTON
98 TE(I,J)=1.E-10
99 QE(I,J)=QEIN
100 QE(I,J)=1.E-6
1270
1300
1340
1350
1360
1370
1380
1390
1400
1420
1430
1440
1450
1460
1470
1480

```

```

101 ED(I,J)=1.E-6
102 U(I,1)=US
103
104 202 U(I,J)=UIN
105 TE(1,2)=TE(2,2)
106 ED(1,2)=ED(2,2)
107 DO 203 I=1,NI
108 T(I,NJ)=TWALLN
109 DO 203 J=1,NJ
110 YPLUSN(I,J)=12.
111 DO 204 J=1,NJ
112 DO 204 I=1,NI
113 XPLUS(I,J)=12.
114 204 CONTINUE
115 CALL PROPS
116
117 C
118 C-----INITIAL OUTPUT
119 C
120 WRITE(6,220) UIN
121 WRITE(6,221) TIN
122 RENOLD=US*X(NI)/NU
123 GR=GRAVITY*BETA*(TWALLN-T(2,1))*Y(NJ)**3/NU**2
124 WRITE(6,222) TWALLN
125 WRITE(6,223) PRANDL
126 WRITE(6,231) RENOLD
127 WRITE(6,232) GR
128 WRITE(6,250) VISCOS
129 WRITE(6,260) DENSIT
130 IF(INCALU) CALL PRINT(2,2,NI,NJ,IT,IT,XU,Y,U,HEDU)
131 IF(INCALV) CALL PRINT(2,2,NI,NJ,IT,IT,X,YV,V,HEDV)
132 IF(INCALP) CALL PRINT(2,2,NI,NJ,IT,IT,X,Y,P,HEDP)
133 INCT=.TRUE.
134 IF(INCALI) CALL PRINT(2,2,NI,NJ,IT,IT,X,Y,T,HEDT)
135 INCI=.FALSE.
136 IE(INCALK) CALL PRINT(2,2,NI,NJ,IT,IT,X,Y,TE,HEDK)
137 IF(INCALD) CALL PRINT(2,2,NI,NJ,IT,IT,X,Y,ED,HEDD)
138 IF(INCALQ) CALL PRINT(2,2,NI,NJ,IT,IT,X,Y,OE,HEDQ)
139 RESORT=0.
140
141 C
142 CHAPTER 3 3 3 3 3 ITERATION LOOP 3 3 3 3 3 3 3 3 3
143 C
144 WRITE(6,310) IMON,JMON
145 300 NITER=NITER+1

```

1680

1690

1720

1770

1780

1790

1800

1810

1820

1830

1920

1930

1940

1950

1960



```

C-----TERMINATION TESTS
C
167   SORCE=AMAX1(RESORH,RESORU,RESORV,RESORT)
168   IF(INITER.EQ.20.AND.SORCE.GT.1.0E4*SORMAX) GO TO 302
169   IF(NITER.EQ.MAXIT) GO TO 302
C
170   GO TO 300
171   302 CONTINUE
C
CHAPTER 4 4 4 4 4 FINAL OPERATIONS AND OUTPUT 4 4 4 4 4
C
172   IF(INCALU) CALL PRINT(2,2,NI,NJ,IT,JT,XU,Y,U,HEDU)
173   IF(INCALV) CALL PRINT(2,2,NI,NJ,IT,JT,X,YU,V,HEDV)
174   IF(INCALP) CALL PRINT(2,2,NI,NJ,IT,JT,X,Y,P,HEDP)
175   INCT=.TRUE.
176   IF(INCALT) CALL PRINT(2,2,NI,NJ,IT,JT,X,Y,T,HEDT)
177   INCT=.FALSE.
178   IF(INCALK) CALL PRINT(2,2,NI,NJ,IT,JT,X,Y,TE,HEDK)
179   IF(INCALD) CALL PRINT(2,2,NI,NJ,IT,JT,X,Y,ED,HEDD)
180   IF(INCALO) CALL PRINT(2,2,NI,NJ,IT,JT,X,Y,VIS,HEDM)
181   IF(INCALQ) CALL PRINT(2,2,NI,NJ,IT,JT,X,Y,QE,HEDQ)
182   J=NJMI
183   CDTERM=CMU**0.25
184   DYN=YV(NJ)-Y(NJMI)
C
C CALCULATION OF THE LOCAL AND AVERAGE NUSSELT NUMBER ALONG THE TOP WALL
C
185   XREF=X(NIMI)-X(2)
186   TREF=TWALLN-TBOTOM
187   AVNUUL=0.
188   AVNUUT=0.
189   AVNUWL=0.
190   AVNUWL=0.
191   WRITE(6,402)
192   DO 401 I=2,NIMI
193     UPLUSN=ALOG(ELOG*YPLUSN(I,NJMI))/CAPPA
194     HFLUXT=DEN(I,J)*CPP*SORT(TE(I,J))*CDTERM*(TWALLN-T(I,NJMI))/
      1*(PRANDT*(UPLUSN+PFUN))
195     HFLUXL=TK*(TWALLN-T(I,NJMI))/DYNP(NJMI)
196     HFLUXL=ABS(HFLUXL)
197     HFLUXT=ABS(HFLUXT)

```

2220

2240  
2250  
2290

2310  
2320  
2330  
2340  
2350  
2360  
2370

2380  
2390  
2400

2490  
2500

```

198 ALNUUL(I)=HFLUXL*1./(TK*TREF)
199 ALNUWL(I)=HFLUXL*XREF/(TK*TREF)
200 ALNUUT(I)=HFLUXT*1./(TK*TREF)
201 ALNUWT(I)=HFLUXT*XREF/(TK*TREF)
202 AVNUUL=AVNUUL+ALNUUL(I)*DXEP(I)
203 AVNUWL=AVNUWL+ALNUWL(I)*DXEP(I)
204 AVNUUT=AVNUUT+ALNUUT(I)*DXEP(I)
205 AVNUWT=AVNUWT+ALNUWT(I)*DXEP(I)
206 WRITE(6,403) I,ALNUUL(I),ALNUWL(I),ALNUUT(I),ALNUWT(I)
207 CONTINUE
401
208 AVNUUL=AVNUUL/XREF
209 AVNUWL=AVNUWL/XREF
210 AVNUUT=AVNUUT/XREF
211 AVNUWT=AVNUWT/XREF
212 WRITE(6,410) AVNUUL,AVNUWL,AVNUUT,AVNUWT

```

C CALCULATION OF NON-DIMENSIONAL TEMPERATURE AND RESULTANT VELOCITY

```

213 TREF=TWALLN-TBOTOM
214 DO 510 I=1,NI
215 DO 510 J=1,NJ
216 RA(I,J)=0.
217 ANGLE(I,J)=0.
510 CONTINUE
DO 500 I=2,NIM1
DO 500 J=2,NJM1
T(I,J)=(T(I,J)-TBOTOM)/TREF
UAVR(I,J)=0.5*(U(I,J)+U(I+1,J))
VAVR(I,J)=0.5*(V(I,J)+V(I,J+1))
RA(I,J)=SQRT(UAVR(I,J)**2+VAVR(I,J)**2)
ANGLE(I,J)=ATAN(VAVR(I,J)/UAVR(I,J))
ANGLE(I,J)=ANGLE(I,J)*180./3.14159
IF(UAVR(I,J).LT.0.) ANGLE(I,J)=ANGLE(I,J)+180.
500 CONTINUE
IF(INCALT) CALL PRINT(2,2,NI,NJ,IT,IT,X,Y,T,HEDT)
IF(INCALR) CALL PRINT(2,2,NI,NJ,IT,IT,X,Y,RA,HEDR)
IF(INCALG) CALL PRINT(2,2,NI,NJ,IT,IT,X,Y,ANGLE,HEDG)
STOP

```

```

C-----FORMAT STATEMENTS
C
C
233 221 FORMAT(1H0,25X,'INITIAL FLUID TEMPERATURE ',T60,1H=,3X,1PE11.3)
234 220 FORMAT(//1H0,15X,'INITIAL FLUID VELOCITY',T60,3X,1PE11.3)
235 222 FORMAT(//1H0,15X,'THERMAL BOUNDARY CONDITIONS ARE '///
11H0,25X,'PRESCRIBED TOP WALL TEMPERATURE= ',1PE11.3//
11H0,25X,'ADIBATIC SIDE WALL '///)
236 223 FORMAT(1H0,15X,'RPAIDL NUMBER',T60,1H=,3X,1PE11.3)
237 231 FORMAT(1H0,15X,16HREYNOLDS NUMBER ,T60,1H=,3X,1PE11.3)
238 232 FORMAT(1H0,15X,16HGRASHOF NUMBER ,T60,1H=,3X,1PE11.3)
239 250 FORMAT(1H0,15X,18HLAMINAR VISCOSITY ,T60,1H=,3X,1PE11.3)
240 260 FORMAT(1H0,15X,14HFLUID DENSITY ,T60,1H=,3X,1PE11.3)
241 310 FORMAT(1H0,4HITER,4X,106HI-----ABSOLUTE RESIDUAL SOURCE SUM
1S-----1
2 1H(I,12,1H,I2,1H),9H-----I/2X,2HNO,6X,4HUMOM,6X,4HVMDM,6X,
34HMASS,6X,4HENER,6X,4HTKIN,6X,4HDISP,10X,1HU,9X,1HV,9X,1HP,9X,1HT,
49X,1HK,9X,1HD/)
242 311 FORMAT(1H,I3,4X,1P6E10.3,3X,1P6E10.3)
243 410 FORMAT(//5X,'AV.LAM.NU/UL =',F10.5,2X,'AV.LAM.NU/L =',F10.5,
1'AV.TUR.NU/UL =',F10.5,2X,'AV.TUR.NU/L =',F10.5)
244 402 FORNAT(//5X,1H1,5X,
1'L.LAM.NU/UL',2X,'L.LAM.NU/L',2X,'L.TUR.NU/UL',2X,
2'L.TUR.NU/L')
245 403 FORMAT(/5X,I2,6X,E10.3,5X,E10.3,3X,E10.3,2X,E10.3)
246 END

```

2560

2  
26  
2630  
2640  
2650  
2660  
2670  
2680  
2690  
2700

2730























```

504 C-----COMPUTE SUM OF ABSOLUTE MASS SOURCES
505 RESORM=RESORH+ABS(SKP)
506 101 CONTINUE
507 100 CONTINUE
508 C
509 CHAPTER 2 2 2 2 2 2 2 2 2 2 2 2 2 2 2 2 2
510 CALL MODP
511 C
512 CHAPTER 3 3 3 3 3 3 3 3 3 3 3 3 3 3 3 3 3
513 C
514 DO 300 I=2,NIM1
515 DO 301 J=2,NJM1
516 301 AP(I,J)=AM(I,J)+AS(I,J)+AE(I,J)+AM(I,J)-SP(I,J)
517 300 CONTINUE
518 C
519 CHAPTER 4 4 4 4 4 4 4 4 4 4 4 4 4 4 4 4 4
520 C
521 C
522 CHAPTER 5 5 5 5 5 5 5 5 5 5 5 5 5 5 5 5 5
523 DO 400 N=1,NSUPP
524 400 CALL LISOLV(2,2,NI,NJ,IT,JT,PP)
525 C
526 C-----VELOCITIES
527 DO 500 I=2,NIM1
528 DO 501 J=2,NJM1
529 IF(I.NE.2) U(I,J)=U(I,J)+DU(I,J)*(PP(I-1,J)-PP(I,J))
530 IF(J.NE.2) V(I,J)=V(I,J)+DV(I,J)*(PP(I,J-1)-PP(I,J))
531 501 CONTINUE
532 500 CONTINUE
533 C-----PRESSURES (WITH PROVISION FOR UNDER-RELAXATION)
534 PPREF=PP(IPREF,JPREF)
535 DO 502 I=2,NIM1
536 DO 503 J=2,NJM1
537 P(I,J)=P(I,J)+URFP*(PP(I,J)-PPREF)
538 PP(I,J)=0.0
539 503 CONTINUE
540 502 CONTINUE
541 RETURN
542 END
543 CALCP
544 CALCP
545 CALCP
546 CALCP
547 CALCP
548 CALCP
549 CALCP
550 CALCP
551 CALCP
552 CALCP
553 CALCP
554 CALCP
555 CALCP
556 CALCP
557 CALCP
558 CALCP
559 CALCP
560 CALCP
561 CALCP
562 CALCP
563 CALCP
564 CALCP
565 CALCP
566 CALCP
567 CALCP
568 CALCP
569 CALCP
570 CALCP
571 CALCP
572 CALCP
573 CALCP
574 CALCP
575 CALCP
576 CALCP
577 CALCP
578 CALCP
579 CALCP
580 CALCP
581 CALCP
582 CALCP
583 CALCP
584 CALCP
585 CALCP
586 CALCP
587 CALCP
588 CALCP
589 CALCP
590 CALCP
591 CALCP
592 CALCP
593 CALCP
594 CALCP
595 CALCP
596 CALCP
597 CALCP
598 CALCP
599 CALCP
600 CALCP
601 CALCP
602 CALCP
603 CALCP
604 CALCP
605 CALCP
606 CALCP
607 CALCP
608 CALCP
609 CALCP
610 CALCP
611 CALCP
612 CALCP
613 CALCP
614 CALCP
615 CALCP
616 CALCP
617 CALCP
618 CALCP
619 CALCP
620 CALCP
621 CALCP
622 CALCP
623 CALCP
624 CALCP
625 CALCP
626 CALCP
627 CALCP
628 CALCP
629 CALCP
630 CALCP
631 CALCP
632 CALCP
633 CALCP
634 CALCP
635 CALCP
636 CALCP
637 CALCP
638 CALCP
639 CALCP
640 CALCP
641 CALCP
642 CALCP
643 CALCP
644 CALCP
645 CALCP
646 CALCP
647 CALCP
648 CALCP
649 CALCP
650 CALCP
651 CALCP
652 CALCP
653 CALCP
654 CALCP
655 CALCP
656 CALCP
657 CALCP
658 CALCP
659 CALCP
660 CALCP
661 CALCP
662 CALCP
663 CALCP
664 CALCP
665 CALCP
666 CALCP
667 CALCP
668 CALCP
669 CALCP
670 CALCP
671 CALCP
672 CALCP
673 CALCP
674 CALCP
675 CALCP
676 CALCP
677 CALCP
678 CALCP
679 CALCP
680 CALCP
681 CALCP
682 CALCP
683 CALCP
684 CALCP
685 CALCP
686 CALCP
687 CALCP
688 CALCP
689 CALCP
690 CALCP
691 CALCP
692 CALCP
693 CALCP
694 CALCP
695 CALCP
696 CALCP
697 CALCP
698 CALCP
699 CALCP
700 CALCP
701 CALCP
702 CALCP
703 CALCP
704 CALCP
705 CALCP
706 CALCP
707 CALCP
708 CALCP
709 CALCP
710 CALCP
711 CALCP
712 CALCP
713 CALCP
714 CALCP
715 CALCP
716 CALCP
717 CALCP
718 CALCP
719 CALCP
720 CALCP
721 CALCP
722 CALCP
723 CALCP
724 CALCP
725 CALCP
726 CALCP
727 CALCP
728 CALCP
729 CALCP
730 CALCP
731 CALCP
732 CALCP
733 CALCP
734 CALCP
735 CALCP
736 CALCP
737 CALCP
738 CALCP
739 CALCP
740 CALCP
741 CALCP
742 CALCP
743 CALCP
744 CALCP
745 CALCP
746 CALCP
747 CALCP
748 CALCP
749 CALCP
750 CALCP
751 CALCP
752 CALCP
753 CALCP
754 CALCP
755 CALCP
756 CALCP
757 CALCP
758 CALCP
759 CALCP
760 CALCP
761 CALCP
762 CALCP
763 CALCP
764 CALCP
765 CALCP
766 CALCP
767 CALCP
768 CALCP
769 CALCP
770 CALCP
771 CALCP
772 CALCP
773 CALCP
774 CALCP
775 CALCP
776 CALCP
777 CALCP
778 CALCP
779 CALCP
780 CALCP
781 CALCP
782 CALCP
783 CALCP
784 CALCP
785 CALCP
786 CALCP
787 CALCP
788 CALCP
789 CALCP
790 CALCP
791 CALCP
792 CALCP
793 CALCP
794 CALCP
795 CALCP
796 CALCP
797 CALCP
798 CALCP
799 CALCP
800 CALCP
801 CALCP
802 CALCP
803 CALCP
804 CALCP
805 CALCP
806 CALCP
807 CALCP
808 CALCP
809 CALCP
810 CALCP
811 CALCP
812 CALCP
813 CALCP
814 CALCP
815 CALCP
816 CALCP
817 CALCP
818 CALCP
819 CALCP
820 CALCP
821 CALCP
822 CALCP
823 CALCP
824 CALCP
825 CALCP
826 CALCP
827 CALCP
828 CALCP
829 CALCP
830 CALCP
831 CALCP
832 CALCP
833 CALCP
834 CALCP
835 CALCP
836 CALCP
837 CALCP
838 CALCP
839 CALCP
840 CALCP
841 CALCP
842 CALCP
843 CALCP
844 CALCP
845 CALCP
846 CALCP
847 CALCP
848 CALCP
849 CALCP
850 CALCP
851 CALCP
852 CALCP
853 CALCP
854 CALCP
855 CALCP
856 CALCP
857 CALCP
858 CALCP
859 CALCP
860 CALCP
861 CALCP
862 CALCP
863 CALCP
864 CALCP
865 CALCP
866 CALCP
867 CALCP
868 CALCP
869 CALCP
870 CALCP
871 CALCP
872 CALCP
873 CALCP
874 CALCP
875 CALCP
876 CALCP
877 CALCP
878 CALCP
879 CALCP
880 CALCP
881 CALCP
882 CALCP
883 CALCP
884 CALCP
885 CALCP
886 CALCP
887 CALCP
888 CALCP
889 CALCP
890 CALCP
891 CALCP
892 CALCP
893 CALCP
894 CALCP
895 CALCP
896 CALCP
897 CALCP
898 CALCP
899 CALCP
900 CALCP

```

6

```

529 SUBROUTINE CALCT
530 COHON
1/VAR/U(30,30),V(30,30),P(30,30),PP(30,30),TE(30,30),ED(30,30) 0420
1/ALL/IT,IT,NI,NJ,NIM,NJM,GREAT
COHON
1/GEON/INDCOS,X(32),Y(32),DXEP(32),DXPM(32),DYNP(32),DYPS(32), 0450
1 SNS(32),SEW(32),XU(32),YU(32),S(32),RV(32)
1/FLUPR/URFVIS,VISCOS,DENSIT,PRANDT,DEN(30,30),VIS(30,30),
2 VISD(30,30)
1/PROB1/VIIN,TEIN,EDIN,FLOWIN,ALANDA,
2 RSHALL,RLARGE,AL1,AL2,JSTEP,ISTEP,JSTP1,JSTH1,ISTP1,ISTH1,
3 MITER,US
1/COEF/AP(30,30),AN(30,30),AS(30,30),AE(30,30),AW(30,30),SU(30,30), 0510
1 SP(30,30)
1/TEMP/T(30,30),GAHH(30,30),RESORT,NSWPT,URFT,PRANDL,PFUN,
2 TWALLN,TIN,GARB(30,30),TBOTON
LOGICAL INCI

```

```

C
CHAPTER 1 1 1 1 1 ASSEMBLY OF COEFFICIENTS 1 1 1 1 1
C

```

```

533 DO 100 I=2,NIM1
534 DO 101 J=2,NJM1
C----- COMPUTE AREAS VOLUME
535 AREAN=RV(J+1)*SEW(I)
536 AREAS=RV(J)*SEW(I)
537 AREAEU=R(J)*SNS(J)
538 VOL=R(J)*SNS(J)*SEW(I)
C CALCULATE CONVECTION COEFFICIENTS
539 GN=0.5*(DEN(I,J)+DEN(I,J+1))*V(I,J+1)
540 GS=0.5*(DEN(I,J)+DEN(I,J-1))*V(I,J)
541 GE=0.5*(DEN(I,J)+DEN(I+1,J))*U(I+1,J)
542 GU=0.5*(DEN(I,J)+DEN(I-1,J))*U(I,J)
543 CN=GN*AREAN
544 CS=GS*AREAS
545 CE=GE*AREAEU
546 CW=GU*AREAEW

```

```

C CALCULATE DIFFUSION COEFFICIENTS
547 GANH=0.5*(GANH(I,J)+GANH(I,J+1))
548 GANS=0.5*(GANH(I,J)+GANH(I,J-1))
549 GANE=0.5*(GANH(I,J)+GANH(I+1,J))
550 GANW=0.5*(GANH(I,J)+GANH(I-1,J))
551 DN=GANH*AREAN/DYNP(J)
552 DS=GANS*AREAS/DYPS(J)

```



586

SUBROUTINE CALCTE

C CHAPTER 0 0 0 0 0 0 PRELIMINARIES 0 0 0 0 0 0 0

KINE  
KINE  
KINE  
KINE  
KINE  
KINE  
0420

587

COMMON

1/TEN/RESORK,NSUPK,URFK  
1/VAR/U(30,30),V(30,30),P(30,30),PP(30,30),TE(30,30),ED(30,30)  
1/ALL/IT,JT,NI,NJ,NIM1,NJM1,GREAT  
COMMON  
1/GEOM/INDCOS,X(32),Y(32),DXEP(32),DXPW(32),DYNP(32),DYPS(32),  
1 SNS(32),SEW(32),XU(32),YU(32),R(32),RV(32)  
1/FLUPR/URFVIS,VISCOS,DENSIT,PRANDT,DEN(30,30),VIS(30,30),  
2 VISD(30,30)  
1/COEF/AP(30,30),AN(30,30),AS(30,30),AE(30,30),AV(30,30),SU(30,30),  
1 SP(30,30)  
1/TURB/GEN(30,30),CD,CNU,C1,C2,CAPPA,ELOG,PRED,PRTE  
1/WALLF/YPLUSN(30,30),XPLUSU(30,30),TAUN(30,30),TAUW(30,30)  
1/PROB1/UIN,TEIN,EDIN,FLOWIN,ALANDA,  
2 RSHALL,RLARGE,AL1,AL2,JSTEP,ISTEP,JSTP1,JSTH1,ISTP1,ISTH1,  
3 NIJER,US MODA

KINE  
KINE  
0510  
0490

589

PRTE=1.0

DO 100 I=2,NIM1  
DO 101 J=2,NJM1  
C-----COMPUTE AREAS AND VOLUME  
U(I,1)=US  
AREAN=RV(J+1)\*SEW(I)  
AREAS=RV(J)\*SEW(I)  
AREAEW=R(J)\*SNS(J)  
VOL=R(J)\*SNS(J)\*SEW(I)  
C-----CALCULATE CONVECTION COEFFICIENTS  
GN=0.5\*(DEN(I,J)+DEN(I,J+1))\*V(I,J+1)  
GS=0.5\*(DEN(I,J)+DEN(I,J-1))\*V(I,J)  
GE=0.5\*(DEN(I,J)+DEN(I+1,J))\*U(I+1,J)  
GW=0.5\*(DEN(I,J)+DEN(I-1,J))\*U(I,J)  
CN=GN\*AREAN  
CS=GS\*AREAS

KINE  
KINE  
KINE

590

PRTE=1.0

DO 100 I=2,NIM1  
DO 101 J=2,NJM1  
C-----COMPUTE AREAS AND VOLUME  
U(I,1)=US  
AREAN=RV(J+1)\*SEW(I)  
AREAS=RV(J)\*SEW(I)  
AREAEW=R(J)\*SNS(J)  
VOL=R(J)\*SNS(J)\*SEW(I)  
C-----CALCULATE CONVECTION COEFFICIENTS  
GN=0.5\*(DEN(I,J)+DEN(I,J+1))\*V(I,J+1)  
GS=0.5\*(DEN(I,J)+DEN(I,J-1))\*V(I,J)  
GE=0.5\*(DEN(I,J)+DEN(I+1,J))\*U(I+1,J)  
GW=0.5\*(DEN(I,J)+DEN(I-1,J))\*U(I,J)  
CN=GN\*AREAN  
CS=GS\*AREAS

KINE  
KINE  
KINE

591

PRTE=1.0

DO 100 I=2,NIM1  
DO 101 J=2,NJM1  
C-----COMPUTE AREAS AND VOLUME  
U(I,1)=US  
AREAN=RV(J+1)\*SEW(I)  
AREAS=RV(J)\*SEW(I)  
AREAEW=R(J)\*SNS(J)  
VOL=R(J)\*SNS(J)\*SEW(I)  
C-----CALCULATE CONVECTION COEFFICIENTS  
GN=0.5\*(DEN(I,J)+DEN(I,J+1))\*V(I,J+1)  
GS=0.5\*(DEN(I,J)+DEN(I,J-1))\*V(I,J)  
GE=0.5\*(DEN(I,J)+DEN(I+1,J))\*U(I+1,J)  
GW=0.5\*(DEN(I,J)+DEN(I-1,J))\*U(I,J)  
CN=GN\*AREAN  
CS=GS\*AREAS

KINE  
KINE  
KINE

592

PRTE=1.0

DO 100 I=2,NIM1  
DO 101 J=2,NJM1  
C-----COMPUTE AREAS AND VOLUME  
U(I,1)=US  
AREAN=RV(J+1)\*SEW(I)  
AREAS=RV(J)\*SEW(I)  
AREAEW=R(J)\*SNS(J)  
VOL=R(J)\*SNS(J)\*SEW(I)  
C-----CALCULATE CONVECTION COEFFICIENTS  
GN=0.5\*(DEN(I,J)+DEN(I,J+1))\*V(I,J+1)  
GS=0.5\*(DEN(I,J)+DEN(I,J-1))\*V(I,J)  
GE=0.5\*(DEN(I,J)+DEN(I+1,J))\*U(I+1,J)  
GW=0.5\*(DEN(I,J)+DEN(I-1,J))\*U(I,J)  
CN=GN\*AREAN  
CS=GS\*AREAS

KINE  
KINE  
KINE

593

PRTE=1.0

DO 100 I=2,NIM1  
DO 101 J=2,NJM1  
C-----COMPUTE AREAS AND VOLUME  
U(I,1)=US  
AREAN=RV(J+1)\*SEW(I)  
AREAS=RV(J)\*SEW(I)  
AREAEW=R(J)\*SNS(J)  
VOL=R(J)\*SNS(J)\*SEW(I)  
C-----CALCULATE CONVECTION COEFFICIENTS  
GN=0.5\*(DEN(I,J)+DEN(I,J+1))\*V(I,J+1)  
GS=0.5\*(DEN(I,J)+DEN(I,J-1))\*V(I,J)  
GE=0.5\*(DEN(I,J)+DEN(I+1,J))\*U(I+1,J)  
GW=0.5\*(DEN(I,J)+DEN(I-1,J))\*U(I,J)  
CN=GN\*AREAN  
CS=GS\*AREAS

KINE  
KINE  
KINE

594

PRTE=1.0

DO 100 I=2,NIM1  
DO 101 J=2,NJM1  
C-----COMPUTE AREAS AND VOLUME  
U(I,1)=US  
AREAN=RV(J+1)\*SEW(I)  
AREAS=RV(J)\*SEW(I)  
AREAEW=R(J)\*SNS(J)  
VOL=R(J)\*SNS(J)\*SEW(I)  
C-----CALCULATE CONVECTION COEFFICIENTS  
GN=0.5\*(DEN(I,J)+DEN(I,J+1))\*V(I,J+1)  
GS=0.5\*(DEN(I,J)+DEN(I,J-1))\*V(I,J)  
GE=0.5\*(DEN(I,J)+DEN(I+1,J))\*U(I+1,J)  
GW=0.5\*(DEN(I,J)+DEN(I-1,J))\*U(I,J)  
CN=GN\*AREAN  
CS=GS\*AREAS

KINE  
KINE  
KINE

595

PRTE=1.0

DO 100 I=2,NIM1  
DO 101 J=2,NJM1  
C-----COMPUTE AREAS AND VOLUME  
U(I,1)=US  
AREAN=RV(J+1)\*SEW(I)  
AREAS=RV(J)\*SEW(I)  
AREAEW=R(J)\*SNS(J)  
VOL=R(J)\*SNS(J)\*SEW(I)  
C-----CALCULATE CONVECTION COEFFICIENTS  
GN=0.5\*(DEN(I,J)+DEN(I,J+1))\*V(I,J+1)  
GS=0.5\*(DEN(I,J)+DEN(I,J-1))\*V(I,J)  
GE=0.5\*(DEN(I,J)+DEN(I+1,J))\*U(I+1,J)  
GW=0.5\*(DEN(I,J)+DEN(I-1,J))\*U(I,J)  
CN=GN\*AREAN  
CS=GS\*AREAS

KINE  
KINE  
KINE

596

PRTE=1.0

DO 100 I=2,NIM1  
DO 101 J=2,NJM1  
C-----COMPUTE AREAS AND VOLUME  
U(I,1)=US  
AREAN=RV(J+1)\*SEW(I)  
AREAS=RV(J)\*SEW(I)  
AREAEW=R(J)\*SNS(J)  
VOL=R(J)\*SNS(J)\*SEW(I)  
C-----CALCULATE CONVECTION COEFFICIENTS  
GN=0.5\*(DEN(I,J)+DEN(I,J+1))\*V(I,J+1)  
GS=0.5\*(DEN(I,J)+DEN(I,J-1))\*V(I,J)  
GE=0.5\*(DEN(I,J)+DEN(I+1,J))\*U(I+1,J)  
GW=0.5\*(DEN(I,J)+DEN(I-1,J))\*U(I,J)  
CN=GN\*AREAN  
CS=GS\*AREAS

KINE  
KINE  
KINE

597

PRTE=1.0

DO 100 I=2,NIM1  
DO 101 J=2,NJM1  
C-----COMPUTE AREAS AND VOLUME  
U(I,1)=US  
AREAN=RV(J+1)\*SEW(I)  
AREAS=RV(J)\*SEW(I)  
AREAEW=R(J)\*SNS(J)  
VOL=R(J)\*SNS(J)\*SEW(I)  
C-----CALCULATE CONVECTION COEFFICIENTS  
GN=0.5\*(DEN(I,J)+DEN(I,J+1))\*V(I,J+1)  
GS=0.5\*(DEN(I,J)+DEN(I,J-1))\*V(I,J)  
GE=0.5\*(DEN(I,J)+DEN(I+1,J))\*U(I+1,J)  
GW=0.5\*(DEN(I,J)+DEN(I-1,J))\*U(I,J)  
CN=GN\*AREAN  
CS=GS\*AREAS

KINE  
KINE  
KINE

598

PRTE=1.0

DO 100 I=2,NIM1  
DO 101 J=2,NJM1  
C-----COMPUTE AREAS AND VOLUME  
U(I,1)=US  
AREAN=RV(J+1)\*SEW(I)  
AREAS=RV(J)\*SEW(I)  
AREAEW=R(J)\*SNS(J)  
VOL=R(J)\*SNS(J)\*SEW(I)  
C-----CALCULATE CONVECTION COEFFICIENTS  
GN=0.5\*(DEN(I,J)+DEN(I,J+1))\*V(I,J+1)  
GS=0.5\*(DEN(I,J)+DEN(I,J-1))\*V(I,J)  
GE=0.5\*(DEN(I,J)+DEN(I+1,J))\*U(I+1,J)  
GW=0.5\*(DEN(I,J)+DEN(I-1,J))\*U(I,J)  
CN=GN\*AREAN  
CS=GS\*AREAS

KINE  
KINE  
KINE

599

PRTE=1.0

DO 100 I=2,NIM1  
DO 101 J=2,NJM1  
C-----COMPUTE AREAS AND VOLUME  
U(I,1)=US  
AREAN=RV(J+1)\*SEW(I)  
AREAS=RV(J)\*SEW(I)  
AREAEW=R(J)\*SNS(J)  
VOL=R(J)\*SNS(J)\*SEW(I)  
C-----CALCULATE CONVECTION COEFFICIENTS  
GN=0.5\*(DEN(I,J)+DEN(I,J+1))\*V(I,J+1)  
GS=0.5\*(DEN(I,J)+DEN(I,J-1))\*V(I,J)  
GE=0.5\*(DEN(I,J)+DEN(I+1,J))\*U(I+1,J)  
GW=0.5\*(DEN(I,J)+DEN(I-1,J))\*U(I,J)  
CN=GN\*AREAN  
CS=GS\*AREAS

KINE  
KINE  
KINE

600

PRTE=1.0

DO 100 I=2,NIM1  
DO 101 J=2,NJM1  
C-----COMPUTE AREAS AND VOLUME  
U(I,1)=US  
AREAN=RV(J+1)\*SEW(I)  
AREAS=RV(J)\*SEW(I)  
AREAEW=R(J)\*SNS(J)  
VOL=R(J)\*SNS(J)\*SEW(I)  
C-----CALCULATE CONVECTION COEFFICIENTS  
GN=0.5\*(DEN(I,J)+DEN(I,J+1))\*V(I,J+1)  
GS=0.5\*(DEN(I,J)+DEN(I,J-1))\*V(I,J)  
GE=0.5\*(DEN(I,J)+DEN(I+1,J))\*U(I+1,J)  
GW=0.5\*(DEN(I,J)+DEN(I-1,J))\*U(I,J)  
CN=GN\*AREAN  
CS=GS\*AREAS

KINE  
KINE  
KINE

601

PRTE=1.0

DO 100 I=2,NIM1  
DO 101 J=2,NJM1  
C-----COMPUTE AREAS AND VOLUME  
U(I,1)=US  
AREAN=RV(J+1)\*SEW(I)  
AREAS=RV(J)\*SEW(I)  
AREAEW=R(J)\*SNS(J)  
VOL=R(J)\*SNS(J)\*SEW(I)  
C-----CALCULATE CONVECTION COEFFICIENTS  
GN=0.5\*(DEN(I,J)+DEN(I,J+1))\*V(I,J+1)  
GS=0.5\*(DEN(I,J)+DEN(I,J-1))\*V(I,J)  
GE=0.5\*(DEN(I,J)+DEN(I+1,J))\*U(I+1,J)  
GW=0.5\*(DEN(I,J)+DEN(I-1,J))\*U(I,J)  
CN=GN\*AREAN  
CS=GS\*AREAS

KINE  
KINE  
KINE

602

PRTE=1.0

DO 100 I=2,NIM1  
DO 101 J=2,NJM1  
C-----COMPUTE AREAS AND VOLUME  
U(I,1)=US  
AREAN=RV(J+1)\*SEW(I)  
AREAS=RV(J)\*SEW(I)  
AREAEW=R(J)\*SNS(J)  
VOL=R(J)\*SNS(J)\*SEW(I)  
C-----CALCULATE CONVECTION COEFFICIENTS  
GN=0.5\*(DEN(I,J)+DEN(I,J+1))\*V(I,J+1)  
GS=0.5\*(DEN(I,J)+DEN(I,J-1))\*V(I,J)  
GE=0.5\*(DEN(I,J)+DEN(I+1,J))\*U(I+1,J)  
GW=0.5\*(DEN(I,J)+DEN(I-1,J))\*U(I,J)  
CN=GN\*AREAN  
CS=GS\*AREAS

KINE  
KINE  
KINE



```

639      C      2 2 2 2 2 2 2 2 2 2 2 2 2 2 2 2
      C      CALL MODTE
      C      CHAPTER 3 FINAL COEFFICIENT ASSEMBLY AND RESIDUAL-SOURCE CALCULATION 3
      C
      RESOR=0.0
      DO 300 I=2,NIM1
      DO 301 J=2,NJM1
      AP(I,J)=AN(I,J)+AS(I,J)+AE(I,J)+AV(I,J)-SP(I,J)
      RESOR=AN(I,J)*TE(I,J+1)+AS(I,J)*TE(I,J-1)+AE(I,J)*TE(I+1,J)
      +AV(I,J)*TE(I-1,J)-AP(I,J)*TE(I,J)+SU(I,J)
      VOL=R(J)*SEU(I)*SNS(J)
      SORVOL=GREAT*VOL
      IF(-SP(I,J).GT.0.5*SORVOL) RESOR=RESOR/SORVOL
      RESOR=RESOR+ABS(RESOR)
      C-----UNDER-RELAXATION
      AP(I,J)=AP(I,J)/URFK
      SU(I,J)=SU(I,J)+(1.-URFK)*AP(I,J)*TE(I,J)
      301 CONTINUE
      300 CONTINUE
      C      CHAPTER 4 4 4 4 4 SOLUTION OF DIFFERENCE EQUATIONS 4 4 4 4 4
      C
      DO 400 N=1,NSUPK
      400 CALL LISOLV(2,2,NI,NJ,IT,JT,TE)
      RETURN
      END
653
654
655
656

```

KINE  
KINE  
KINE  
KINE  
KINE  
KINE  
KINE  
KINE  
KINE  
KINE  
KINE  
KINE

MODA  
KINE  
KINE  
MODA  
KINE  
KINE  
KINE  
KINE  
KINE  
KINE  
MODA  
KINE  
KINE  
KINE





```

701. C CHAPTER 3 FINAL COEFFICIENT ASSEMBLY AND RESIDUAL SOURCE CALCULATION 3
      RESORE=0.0
      DISP
702. DO 300 I=2,NIMI
      DISP
703. DO 301 J=2,NJMI
      DISP
704. AP(I,J)=AN(I,J)+AS(I,J)+AE(I,J)+AW(I,J)-SP(I,J)
      DISP
705. RESOR=AN(I,J)*ED(I,J+1)+AS(I,J)*ED(I,J-1)+AE(I,J)*ED(I+1,J)
      DISP
      1 +AW(I,J)*ED(I-1,J)-AP(I,J)*ED(I,J)+SU(I,J)
      MODA
706. VOL=R(J)*SNS(J)*SEW(I)
      DISP
707. SORVOL=GREAT*VOL
      DISP
708. IF(-SP(I,J).GT.0.5*SORVOL) RESOR=RESOR/SORVOL
      DISP
709. RESORE=RESORE+ABS(RESOR)
      MODA
      C-----UNDER-RELAXATION
      DISP
710. AP(I,J)=AP(I,J)/URFE
      DISP
711. SU(I,J)=SU(I,J)*(1.-URFE)*AP(I,J)*ED(I,J)
      MODA
712. 301 CONTINUE
      DISP
713. 300 CONTINUE
      DISP
      C
714. C CHAPTER 4 4 4 4 SOLUTION OF DIFFERENCE EQUATIONS 4 4 4 4 4
      DISP
715. DO 400 N=1,NSUPD
      DISP
716. 400 CALL LISOLV(2,2,NI,NJ,IT,JT,ED)
      DISP
717. RETURN
      END
      DISP

```





C CHAPTER 3 FINAL COEFFICIENT ASSEMBLY AND RESIDUAL-SOURCE CALCULATION 3

```
766 RESOR=0.0
767 DO 300 I=2,NIM1
768 DO 301 J=2,NJM1
769   AP(I,J)=AN(I,J)+AS(I,J)+AE(I,J)-SP(I,J)
770   RESOR=AN(I,J)*QE(I,J+1)+AS(I,J)*QE(I,J-1)+AE(I,J)*QE(I+1,J)
771   AU(I,J)*QE(I-1,J)-AP(I,J)*QE(I,J)+SU(I,J)
772   VOL=R(I)*SER(I)*SNS(J)
773   SORVOL=GREAT*VOL
774   IF(-SP(I,J).GT.0.5*SORVOL) RESOR=RESOR/SORVOL
775   RESOR=RESOR+ABS(RESOR)
776   UNDER_RELAXATION
777   AP(I,J)=AP(I,J)/URFO
778   SU(I,J)=SU(I,J)+(1.-URFO)*AP(I,J)*QE(I,J)
301 CONTINUE
300 CONTINUE
```

C CHAPTER 4 4 4 4 4 SOLUTION OF DIFFERENCE EQUATIONS 4 4 4 4 4

```
779 DO 400 N=1,NSUPO
780 CALL LISOLV(2,2,NI,NJ,IT,JT,QE)
781 RETURN
782 END
```



```

809 SUBROUTINE PRINT(ISTART,JSTART,NI,NJ,IT,JT,X,Y,PHI,HEAD)
810 COMMON
      1/AREAL/INCT
      DIMENSION PHI(IT,JT),X(IT),Y(JT),HEAD(9),STORE(50)
811 DIMENSION F(7),F4(11)
812 LOGICAL INCT
813 DATA F/4H(1H,4H,A4,4H13,4H11I,4H10,4H7X,
814 14H6) /
815 DATA F4/4H(1I,4H 2I,4H 3I,4H 4I,4H 5I,4H 6I,
      4H 7I,4H 8I,4H 9I,4H10I,4H11I) /
816 DATA HI,HY/4H(1=,4H Y =/
817 ISKIP=1
818 JSKIP=1
819 WRITE(6,110)HEAD
820 ISTA=ISTART-12
821 100 CONTINUE
822 ISTA=ISTA+12
823 IEND=ISTA+11
824 IEND=MINO(NI,IEND)
825 F(4)=F4(IEND-ISTA)
826 WRITE(6,F) HI, (I,I=ISTA,IEND,ISKIP), HY
827 WRITE(6,112)
828 DO 101 JJ=JSTART,NJ,JSKIP
829 J=JSTART+NJ-JJ
830 DO 120 I=ISTA,IEND
831 A=PHI(I,J)
832 IF(ABS(A).LT.1.E-20) A=0.0
833 120 STORE(I)=A
834 IF(INCT) GO TO 200
835 WRITE(6,113) J,(STORE(I),I=ISTA,IEND,ISKIP),Y(J)
836 GO TO 300
837 200 WRITE(6,150) J,(STORE(I),I=ISTA,IEND,ISKIP),Y(J)
838 300 CONTINUE
839 101 CONTINUE
840 WRITE(6,114) (X(I),I=ISTA,IEND,ISKIP)
C-----
841 IF(IEND.LI.NI)GO TO 100
842 RETURN
843 110 FORMAT(1H0,20(2H*-),7X,9A4,7X,20(2H-*))
844 112 FORMAT(3H J)
845 113 FORMAT(1H ,I3,1P12E10.2,0PF7.3)
846 114 FORMAT(6H0X= ,F7.3,11F10.3)
847 150 FORMAT(1H ,I3,1P12E10.3,0PF7.3)
848 END

```

```

0010
0020
0030
0040
0050
0060
0070
0080
0090
0100
0110
0120
0130
0140
0150
0160
0170
0180
0190
0200
0210
0220
0230
0240
0250
0260
0270
0280
0290
0300
0310
0320
0330
0340
0330

```



```

861 DO 210 I=3,NIM1
862 SORTK=SQRT(0.5*(TE(I,J)+TE(I-1,J)))
863 DENU=0.5*(DEN(I,J)+DEN(I-1,J))
864 YPLUSA=0.5*(YPLUSN(I,NJM1)+YPLUSN(I-1,NJM1))
865 IF(YPLUSA.LE.11.63) GO TO 211
866 THULT=DENU*CDTERM*SORTK*CAPPA/ALOG(ELOG*YPLUSA)
867 GO TO 212
868 MODA
869 211 THULT=VISCOS/YP
870 TAUN(I,NJM1)=-THULT*U(I,J)
871 SP(I,J)=SP(I,J)-THULT*SEMU(I)*RV(NJ)
872 210 AN(I,J)=0.0
873 TAUN(2,NJM1)=TAUN(3,NJM1)
874 TAUN(NI,NJM1)=TAUN(NIM1,NJM1)
875 C-----LEFT SIDE WALL
876 DO 213 J=2,NJH1
877 U(1,J)=0.
878 AV(2,J)=0.
879 213 CONTINUE
880 C-----BOTTOM WALL
881 YP=YV(2)-Y(1)
882 CDTERM=CMU**0.25
883 J=2
884 DO 4210 I=3,NIM1
885 SORTK=SQRT(0.5*(TE(I,J)+TE(I-1,J)))
886 DENU=0.5*(DEN(I,J)+DEN(I-1,J))
887 YPLUSA=0.5*(YPLUSN(I,2)+YPLUSN(I-1,2))
888 IF(YPLUSA.LE.11.63) GO TO 4211
889 THULT=DENU*CDTERM*SORTK*CAPPA/ALOG(ELOG*YPLUSA)
890 GO TO 4212
891 4211 THULT=VISCOS/YP
892 TAUN(I,2)=-THULT*U(I,J)+THULT*US
893 SP(I,J)=SP(I,J)-THULT*SEMU(I)*RV(NJ)
894 SU(I,J)=SU(I,J)+THULT*US*SEMU(I)*RV(NJ)
895 U(I,1)=US
896 U(2,1)=US
897 AS(I,J)=0.
898 4210 CONTINUE
899 TAUN(2,2)=TAUN(3,2)
900 TAUN(NI,2)=TAUN(NIM1,2)
901 C-----RIGHT SIDE WALL
902 DO 3203 J=1,NJ
903 U(NI,J)=0.0
904 AE(RIH1,J)=0.0
905 3203 CONTINUE
906 RETURN
907 PROMOD

```

MODA

MODA

MODA

MODA

MODA

MODA

MODA

MODA

MODA

MODA

MODA

MODA

MODA

MODA

MODA

MODA

PROMOD





```

967 C-----LEFT SIDE WALL
968 XP=X(2)-XU(2)
969 I=2
970 DO 620 J=2,NJH1
971 DENV=DEN(I,J)
972 SORTK=SQRT(TE(I,J))
973 VOL=R(J)*SNS(J)*SEW(I)
974 XPLUSW(2,J)=DENV*SORTK*CDTERM*XP/VISCOS
975 GENCOU=0.5*(ABS(TAUW(2,J+1)*V(I,J+1))+ABS(TAUW(2,J)
976 1*V(I,J)))/XP
977 DVDX=((V(I,J)+V(I,J+1)+V(I+1,J)+V(I+1,J+1))/4.-(V(I,J)+V(I,J+1)+V(
978 I-1,J)+V(I-1,J+1))/4.)/SEW(I)
979 GENRES=GEN(I,J)-VIS(I,J)*DVDX**2
980 GEN(I,J)=GENRES+GENCOU
981 IF(XPLUSW(2,J).LE.11.63) GO TO 621
982 DITERM=DEN(I,J)*(CHU**0.75)*SORTK*ALOG(ELOG*XPLUSW(2,J))/
983 1CAPPA*XP)
984 GO TO 622
985 621 CONTINUE
986 DITERM=DEN(I,J)*(CHU**0.75)*SORTK*XPLUSW(2,J)/XP
987 622 CONTINUE
988 SU(I,J)=SUKD(I,J)+GEN(I,J)*VOL
989 SP(I,J)=SPKD(I,J)-DITERM*VOL
990 AN(I,J)=0.0
991 C-----RIGHT SIDE WALL
992 I=NIM1
993 DO 1620 J=2,NJH1
994 DENV=DEN(I,J)
995 SORTK=SQRT(TE(I,J))
996 XPLUSW(NIM1,J)=DENV*SORTK*CDTERM*XP/VISCOS
997 VOL=R(J)*SNS(J)*SEW(I)
998 GENCOU=0.5*(ABS(TAUN(NIM1,J+1)*V(I,J+1))+ABS(TAUN(NIM1,J)*V(I,
999 1))/XP)
1000 DVDX=((V(I,J)+V(I,J+1)+V(I+1,J)+V(I+1,J+1))/4.-(V(I,J)+V(I,J+1)+V(
1001 I-1,J)+V(I-1,J+1))/4.)/SEW(I)
1002 GENRES=GEN(I,J)-VIS(I,J)*DVDX**2
1003 GEN(I,J)=GENRES+GENCOU
1004 IF(XPLUSW(NIM1,J).LE.11.63) GO TO 1621
1005 DITERM=DEN(I,J)*(CHU**0.75)*SORTK*ALOG(ELOG*XPLUSW(NIM1,J))
1006 1/(CAPPA*XP)
1007 GO TO 1622
1008 1621 CONTINUE

```

MODA  
MODA

MODA  
MODA  
MODA

MODA  
MODA  
MODA

MODA  
MODA  
MODA  
MODA

MODA  
MODA  
MODA

MODA  
MODA  
MODA

MODA  
MODA  
MODA

```

1001 DITERM=DEN(I,J)*(CMU**.75)*SORTK*PLUSW(NIMI,J)/XP
1002 1622 CONTINUE
1003 SU(I,J)=SUKD(I,J)+GEN(I,J)*VOL
1004 SP(I,J)=SPKD(I,J)-DITERM*VOL
1005 1620 AV(I,J)=0.0
C-----BOTTOM WALL
1006 J=2
1007 YP=YV(2)-Y(1)
1008 DO 3630 I=2,NIMI
1009 DENU=DEN(I,J)
1010 SORTK=SORT(TE(I,J))
1011 VOL=R(J)*SNS(J)*SEM(I)
1012 GENCOU=0.5*(ABS(TAUN(I+1,2))*(U(I+1,J)-US))
+ABS(TAUN(I,2))*(U(I,J)-US))/YP
1013 YPLUSN(I,2)=DENU*SORTK*EDITERM*YP/VISCOS
1014 DUDY=((U(I,J)+U(I+1,J)+U(I,J+1)+U(I+1,J+1))/4.
1-(U(I,J)+U(I+1,J)+U(I,J-1)+U(I+1,J-1))/4.)/SNS(J)
1015 GENRES=GEN(I,J)-VIS(I,J)*DUDY**2
1016 GEN(I,J)=GENRES+GENCOU
1017 IF(YPLUSN(I,2).LE.11.63) GO TO 3631
1018 DITERM=DEN(I,J)*(CMU**.75)*SORTK*ALOG(ELOG*YPLUSN(I,2)
1/(CAPPA*YP)
GO TO 3632
1019 3631 CONTINUE
1020 DITERM=DEN(I,J)*(CMU**.75)*SORTK*YPLUSN(I,2)/(CAPPA*YP)
1021 3632 CONTINUE
1023 SU(I,J)=GEN(I,J)*VOL+SUKD(I,J)
1024 SP(I,J)=-DITERM*VOL+SPKD(I,J)
1025 AS(I,J)=0.0
1026 RETURN
C
CHAPTER 7 7 7 7 7 7 7 DISSIPATION
C
ENTRY HODED
C-----TOP WALL
1027 YP=YV(NJ)-Y(NJN1)
1028 J=NJN1
1029 TERH=(CMU**.75)/(CAPPA*YP)
1030 DO 710 I=2,NIMI
1031 SU(I,J)=GREAT*TERM*TE(I,J)**1.5
1032 SP(I,J)=-GREAT
1033 710 SP(I,J)=-GREAT

```

MODA  
MODA

PROM  
PROMOD  
PROMOD  
PROMOD

MODA  
MODA  
MODA  
MODA  
MODA

NODA  
MODA  
NODA

```
1034 C-----LEFT SIDE WALL  
1035 XP=X(2)-XU(2)  
1036 I=2  
1037 TERM=(CHU**.75)/(CAPPA*YP)  
1038 NJH2=NJ-2  
1039 DO 720 J=2,NJH2  
1040 AV(2,J)=0.0  
1041 SU(I,J)=GREAT*TERM*TE(I,J)**1.5  
1042 720 SP(I,J)=-GREAT  
1043 C-----RIGHT SIDE WALL  
1044 NJH2=RJ-2  
1045 NINI  
1046 DO 1720 J=2,NJH2  
1047 XP=X(2)-XU(2)  
1048 TERM=(CHU**.75)/(CAPPA*XP)  
1049 SU(I,J)=GREAT*TERM*TE(I,J)**1.5  
1050 SP(I,J)=-GREAT  
1051 C-----BOTTOM WALL  
1052 J=2  
1053 DO 1730 I=2,NINI  
1054 YP=YV(2)-Y(1)  
1055 J=2  
1056 TERM=(CHU**.75)/(CAPPA*XP)  
1057 SU(I,J)=GREAT*TERM*TE(I,J)**1.5  
1058 SP(I,J)=-GREAT  
1059 RETURN  
1060 C  
1061 ENTRY MODT  
1062 C-----TOP WALL (CONSTANT TEMPERATURE)  
1063 CDTERM=CHU**0.25  
1064 J=NJH1  
1065 DYN=YV(NJ)-YV(NJH1)  
1066 DO 500 I=2,NINI  
1067 T(I,NJ)=TWALL  
1068 AN(I,J)=0.0  
1069 AREA=RV(J+1)*SEU(I)  
1070 IF(YPLUS(I,NJH1).LE.11.63) GO TO 510  
1071 UPLUS=ALOG(ELOG*YPLUS(I,NJH1))/CAPPA  
1072 GT=DEN(I,J)*CDTERM*SQRT(TE(I,J))/(PRANDT*(UPLUS*PFUN))  
1073 GO TO 511  
1074 510 GT=VISCOS/(PRANDL*DYN)  
1075 511 TERM=GT*AREA
```

```

1083
1084
1085
1086
1087
1088
1089
1090
1091
1092
1093
1094
1095
1096
1097
1098
1099
1100
1101

AREA=0.0
IF (PLUSM(1,2).LE.11.63) GO TO 5510
UPLUS=ALOG(10*PLUSM(1,2))/CAPPA
GT=DER(I,J)*CDTERM+SORT(TE(I,J))/(PRANDT*(UPLUS+PFUN))
GO TO 5511

5510 GT=VISCOS/(PRANDL*DYN)
5511 TERM=GT*AREA
SU(I,J)=SU(I,J)+TERM+TBOTOM
SP(I,J)=SP(I,J)-TERM
AS(I,J)=0.0
1502 CONTINUE
C-----RIGHT SIDE WALL
I=NIMI
DYN=XU(NIMI)-XU(NIMI)
DO 7500 J=2,NJM1
AE(I,J)=0.
T(NI,J)=T(NIMI,J)
7500 CONTINUE
RETURN
C
CHAPTER 8 8 8 8 MEAN SQUARE TEMPERATURE FLUCTUATION
C
ENTRY MODDE
CO1=2.8
CO2=1.7

```

```

1105 C-----LEFT SIDE WALL
1106 XP=X(3)-X(2)
1107 I=2
1108 DO 6610 J=2,NJM1
1109 VOL=R(J)*SNS(J)*SEU(I)
1110 DTDX=((T(I+1,J)+T(I,J))/2.-((T(I-1,J)+T(I,J))/2.)/SEU(I)
1111 GENQ(I,J)=(DTDY**2)*VIS(I,J)
1112 QETERM=CQ1*TE(I,J)*GENQ(I,J)/(CQ2*DEN(I,J)*ED(I,J))
1113 SU(I,J)=GREAT*QETERM
1114 SP(I,J)=-GREAT
1115 AV(I,J)=0.
1116 6610 CONTINUE
1117 C-----RIGHT SIDE WALL
1118 I=NIM1
1119 XP=X(NI)-XU(NI)
1120 DO 6310 J=2,NJM1
1121 VOL=R(J)*SNS(J)*SEU(I)
1122 DTDX=((T(I+1,J)+T(I,J))/2.-((T(I-1,J)+T(I,J))/2.)/SEU(I)
1123 GENQ(I,J)=(DTDY**2)*VIS(I,J)
1124 QETERM=CQ1*TE(I,J)*GENQ(I,J)/(CQ2*DEN(I,J)*ED(I,J))
1125 SU(I,J)=GREAT*QETERM
1126 SP(I,J)=-GREAT
1127 AE(I,J)=0.
1128 6310 CONTINUE
1129 C-----BOTTOM WALL
1130 J=2
1131 DO 9630 I=2,NIM1
1132 YP=Y(3)-Y(2)
1133 VOL=R(J)*SNS(J)*SEU(I)
1134 DTDY=(T(I,J+1)-T(I,J))/DYNP(J)
1135 GENQ(I,J)=(DTDY**2)*VIS(I,J)
1136 QETERM=CQ1*TE(I,J)*GENQ(I,J)/(CQ2*DEN(I,J)*ED(I,J))
1137 SU(I,J)=GREAT*QETERM
1138 SP(I,J)=-GREAT
1139 AS(I,J)=0.
1140 9630 CONTINUE
1141 C-----TOP WALL
1142 J=NJM1
1143 DO 8610 I=2,NIM1
1144 DTDY=(T(I,J)-T(I,J-1))/DYPS(J)
1145 GENQ(I,J)=(DTDY**2)*VIS(I,J)

```

1142 DETERM = CQ1\*TE(I,J)\*GENQ(I,J)/(CQ2\*DEN(I,J)\*ED(I,J))  
1143 SU(I,J)=GREAT\*DETERM  
1144 SP(I,J)=-GREAT  
1145 AN(I,J)=0.  
1146 8610 CONTINUE  
1147 RETURN  
1148 END

PROMOD









3594. I= 2 3 4 5 6 7 8 9 10 11 Y =

J	18	17	16	15	14	13	12	11	10	9	8	7	6	5	4	3	2	1	
3595.	0.0	7.08E-10	7.90E-10	0.0	0.0	0.0	0.0	0.0	0.0	0.0	0.0	0.0	0.0	0.0	0.0	0.0	0.0	0.0	
3596.	6.72E-10	7.27E-10	8.19E-10	9.01E-10	9.70E-10	9.27E-10	1.12E-09	1.36E-09	1.66E-09	1.94E-09	2.00E-09	2.00E-09	2.00E-09	2.00E-09	2.00E-09	2.00E-09	2.00E-09	2.00E-09	2.00E-09
3597.	6.86E-10	7.83E-10	9.01E-10	1.05E-09	1.26E-09	1.50E-09	1.75E-09	1.98E-09	2.22E-09	2.48E-09	2.73E-09	2.96E-09	3.16E-09	3.45E-09	3.71E-09	3.95E-09	4.10E-09	4.25E-09	4.40E-09
3598.	7.28E-10	8.93E-10	1.05E-09	1.26E-09	1.49E-09	1.74E-09	1.99E-09	2.22E-09	2.45E-09	2.73E-09	2.96E-09	3.16E-09	3.45E-09	3.71E-09	3.95E-09	4.10E-09	4.25E-09	4.40E-09	4.55E-09
3599.	8.15E-10	1.06E-09	1.26E-09	1.49E-09	1.74E-09	1.99E-09	2.22E-09	2.45E-09	2.73E-09	2.96E-09	3.16E-09	3.45E-09	3.71E-09	3.95E-09	4.10E-09	4.25E-09	4.40E-09	4.55E-09	4.70E-09
3600.	9.52E-10	1.27E-09	1.49E-09	1.74E-09	1.99E-09	2.22E-09	2.45E-09	2.73E-09	2.96E-09	3.16E-09	3.45E-09	3.71E-09	3.95E-09	4.10E-09	4.25E-09	4.40E-09	4.55E-09	4.70E-09	4.85E-09
3601.	1.15E-09	1.49E-09	1.74E-09	1.99E-09	2.22E-09	2.45E-09	2.73E-09	2.96E-09	3.16E-09	3.45E-09	3.71E-09	3.95E-09	4.10E-09	4.25E-09	4.40E-09	4.55E-09	4.70E-09	4.85E-09	5.00E-09
3602.	1.41E-09	1.50E-09	1.74E-09	1.99E-09	2.22E-09	2.45E-09	2.73E-09	2.96E-09	3.16E-09	3.45E-09	3.71E-09	3.95E-09	4.10E-09	4.25E-09	4.40E-09	4.55E-09	4.70E-09	4.85E-09	5.00E-09
3603.	1.83E-09	2.03E-09	2.05E-09	2.14E-09	2.24E-09	2.33E-09	2.42E-09	2.51E-09	2.60E-09	2.69E-09	2.78E-09	2.87E-09	2.96E-09	3.05E-09	3.14E-09	3.23E-09	3.32E-09	3.41E-09	3.50E-09
3604.	2.25E-09	2.15E-09	2.03E-09	1.99E-09	2.05E-09	2.14E-09	2.24E-09	2.33E-09	2.42E-09	2.51E-09	2.60E-09	2.69E-09	2.78E-09	2.87E-09	2.96E-09	3.05E-09	3.14E-09	3.23E-09	3.32E-09
3605.	2.50E-09	2.19E-09	1.99E-09	1.97E-09	2.05E-09	2.14E-09	2.24E-09	2.33E-09	2.42E-09	2.51E-09	2.60E-09	2.69E-09	2.78E-09	2.87E-09	2.96E-09	3.05E-09	3.14E-09	3.23E-09	3.32E-09
3606.	2.60E-09	2.19E-09	1.99E-09	1.97E-09	2.05E-09	2.14E-09	2.24E-09	2.33E-09	2.42E-09	2.51E-09	2.60E-09	2.69E-09	2.78E-09	2.87E-09	2.96E-09	3.05E-09	3.14E-09	3.23E-09	3.32E-09
3607.	2.68E-09	2.20E-09	2.14E-09	2.14E-09	2.14E-09	2.14E-09	2.14E-09	2.14E-09	2.14E-09	2.14E-09	2.14E-09	2.14E-09	2.14E-09	2.14E-09	2.14E-09	2.14E-09	2.14E-09	2.14E-09	2.14E-09
3608.	2.98E-09	2.30E-09	2.14E-09	2.14E-09	2.14E-09	2.14E-09	2.14E-09	2.14E-09	2.14E-09	2.14E-09	2.14E-09	2.14E-09	2.14E-09	2.14E-09	2.14E-09	2.14E-09	2.14E-09	2.14E-09	2.14E-09
3609.	3.19E-09	3.19E-09	3.19E-09	3.19E-09	3.19E-09	3.19E-09	3.19E-09	3.19E-09	3.19E-09	3.19E-09	3.19E-09	3.19E-09	3.19E-09	3.19E-09	3.19E-09	3.19E-09	3.19E-09	3.19E-09	3.19E-09
3610.	8.47E-09	8.83E-09	9.86E-09	1.07E-08	1.11E-08	1.11E-08	1.11E-08	1.11E-08	1.11E-08	1.11E-08	1.11E-08	1.11E-08	1.11E-08	1.11E-08	1.11E-08	1.11E-08	1.11E-08	1.11E-08	1.11E-08
3611.	2.77E-08	2.47E-08	2.17E-08	1.93E-08	1.72E-08	1.53E-08	1.36E-08	1.21E-08	1.06E-08	9.27E-09	8.15E-09	7.27E-09	6.58E-09	6.00E-09	5.50E-09	5.00E-09	4.50E-09	4.00E-09	3.50E-09
3612.	0.010	0.025	0.045	0.070	0.100	0.135	0.180	0.240	0.300	0.345	0.380	0.410	0.430	0.450	0.470	0.480	0.490	0.500	0.510
3613.	0.010	0.025	0.045	0.070	0.100	0.135	0.180	0.240	0.300	0.345	0.380	0.410	0.430	0.450	0.470	0.480	0.490	0.500	0.510
3614.	0.010	0.025	0.045	0.070	0.100	0.135	0.180	0.240	0.300	0.345	0.380	0.410	0.430	0.450	0.470	0.480	0.490	0.500	0.510
3615.	0.010	0.025	0.045	0.070	0.100	0.135	0.180	0.240	0.300	0.345	0.380	0.410	0.430	0.450	0.470	0.480	0.490	0.500	0.510
3616.	0.010	0.025	0.045	0.070	0.100	0.135	0.180	0.240	0.300	0.345	0.380	0.410	0.430	0.450	0.470	0.480	0.490	0.500	0.510
3617.	0.010	0.025	0.045	0.070	0.100	0.135	0.180	0.240	0.300	0.345	0.380	0.410	0.430	0.450	0.470	0.480	0.490	0.500	0.510
3618.	9.41E-10	6.17E-10	3.19E-10	9.97E-11	9.97E-11	9.97E-11	9.97E-11	9.97E-11	9.97E-11	9.97E-11	9.97E-11	9.97E-11	9.97E-11	9.97E-11	9.97E-11	9.97E-11	9.97E-11	9.97E-11	9.97E-11
3619.	1.00E-09	6.54E-10	3.37E-10	9.99E-11	9.99E-11	9.99E-11	9.99E-11	9.99E-11	9.99E-11	9.99E-11	9.99E-11	9.99E-11	9.99E-11	9.99E-11	9.99E-11	9.99E-11	9.99E-11	9.99E-11	9.99E-11
3620.	1.16E-09	7.59E-10	3.91E-10	1.00E-10	1.00E-10	1.00E-10	1.00E-10	1.00E-10	1.00E-10	1.00E-10	1.00E-10	1.00E-10	1.00E-10	1.00E-10	1.00E-10	1.00E-10	1.00E-10	1.00E-10	1.00E-10
3621.	1.44E-09	9.54E-10	4.97E-10	1.01E-10	1.01E-10	1.01E-10	1.01E-10	1.01E-10	1.01E-10	1.01E-10	1.01E-10	1.01E-10	1.01E-10	1.01E-10	1.01E-10	1.01E-10	1.01E-10	1.01E-10	1.01E-10
3622.	1.82E-09	1.24E-09	6.58E-10	1.03E-10	1.03E-10	1.03E-10	1.03E-10	1.03E-10	1.03E-10	1.03E-10	1.03E-10	1.03E-10	1.03E-10	1.03E-10	1.03E-10	1.03E-10	1.03E-10	1.03E-10	1.03E-10
3623.	2.35E-09	1.64E-09	8.89E-10	1.17E-10	1.17E-10	1.17E-10	1.17E-10	1.17E-10	1.17E-10	1.17E-10	1.17E-10	1.17E-10	1.17E-10	1.17E-10	1.17E-10	1.17E-10	1.17E-10	1.17E-10	1.17E-10
3624.	3.09E-09	2.24E-09	1.25E-09	1.70E-10	1.70E-10	1.70E-10	1.70E-10	1.70E-10	1.70E-10	1.70E-10	1.70E-10	1.70E-10	1.70E-10	1.70E-10	1.70E-10	1.70E-10	1.70E-10	1.70E-10	1.70E-10
3625.	4.18E-09	3.24E-09	1.94E-09	3.63E-10	3.63E-10	3.63E-10	3.63E-10	3.63E-10	3.63E-10	3.63E-10	3.63E-10	3.63E-10	3.63E-10	3.63E-10	3.63E-10	3.63E-10	3.63E-10	3.63E-10	3.63E-10
3626.	5.48E-09	4.75E-09	3.30E-09	1.11E-09	1.11E-09	1.11E-09	1.11E-09	1.11E-09	1.11E-09	1.11E-09	1.11E-09	1.11E-09	1.11E-09	1.11E-09	1.11E-09	1.11E-09	1.11E-09	1.11E-09	1.11E-09
3627.	6.88E-09	6.61E-09	5.44E-09	2.90E-09	2.90E-09	2.90E-09	2.90E-09	2.90E-09	2.90E-09	2.90E-09	2.90E-09	2.90E-09	2.90E-09	2.90E-09	2.90E-09	2.90E-09	2.90E-09	2.90E-09	2.90E-09
3628.	8.26E-09	8.48E-09	8.01E-09	5.77E-09	5.77E-09	5.77E-09	5.77E-09	5.77E-09	5.77E-09	5.77E-09	5.77E-09	5.77E-09	5.77E-09	5.77E-09	5.77E-09	5.77E-09	5.77E-09	5.77E-09	5.77E-09
3629.	9.65E-09	1.03E-08	1.05E-08	9.29E-09	9.29E-09	9.29E-09	9.29E-09	9.29E-09	9.29E-09	9.29E-09	9.29E-09	9.29E-09	9.29E-09	9.29E-09	9.29E-09	9.29E-09	9.29E-09	9.29E-09	9.29E-09
3630.	1.11E-08	1.22E-08	1.28E-08	1.29E-08	1.29E-08	1.29E-08	1.29E-08	1.29E-08	1.29E-08	1.29E-08	1.29E-08	1.29E-08	1.29E-08	1.29E-08	1.29E-08	1.29E-08	1.29E-08	1.29E-08	1.29E-08
3631.	1.23E-08	1.46E-08	1.55E-08	1.59E-08	1.59E-08	1.59E-08	1.59E-08	1.59E-08	1.59E-08	1.59E-08	1.59E-08	1.59E-08	1.59E-08	1.59E-08	1.59E-08	1.59E-08	1.59E-08	1.59E-08	1.59E-08
3632.	1.26E-08	1.68E-08	1.94E-08	1.93E-08	1.93E-08	1.93E-08	1.93E-08	1.93E-08	1.93E-08	1.93E-08	1.93E-08	1.93E-08	1.93E-08	1.93E-08	1.93E-08	1.93E-08	1.93E-08	1.93E-08	1.93E-08
3633.	1.38E-08	1.71E-08	2.47E-08	2.91E-08	2.91E-08	2.91E-08	2.91E-08	2.91E-08	2.91E-08	2.91E-08	2.91E-08	2.91E-08	2.91E-08	2.91E-08	2.91E-08	2.91E-08	2.91E-08	2.91E-08	2.91E-08
3634.	0.435	0.455	0.470	0.480	0.480	0.480	0.480	0.480	0.480	0.480	0.480	0.480	0.480	0.480	0.480	0.480	0.480	0.480	0.480

J	18	17	16	15	14	13	12	11	10	9	8	7	6	5	4	3	2	1	
3615.	0.0	0.0	0.0	0.0	0.0	0.0	0.0	0.0	0.0	0.0	0.0	0.0	0.0	0.0	0.0	0.0	0.0	0.0	
3616.	4.90E-01	4.80E-01	4.70E-01	4.60E-01	4.50E-01	4.40E-01	4.30E-01	4.20E-01	4.10E-01	4.00E-01	3.90E-01	3.80E-01	3.70E-01	3.60E-01	3.50E-01	3.40E-01	3.30E-01	3.20E-01	3.10E-01
3617.	4.80E-01	4.70E-01	4.60E-01	4.50E-01	4.40E-01	4.30E-01	4.20E-01	4.10E-01	4.00E-01	3.90E-01	3.80E-01	3.70E-01	3.60E-01	3.50E-01	3.40E-01	3.30E-01	3.20E-01	3.10E-01	3.00E-01
3618.	4.70E-01	4.60E-01	4.50E-01	4.40E-01	4.30E-01	4.20E-01	4.10E-01	4.00E-01	3.90E-01	3.80E-01	3.70E-01	3.60E-01	3.50E-01	3.40E-01	3.30E-01	3.20E-01	3.10E-01	3.00E-01	2.90E-01
3619.	4.60E-01	4.50E-01	4.40E-01	4.30E-															

3635.  
3636.  
3637.  
3638.  
3639.  
3640.  
3641.  
3642.  
3643.  
3644.  
3645.  
3646.  
3647.  
3648.  
3649.  
3650.  
3651.  
3652.  
3653.  
3654.  
3655.  
3656.  
3657.

ENERGY DISSIPATION

	2	3	4	5	6	7	8	9	10	11	Y =
18	0.0	0.0	0.0	0.0	0.0	0.0	0.0	0.0	0.0	0.0	4.90E-01
17	1.37E-12	1.47E-12	1.74E-12	2.21E-12	2.93E-12	3.92E-12	5.29E-12	6.67E-12	7.00E-12	6.06E-12	4.80E-01
16	1.41E-12	8.62E-13	8.66E-13	1.06E-12	1.37E-12	1.79E-12	2.33E-12	2.82E-12	2.91E-12	2.54E-12	4.70E-01
15	1.54E-12	6.90E-13	5.22E-13	5.81E-13	7.35E-13	9.36E-13	1.17E-12	1.34E-12	1.37E-12	1.22E-12	4.55E-01
14	1.82E-12	7.23E-13	4.36E-13	4.18E-13	5.00E-13	6.12E-13	7.27E-13	8.05E-13	8.38E-13	7.97E-13	4.35E-01
13	2.30E-12	8.56E-13	4.55E-13	3.80E-13	4.16E-13	4.84E-13	5.55E-13	6.22E-13	7.01E-13	7.35E-13	4.10E-01
12	3.04E-12	1.07E-12	5.22E-13	3.91E-13	3.91E-13	4.36E-13	5.00E-13	5.95E-13	7.38E-13	8.55E-13	3.80E-01
11	4.17E-12	1.89E-12	7.85E-13	4.24E-13	3.95E-13	4.27E-13	5.01E-13	6.44E-13	8.68E-13	1.10E-12	3.45E-01
10	6.13E-12	2.46E-12	9.54E-13	4.83E-13	4.16E-13	4.40E-13	5.31E-13	7.28E-13	1.05E-12	1.44E-12	3.00E-01
9	8.38E-12	2.84E-12	1.07E-12	5.63E-13	4.32E-13	4.43E-13	5.39E-13	7.72E-13	1.20E-12	1.76E-12	2.40E-01
8	9.83E-12	2.84E-12	1.13E-12	5.77E-13	4.19E-13	4.07E-13	5.39E-13	7.72E-13	1.20E-12	1.76E-12	1.80E-01
7	1.04E-11	3.00E-12	1.13E-12	5.77E-13	4.16E-13	4.00E-13	4.80E-13	7.05E-13	1.18E-12	1.94E-12	1.35E-01
6	1.09E-11	3.07E-12	1.13E-12	5.97E-13	4.73E-13	4.73E-13	6.95E-13	1.05E-12	1.58E-12	2.00E-12	1.35E-01
5	1.27E-11	3.27E-12	1.20E-12	8.20E-13	9.74E-13	1.31E-12	1.85E-12	2.49E-12	3.12E-12	3.83E-12	1.00E-01
4	1.97E-11	4.57E-12	2.89E-12	3.76E-12	4.82E-12	5.75E-12	6.51E-12	7.04E-12	7.45E-12	7.96E-12	7.00E-02
3	6.12E-11	2.33E-11	2.27E-11	2.38E-11	2.36E-11	2.25E-11	2.09E-11	1.92E-11	1.81E-11	1.79E-11	4.50E-02
2	1.81E-10	1.52E-10	1.25E-10	1.05E-10	8.88E-11	7.46E-11	6.20E-11	5.21E-11	4.63E-11	4.43E-11	2.50E-02
X =	0.010	0.025	0.045	0.070	0.100	0.135	0.180	0.240	0.300	0.345	

3658.  
3659.  
3660.  
3661.  
3662.  
3663.  
3664.  
3665.  
3666.  
3667.  
3668.  
3669.  
3670.  
3671.  
3672.  
3673.  
3674.  
3675.

	14	15	16	17	18	Y =
18	0.0	0.0	0.0	0.0	0.0	4.90E-01
17	2.26E-12	1.20E-12	4.47E-13	7.82E-14	1.00E-06	4.80E-01
16	1.05E-12	6.03E-13	2.58E-13	3.92E-14	1.00E-06	4.70E-01
15	5.52E-13	3.37E-13	1.62E-13	3.95E-14	1.00E-06	4.55E-01
14	4.04E-13	2.58E-13	1.35E-13	3.97E-14	1.00E-06	4.35E-01
13	4.44E-13	2.93E-13	1.58E-13	4.10E-14	1.00E-06	4.10E-01
12	6.42E-13	4.39E-13	2.38E-13	4.98E-14	1.00E-06	3.80E-01
11	1.07E-12	7.69E-13	4.29E-13	8.71E-14	1.00E-06	3.45E-01
10	1.95E-12	1.58E-12	9.79E-13	2.71E-13	1.00E-06	3.00E-01
9	3.34E-12	3.29E-12	2.62E-12	1.45E-12	1.00E-06	2.40E-01
8	5.33E-12	6.39E-12	6.71E-12	6.11E-12	1.00E-06	1.80E-01
7	7.59E-12	1.06E-11	1.39E-11	1.72E-11	1.00E-06	1.35E-01
6	9.91E-12	1.51E-11	2.30E-11	3.51E-11	1.00E-06	1.00E-01
5	1.27E-11	2.05E-11	3.32E-11	5.72E-11	1.00E-06	7.00E-02
4	1.69E-11	2.85E-11	4.68E-11	7.89E-11	1.00E-06	4.50E-02
3	2.65E-11	4.34E-11	7.33E-11	1.05E-10	1.00E-06	2.50E-02
2	6.34E-11	8.81E-11	1.52E-10	1.95E-10	1.00E-06	1.00E-02
X =	0.435	0.455	0.470	0.480	0.490	



MEAN SQUARE TEMPERATURE FLUCTUATION											
I =	2	3	4	5	6	7	8	9	10	11	Y =
3717.	0.0	0.0	0.0	0.0	0.0	0.0	0.0	0.0	0.0	0.0	4.90E-01
3718.	1.00E-06	1.00E-06	1.00E-06	1.00E-06	1.00E-06	1.00E-06	1.00E-06	1.00E-06	1.00E-06	1.00E-06	4.80E-01
3719.	1.00E-06	1.00E-06	1.00E-06	1.00E-06	1.00E-06	1.00E-06	1.00E-06	1.00E-06	1.00E-06	1.00E-06	4.70E-01
3720.	1.00E-06	1.00E-06	1.00E-06	1.00E-06	1.00E-06	1.00E-06	1.00E-06	1.00E-06	1.00E-06	1.00E-06	4.55E-01
3721.	1.00E-06	1.00E-06	1.00E-06	1.00E-06	1.00E-06	1.00E-06	1.00E-06	1.00E-06	1.00E-06	1.00E-06	4.35E-01
3722.	1.00E-06	1.00E-06	1.00E-06	1.00E-06	1.00E-06	1.00E-06	1.00E-06	1.00E-06	1.00E-06	1.00E-06	4.10E-01
3723.	1.00E-06	1.00E-06	1.00E-06	1.00E-06	1.00E-06	1.00E-06	1.00E-06	1.00E-06	1.00E-06	1.00E-06	3.80E-01
3724.	1.00E-06	1.00E-06	1.00E-06	1.00E-06	1.00E-06	1.00E-06	1.00E-06	1.00E-06	1.00E-06	1.00E-06	3.45E-01
3725.	1.00E-06	1.00E-06	1.00E-06	1.00E-06	1.00E-06	1.00E-06	1.00E-06	1.00E-06	1.00E-06	1.00E-06	2.40E-01
3726.	1.00E-06	1.00E-06	1.00E-06	1.00E-06	1.00E-06	1.00E-06	1.00E-06	1.00E-06	1.00E-06	1.00E-06	1.80E-01
3727.	1.00E-06	1.00E-06	1.00E-06	1.00E-06	1.00E-06	1.00E-06	1.00E-06	1.00E-06	1.00E-06	1.00E-06	1.35E-01
3728.	1.00E-06	1.00E-06	1.00E-06	1.00E-06	1.00E-06	1.00E-06	1.00E-06	1.00E-06	1.00E-06	1.00E-06	7.00E-02
3729.	1.00E-06	1.00E-06	1.00E-06	1.00E-06	1.00E-06	1.00E-06	1.00E-06	1.00E-06	1.00E-06	1.00E-06	4.50E-02
3730.	1.00E-06	1.00E-06	1.00E-06	1.00E-06	1.00E-06	1.00E-06	1.00E-06	1.00E-06	1.00E-06	1.00E-06	2.50E-02
3731.	1.00E-06	1.00E-06	1.00E-06	1.00E-06	1.00E-06	1.00E-06	1.00E-06	1.00E-06	1.00E-06	1.00E-06	1.00E-02
3732.	1.00E-06	1.00E-06	1.00E-06	1.00E-06	1.00E-06	1.00E-06	1.00E-06	1.00E-06	1.00E-06	1.00E-06	0.345
3733.	1.00E-06	1.00E-06	1.00E-06	1.00E-06	1.00E-06	1.00E-06	1.00E-06	1.00E-06	1.00E-06	1.00E-06	0.300
3734.	1.00E-06	1.00E-06	1.00E-06	1.00E-06	1.00E-06	1.00E-06	1.00E-06	1.00E-06	1.00E-06	1.00E-06	0.240
3735.	1.00E-06	1.00E-06	1.00E-06	1.00E-06	1.00E-06	1.00E-06	1.00E-06	1.00E-06	1.00E-06	1.00E-06	0.180
3736.	1.00E-06	1.00E-06	1.00E-06	1.00E-06	1.00E-06	1.00E-06	1.00E-06	1.00E-06	1.00E-06	1.00E-06	0.135
3737.	0.010	0.025	0.045	0.070	0.100	0.135	0.180	0.240	0.300	0.345	0.345
3738.	I = 14	15	16	17	18	Y =					
3739.	0.0	0.0	0.0	0.0	0.0	4.90E-01					
3740.	1.00E-06	1.00E-06	1.00E-06	1.00E-06	1.00E-06	4.80E-01					
3741.	1.00E-06	1.00E-06	1.00E-06	1.00E-06	1.00E-06	4.70E-01					
3742.	1.00E-06	1.00E-06	1.00E-06	1.00E-06	1.00E-06	4.55E-01					
3743.	1.00E-06	1.00E-06	1.00E-06	1.00E-06	1.00E-06	4.35E-01					
3744.	1.00E-06	1.00E-06	1.00E-06	1.00E-06	1.00E-06	4.10E-01					
3745.	1.00E-06	1.00E-06	1.00E-06	1.00E-06	1.00E-06	3.80E-01					
3746.	1.00E-06	1.00E-06	1.00E-06	1.00E-06	1.00E-06	3.45E-01					
3747.	1.00E-06	1.00E-06	1.00E-06	1.00E-06	1.00E-06	3.00E-01					
3748.	1.00E-06	1.00E-06	1.00E-06	1.00E-06	1.00E-06	2.40E-01					
3749.	1.00E-06	1.00E-06	1.00E-06	1.00E-06	1.00E-06	1.80E-01					
3750.	1.00E-06	1.00E-06	1.00E-06	1.00E-06	1.00E-06	1.35E-01					
3751.	1.00E-06	1.00E-06	1.00E-06	1.00E-06	1.00E-06	1.00E-01					
3752.	1.00E-06	1.00E-06	1.00E-06	1.00E-06	1.00E-06	7.00E-02					
3753.	1.00E-06	1.00E-06	1.00E-06	1.00E-06	1.00E-06	4.50E-02					
3754.	1.00E-06	1.00E-06	1.00E-06	1.00E-06	1.00E-06	2.50E-02					
3755.	1.00E-06	1.00E-06	1.00E-06	1.00E-06	1.00E-06	1.00E-02					
3756.	1.00E-06	1.00E-06	1.00E-06	1.00E-06	1.00E-06	1.00E-06					
3757.	0.435	0.455	0.470	0.480	0.490	1.00E-02					

3758.  
3759.  
3760.  
3761.  
3762.  
3763.  
3764.  
3765.  
3766.  
3767.  
3768.  
3769.  
3770.  
3771.  
3772.  
3773.  
3774.  
3775.  
3776.  
3777.  
3778.  
3779.  
3780.  
3781.  
3782.  
3783.  
3784.  
3785.  
3786.  
3787.  
3788.  
3789.  
3790.  
3791.  
3792.  
3793.  
3794.  
3795.  
3796.

I	L.LAM.NU/UL	L.LAM.NU/L	L.TUR.NU/UL	L.TUR.NU/L
2	0.681E 01	0.320E 01	0.323E 00	0.152E 00
3	0.744E 01	0.350E 01	0.361E 00	0.170E 00
4	0.850E 01	0.400E 01	0.433E 00	0.204E 00
5	0.992E 01	0.466E 01	0.542E 00	0.255E 00
6	0.118E 02	0.553E 01	0.698E 00	0.328E 00
7	0.141E 02	0.661E 01	0.910E 00	0.428E 00
8	0.169E 02	0.795E 01	0.120E 01	0.563E 00
9	0.198E 02	0.929E 01	0.150E 01	0.704E 00
10	0.222E 02	0.104E 02	0.171E 01	0.802E 00
11	0.230E 02	0.108E 02	0.170E 01	0.798E 00
12	0.223E 02	0.105E 02	0.153E 01	0.721E 00
13	0.206E 02	0.970E 01	0.129E 01	0.607E 00
14	0.183E 02	0.859E 01	0.101E 01	0.473E 00
15	0.158E 02	0.743E 01	0.722E 00	0.340E 00
16	0.139E 02	0.654E 01	0.476E 00	0.224E 00
17	0.130E 02	0.613E 01	0.269E 00	0.126E 00

AV.LAM.NU/UL = 16.74229 AV.LAM.NU/L = 7.86888AV.TUR.NU/UL = 1.10472 AV.TUR.NU/L = 0.51922





